GENETICS OF WHEAT DOMESTICATION AND *SEPTORIA NODORUM* BLOTCH SUSCEPTIBILITY IN WHEAT

A Thesis
Submitted to the Graduate Faculty
of the
North Dakota State University
of Agriculture and Applied Science

By

Sapna Sharma

In Partial Fulfillment of the Requirements
for the Degree of
MASTER OF SCIENCE

Major Program:
Genomics and Bioinformatics

February 2019

Fargo, North Dakota

North Dakota State University
Graduate School

Title

GENETICS OF WHEAT DOMESTICATION AND *SEPTORIA NODORUM* BLOTCH SUSCEPTIBILITY IN WHEAT

By

Sapna Sharma

The Supervisory Committee certifies that this ***disquisition*** complies with North Dakota State University's regulations and meets the accepted standards for the degree of

MASTER OF SCIENCE

SUPERVISORY COMMITTEE:

Dr. Justin D. Faris
Chair

Dr. Phillip E. McClean

Dr. Steven S. Xu

Approved:

February 15, 2019
Date

Dr. Phillip E. McClean
Department Chair

ABSTRACT

T. aestivum ssp. *spelta* Iranian type has long been thought to potentially be the direct non-free threshing hexaploid progenitor. I evaluated a RIL population derived from a cross between CS and Iranian spelta accession P503 to identify loci suppressing free-threshabilty in P503. Identification of QTL associated with threshability in region known to harbor the Tg^{2A} gene, and an inactive tg^{2D} allele supported the hypothesis of Iranian spelta being derived from a more recent hybridization between free-threshing hexaploid and emmer wheat.

Parastagonospora nodorum is an important fungal pathogen and secretes necrotrophic effectors that evoke cell death. In this research, a DH population segregating for *Snn5* was used to saturate *Snn5* region of chromosome 4B with molecular markers. The physical distance between *Snn5* flanking markers was narrowed to 1.38 Mb with genetic distance of 2.8 cM. The markers developed in this study will provide a strong foundation for map-based cloning of *Snn5*.

ACKNOWLEDGEMENTS

First of all, I would like to express my deepest gratitude to my major advisor, Dr. Justin Faris for showing faith in me and letting me part of his research team. He is one of the best advisors anyone could ask for and words might fall short of in thanking him for all his persistent help and motivation throughout my program. His love and passion for wheat molecular genetics inspire me to learn more and push beyond my limits to achieve success. I would also like to thank my academic advisor, Dr. Phil McClean for all his support and sharing his knowledge on plant genetics that helped me to gain better understanding of my subject. Furthermore, my special thanks to my committee member Dr. Steven Xu for providing his intellect and insight during the committee meetings.

It was a blessing to work with great and helping labmates: Dr. Jyoti Saini, Sudeshi Seneviratne, Amanda Peters, Katherine Running and Dr. Aliya Momotaz. The assistance provided by Samantha Steckler and Marissa Condron to keep the greenhouse in order was marvelous. My special thanks to Dr. Zengcui Zhang and Megan Overlander who have gone beyond their ways to assist me with the accomplishment of multiple projects. Additionally, I am grateful to genotyping lab of USDA-ARS for letting me use their lab robotics that eased much of my work-load. I would like to appreciate the Department of Plant Sciences faculty and administrative staff for their guidance at campus.

Most importantly, I would like to extend my gratitude to my husband along with my mom and brother for always having my back and putting up with my madness at times. Also, I want to take a chance to remember my father and grandmother who had always believed in me and encouraged me to move forward crossing all the hardships. I am beyond thankful for the support provided by my friends in Fargo who made me feel like home away from home.

DEDICATION

To my mom and dad

TABLE OF CONTENTS

LIST OF TABLES

LIST OF FIGURES

1. INTRODUCTION

Wheat is an ancient food crop and serves as a substantial source of calories for much of the world's population. It was the world's second most widely produced cereal crop in 2016 with a total production of 725 million tones (FAO, December 2018). As per the present trends, the predicted demand of wheat consumption will increase at a rate of around 1.7% per year until 2050, but productivity has been increasing at a rate of 1.1% annually on a global scale and is stagnating in some regions. Because the production is less than the demand, efforts must be employed to improve the inherent potential of wheat to give higher yield to meet the upcoming trends.

The seed of hexaploid bread wheat is free-threshing because of several critical mutations that accumulated over the course of time. These critical mutations resulted in larger and free-threshing seeds with a non-shattering rachis and enabled early gatherers to easily collect and separate the grains from the chaff. Spikelet shattering occurs due to disarticulation of spikelets through the formation of abscission zones along the rachis at the time of ripening. This trait is favorable to wild species because it provides a natural seed dispersal mechanism and ensures their survival. However, it made it very difficult for early farmers to collect grains at harvest. Another critical and widely studied domestication trait is the ease at which the seed is threshed. The cost of processing non-free threshing seed is higher and thereby reduces its market value.

Two wheat domestication genes, *Q* and *Tg* are primarily responsible for the control of the free-threshing character of wheat cultivars (see review by Faris 2014). However, one subspecies of hexaploid wheat known as *Triticum aestivum* ssp. *spelta* Iranian type, has tough glumes and non-free-threshing seed, even though it harbors the free-threshing *Q* allele (Luo et al. 2000). Therefore, the gene(s) present in Iranian spelta that suppress the free threshing character are

unknown, and the dissection of genetics controlling the non-free-threshing character in Iranian spelta was a primary objective of this research.

Another worldwide challenge faced by the wheat industry is its significant yield loss due to biotic threats posed by bacteria, viruses, fungi, and insects. The genome of fungal pathogens are highly plastic in nature and cause 15-20 % yield loss per annum (see review Figueroa et al. 2017). Major fungal diseases of wheat include powdery mildew (*Erysiphe graminis* f. sp. *tritici*), leaf rust (*Puccinia recondite* f. sp. *tritici*), Septoria nodorum blotch (*Parastagonospora nodorum*), tan spot (*Pyrenophora tritici repentis*), Fusarium head blight (*Fusarium graminearum*), and blast (*Magnaporthe oryzae*). The second major objective of this research was to saturate the region of chromosome arm 4BL that carries *P. nodorum*-wheat sensitivity gene *Snn5* (Friesen et al. 2012) with genetic markers.

Findings from this research will further our understanding of the dyanmic nature of genes governing threshability in wheat, which is an important agronomic character. Expanding our knowledge of these genetic mechanisms involved in the evolution of modern day bread wheat from its diploid and tetraploid progenitors will provide us with knowledge of how further improvements can be employed to meet the demands of the growing global population. Apart from this, markers developed in saturation and high-resolution mapping of *P. nodorum*-wheat sensitivity genes will be useful for marker-assisted selection in wheat germplasm.

1.1. References

Faris JD (2014) Wheat Domestication: Key to Agricultural Revolutions Past and Future. In: Tuberosa R, Graner A, Frison E (eds) Genomics of Plant Genetic Resources: Volume 1. Managing, sequencing and mining genetic resources. Springer Netherlands, Dordrecht, pp 439–464

Figueroa M, Hammond-Kosack KE, Solomon PS (2018) A review of wheat diseases- a field perspective. Mol Plant Pathol 19:1523–1536. doi: 10.1111/mpp.12618

Friesen TL, Chu C, Xu SS, Faris JD (2012) SnTox5-*Snn5*: a novel *Stagonospora nodorum* effector-wheat gene interaction and its relationship with the SnToxA-*Tsn1* and SnTox3-*Snn3-B1* interactions. Mol Plant Pathol 13:1101–1109. doi: 10.1111/j.1364-3703.2012.00819.x

FAO Cereal Supply and Demand Brief | World Food Situation | Food and Agriculture Organization of the United Nations. http://www.fao.org/worldfoodsituation/csdb/en/. Accessed 22 Dec 2018

Luo MC, Yang ZL, Dvořák J (2000) The *Q* locus of Iranian and European spelt wheat. Theor Appl Genet 100:602–606. doi: 10.1007/s001220050079

2. LITERATURE REVIEW

2.1. The wheat genome

The large size of the hexaploid wheat genome (~17 Gbp) and the fact that it is an allopolyploid have led to a decade long effort in obtaining the whole genome sequence. The International Wheat Genome Sequencing Consortium (IWGSC) released its first version of reference sequence of the hexaploid wheat landrace Chinese Spring in 2017 (IWGSC RefSeq v1.0) and fully annotated reference genome with estimated coverage of 94% in 2018 (IWGSC et al. 2018). The reference sequence data from IWGSC RefSeq assembly v1.0, IWGSC RefSeq annotation v1.0 and v1.1, IWGSC physical maps for all chromosomes, some sequenced bacterial artificial chromosomes (BACs), MTP BAC WGP^{TM} sequence tags for all chromosomes (except 3B), and genotyping by sequencing (GBS) maps (January 2017) are also available publicly (https://www.wheatgenome.org/News/Latest-news/RefSeq-v1.0-URGI). These recent resources have increased the chromosome scaffold N50 from 7.0 Mb to 22.8 Mb (IWGSC et al. 2018).

BAC-by-BAC sequencing was the first approach that was considered to obtain a finished genome of high quality. The problems with BAC sequencing include high cost, time, and underrepresentation of some regions (http://www.wheatgenome.info/details.php). Gaps that appear in the sequence of a BAC, or certain regions of a clone might not achieve the full shotgun standard. Efforts to finish the sequencing of these specific regions of the genome involve the sequencing of additional subclones of the clones. This, though, is tedious and expensive.

The adoption of whole genome shotgun (WGS) sequencing methods increased the speed and reduced the cost, but presence of highly repetitive regions accounting for about 80% of the wheat genome made the assembly of sequences difficult. However, new, and improved assembly methods that have been implemented over the past couple of years have made the WGS method

extremely efficient, even for organisms with very large genomes such as wheat. The IWGSC WGA v0.4 included Illumina short sequence reads that were assembled with NRGene's DeNovoMAGIC^{TM}software and produced scaffolds with an L50 of 7.1 Mb and totaled 14.5 Gb (https://www.wheatgenome.org/News/Latest-news/IWGSC-Whole-Genome-Assembly-now-available-at-URGI). With the availability of more recent IWGSC physical maps for all chromosomes, some sequenced BACs, and MTP BAC WGP^{TM} sequence tags, chromosome scaffolds showed significant increase to 22.8 Mb (https://www.wheatgenome.org/News/Latest-news/RefSeq-v1.0-URGI). They have been assigned to chromosomal locations using POPSEQ data and a HiC map. As per the sequences assembled by IWGSC (2018), the precise location of 107,891 high-confidence genes (Borrill et al. 2018) and more than 4.7 million molecular markers have been released (Krasileva et al. 2017).

2.2. Evolution of wheat

The basic genome of all wheat species is organized into seven chromosomes ($x = 7$). The various *Triticum* and *Aegilops* species consist of diploids ($2n = 2x = 14$), tetraploids ($2n = 4x = 28$), and hexaploids ($2n = 6x = 42$) (Sax 1922; Kimber and Sears 1987). It is believed that diploid and tetraploid progenitors and close relatives of modern wheat evolved from a common ancestor about 3 million years ago (MYA) (Huang et al. 2002).

Two separate amphiploidization events involving spontaneous chromosome doubling through the functioning of meiotic restitution division, led to the evolution of bread wheat. The first event that occurred about a half million years ago involved the hybridization between wild diploid, *Triticum urartu* Tumanian ex Gandylian ($2n = 2x = 14$, AA genome) and a species similar to *Aegilops speltoides* Tausch ($2n = 2x = 14$, SS genome) (related but distinct form). The tetraploid wheat *Triticum turgidum* ssp. *dicoccoides* Thell ($2n = 4x = 28$, AABB genomes)

known as wild emmer came into existence as the result of this hybridization. Diploid and tetraploid wheat were independently domesticated from its wild relatives 13,000 and 9,000 years ago, respectively (Nesbitt and Samuel 1996). The first transition occurred in wild emmer and consisted of mutations in the homoeologous *Br1 (brittle rachis)* genes on chromosomes 3A and 3B, which led to a type with a non-brittle rachis. This transition abolished the shattering spike trait and gave rise to new subspecies *T. turgidum* ssp. *dicoccum*, which is commonly known as cultivated emmer wheat.

The second major domestication transition occurred in the *q* gene on chromosome 5A where mutation led to formation of the *Q* allele, which is one of the free-threshing genes of wheat. This mutation along with mutations in the *Tg* genes on chromosomes 2A and 2B at about the same time led to the formation of free-threshing tetraploid wheat, which ultimately spawned fully domesticated durum wheat (*T. turgidum* ssp. *durum*).

Then second amphiploidization took place about 8,000 years ago, (Nesbitt and Samuel 1996; Huang et al. 2002) and involved a hybridization between a tetraploid subspecies of *T. turgidum* (most likely a free-threshing form) and the diploid goatgrass *Aegilops tauschii* Coss. ($2n = 2x = 14$, DD genome) (Kihara 1944; McFadden and Sears 1946) which resulted in *T. aestivum* L. ($2n = 6x = 42$, AABBDD genomes). The first amphiploid would have had non-free-threshing seed due to acquisition of the *Tg* gene on chromosome 2D from *Ae. tauschii*. Shortly following the formation of the first hexaploid, a mutation in the *Tg* gene on 2D gave rise to the *tg* allele resulting in the fully domesticated common hexaploid bread wheat (*T. aestivum* ssp. *aestivum*). This common bread wheat had soft glumes (*tg* on group 2 chromosomes), a non-brittle rachis (*br* on group 3 chromosomes) and free-threshing seed (*Q* on chromosome 5A) to make it non-shattering and free-threshing. Based on various findings so far, researchers have

concluded all wild forms of diploid and tetraploid species carry *BrBrTgTgqq* genetic composition whereas, the cultivated ones vary.

Apart from these lineages, some other hybridization events also took place among the subspecies. A cross between club wheat (*T. aestivum* ssp. *compactum*) and cultivated emmer gave rise to European spelta (non-free-threshing) (Bertsch 1943; MacKey 1966; Blatter et al. 2002, 2004; Yan et al. 2003). Another form of spelta-like wheat, Iranian spelta (Kuckuck 1959) was found growing in northern Iran and other Middle East regions. It was assumed to be more primitive than European spelta. According to genetic analysis, European and Iranian spelta have a major allelic difference at the *Q*/*q* locus on chromosome 5A, where European has *q* (non free-threshing) and Iranian spelta has *Q* (free-threshing allele) (Luo et al. 2000). But, in spite of carrying the free-threshing *Q* allele, Iranian spelta has tough glumes and non-free-threshing seed. It resembles what the first *T. aestivum* hexaploid resulting from the amphiploidization event between *T. turgidum* and *Ae. tauschii* is thought to have looked like.

Dvorak et al. (2012) reported a genetic study on the origin of spelta-like wheat. The group hypothesized if Iranian spelta is derived from hybridization of hulled emmer with free-threshing hexaploid wheat, it must have recessive tg^{2D} at chromosome 2D (which would have come from free-threshing parent), and/or may have Tg^{2A} (or *Sog*) or Tg^{2B} alleles. If Iranian spelta is an ancestral hexaploid wheat and derived from hybridization of domesticated emmer with hulled *Ae. tauschii*, it should have the Tg^{2D} allele (from *Ae. tauschii*) and Tg^{2A} (or *Sog*) or Tg^{2B} or both, depending on genotype of emmer parent. Therefore, the genotype at the Tg^{2D} locus remains a critical factor in determining the possible scenario. The group studied 11 accessions of speltas (four European spelta, one Ethiopian spelta, and six Iranian spelta) to infer the Tg^{2D} genotype by using simple sequence repeat (SSR) markers linked to the Tg^{2D} locus (Dvorak et al. 2012). Ten

accessions had inactive tg^{2D} alleles on chromosome 2D, which agreed with their first hypothesis that one parent was a free-threshing hexaploid wheat. The presence of the Tg^{2B} allele on chromosome 2B was consistent with the assumption of other parent being hulled tetraploid wheat.

Phenotypic analysis of 11 spelta-like wheat accessions, four disomic substitution (DS) lines with chromosome 2D replaced by *Ae. tauschii* in the CS genetic background, TetraCanthatch (tetraploid wheat), and CS revealed the most tough glumes were present in the spelta-like accessions (Dvorak et al. 2012). Softer glumes in DS lines suggested the presence of additional genes that affect glume tenacity in *Ae. tauschii*. Tg^{2D} was mapped to a 9.7 cM interval between markers *Xwmc112* and *XBG263347*. Homoeologous Tg^{2B} was mapped to a 15.8 cM interval between SNPs *XCJ600989* and *XBE518440*. Evidence for a homoeologous Tg^{2A} allele was not conclusive and the authors suggested that more research was needed to determine if a *Tg* homoeoallele on chromosome 2A was a factor in wheat domestication.

Other hexaploid subspecies also exist that differ from common wheat primarily by single gene mutations. These include *T. aestivum* spp. *compactum* (the *C* gene confers a compact spike), *sphaerococcum* (carries the *S* gene conferring spherical grains), and *macha*. *Triticum aestivum* ssp. *sphaerococcum* is commonly known as Indian dwarf wheat or shot wheat and is endemic to southern Pakistan and Northwestern India (Percival 1921). It is considered as one of the important winter crops being grown by ancient Indians. The characteristics that make it different from others are its semi-dwarf growth, erect and firm appearance (60-70 cm), short culms, small ears, and spherical grains (Mori et al. 2013).

2.3. Major wheat domestication genes

The wild forms of wheat species ensured their continuity via natural seed dispersal. The spikelets would break and shatter to the ground upon maturity, due to the brittle rachis controlled by the brittle rachis (*Br)* gene. The spontaneous mutation in wild emmer (*Br*) resulted in cultivated emmer (*br*). Another major dominant gene mutation occurred in the *q* gene, most likely in cultivated emmer. The *Q* gene, considered as the super domestication gene (Faris et al. 2003; Simons et al. 2006), pleiotropically affects various traits like glume shape, spike length, rachis fragility, plant height, and ear emergence time. Additionally, it results in the free-threshing character when *Tg* alleles are present in their recessive forms. This is evident in common bread wheat, which resulted from a recessive gene mutation at the *Tg* locus. *Tg* controls the tough glume trait, which protects seeds by enveloping them tightly during natural seed dispersal.

2.4. Evolution and genetics of *Q, Br,* and *Tg* genes

The natural seed dispersal mechanism, though useful for propagation of wild forms, is quite undesirable for cultivated forms. The seeds would fall to ground upon maturity because of formation of abscission zones and would be lost. The mutation of *Br* to *br* was one of the first and most important domestication traits acquired by cultivated forms. Two types of disarticulation are found in wheat, spike and spikelet type (Gill et al. 2008). In spike type, the whole spike breaks as a single unit at its base as found in *Ae. speltoides* var *speltoides*. Spikelet type is further subdivided into the common wedge type (W-type), found in *Ae. speltoides* ssp. *ligustica* and *T. mononcoccum* ssp. *aegilopoides;* and barrel type (B-type), found in *Ae. tauschii*. W-type disarticulation was mapped to 3DS in *T. aestivum* (Chen et al. 1998; Watanabe et al. 2003). It is also found that the dominant allelic form of *Br* gene is responsible for W-type

detachment as found in wild emmer whereas the recessive allele controls spike type drop (Li and Gill 2006).

Mapping of recombinant inbred lines (RILs), obtained from the genetic stocks assessed by Watanabe and Ikebata (2000) not only identified the chromosomal location of *Br* genes on 3AS and 3BS but also indicated that *T. urartu* was the donor of *Br1* on chromosome 3A, and the B-genome donor contributed *Br1* on chromosome 3B. W-type is controlled by *Br1* on chromosomes 3A, 3B, and 3D, whereas B-type is controlled by *Br2* on chromosome 3D (Li and Gill 2006). Recessive mutations at these loci resulted in a tough rachis. The recent cloning of *Br* genes on chromosome 3A (*Ttbtr1-A*) and 3B (*Ttbtr1-B*) by Avni et al. (2017) has shown that homozygous recessive mutation at both *TtBtr1* alleles is required for a non-brittle phenotype as in cultivated emmer.

It is well known that mutations at the *Br* loci occurred before the second amphiploidization event. Moreover, it is assumed that the *Br* genes from the D-genome progenitor have either undergone mutation before amphiploidization or their effects are greatly reduced in the hexaploid background. Therefore, none of the hexaploid wheat subspecies (except *T. aestivum* ssp. *macha*) have primitive *Br* alleles.

The *Q* gene is referred to as a super gene (Faris et al. 2003) because of its effects on numerous traits including glume shape and tenacity (Muramatsu 1963, 1986; Singh 1969), spike length (Muramatsu 1963; Kato et al. 1999), rachis fragility (Leighty and Boshnakian 1921; Mackey 1954; Singh et al. 1957; Jantasuriyarat et al. 2004), ear emergence time (Kato et al. 1999), and plant height (Muramatsu 1963; Kato et al. 1999, 2003). The *q* allele is responsible for the speltoid type spike (Nilsson-Ehle 1917, 1920) in European spelta. *Q* is incompletely dominant to *q*, and plants having *Qq* genotype result in an intermediate spike to speltoid and

squareheaded. Muramatsu (1963) gave the idea of dosage effect of *Q*. He concluded *q* was hypomorphic to *Q* and ~2.5 doses of *q* equaled to 1 dose of *Q*.

The mutation from *q* to *Q* is considered as the master switch that resulted in square headed and free-threshing spikes. Other hypotheses have been made regarding the evolution of *Q*. Kuckuck (1959) suggested occurrence of *Q* is derived from duplication of *q*, and Swaminathan (1963) argued that the presence of tandem repeats and unequal crossing within the *Q* locus potentially caused its differential expression from speltoides to compactoides. However, the cloning of *Q* by Simons et al. (2006) refuted both theories.

Q was physically mapped to the long arm of chromosome 5A using deletion lines (Miller and Reader 1982; Endo and Mukai 1988; Tsujimoto and Noda 1989, 1990; Ogihara et al. 1994; Endo and Gill 1996) and eventually to submicroscopic deletion interval (Endo and Gill 1996). Faris and Gill (2002) conducted high-resolution mapping of *Q* to identify markers tightly linked to the locus. This was followed by chromosome walking and BAC sequencing using a *T. monococcum* BAC library, which led to the identification of a candidate gene with similarity to the *APETALA2* (*AP2*) gene in Arabidopsis and *indeterminate spikelet1* (*ids1*) in maize (Faris et al. 2003). Both genes are responsible for flower and seed development. *Q* is a member of *APETALA2* (*AP2*) family of transcription factors. *AP2* is a class A type gene of the ABC model of flower development and controls the transition from vegetative to reproductive development and specifies floral organ identity (Jofuku et al. 1994). DNA binding domain is characteristic feature of *AP2* family, unique to plants, and is named after the Arabidopsis *AP2* gene (Jofuku et al. 1994).

Simons et al. (2006) determined the structural composition of *Q* using the wild-type *WAP2* gene genomic sequence from Chinese Spring. The gene contains 10 exons and 9 introns

adding to 3229 bp, and had a GC content of 54%. The coding sequence is 1344 bp and it has 128 bp and 255 bp of 5' and 3' untranslated regions (UTRs), respectively. Finally, it encodes a protein consisting of 447 amino acids. *Q* has more abundant transcription levels than *q* by a factor of >2 (Simons et al. 2006). Increased transcription is reported to be related to single point mutation in the miR172 binding site in exon 10 (Greenwood et al. 2017; Debernardi et al. 2017). The *q* allele has stronger binding affinity than *Q* for miR172 and, upon binding to *q*, miR172 would suppress transcription of *q* resulting in speltoid-type spikes. This finding was consistent with the Muramatsu (1963) reports of dosage effect of *Q*.

Another gene having major effects on the free-threshing character is *Tg*, which confers tenacious glumes (Kerber and Dyck 1969). The dominant allele is responsible for tough glumes that adhere strongly to the kernels. The tough glumes help to protect the seed from damage, ensuring propagation, but they make threshing of the seed difficult. Early cytogenetic studies along with the recent molecular mapping studies have corroborated the position of Tg^{2D} on short arm of chromosome 2D (Kerber and Rowland 1974; Jantasuriyarat et al. 2004; Nalam et al. 2007; Sood et al. 2009).

Efforts were taken by Simonetti et al. (1999) to map other quantitative trait loci (QTLs) controlling the tough glume trait. They developed a tetraploid population from the cross between *T. turgidum* ssp. *dicoccoides* (non-free-threshing due to tough glumes) and durum (free-threshing). After their evaluation, the group found a major QTL on 5AL that corresponded to the *Q* gene, and also a second major QTL on 2BS. The latter QTL was thought to be a homoeoallele of Tg^{2D}.

Some hypothesize *Tg* to be dominantly epistatic to *Q*. Work by Muramatsu (1979) and Simons et al. (2006) on *T. turgidum* ssp. *dicoccum* var. *liguliforme* (carrying the *Q* allele)

indicated that the dominant allele of *Tg* indeed inhibits the expression of *Q*. It was also suggested that cultivated emmer carries Tg^{2B} on chromosome 2B. The species carrying recessive alleles at the *Br* and *Tg* loci but lacking the *Q* allele behave as primitive species with speltoid-type spike, partially tough glumes, semi-brittle rachis, taller plant height, early flowering, and variable yield expectancies. Such immense control of a single gene over numerous characters makes it important to study and understand its evolution and genetic control in different polyploid backgrounds.

Faris et al. (2014a) evaluated disomic substitution lines involving chromosomes 2A and 2B of wild emmer accessions substituted for homologous chromosomes in tetraploid and hexaploid backgrounds. Phenotypic analysis of these lines suggested the possibility of presence of genes on 2A and 2B that inhibit the free-threshing trait in the tetraploid background. Additionally, the group evaluated RILs that were developed by crossing tetraploid durum and a *T. turgidum* ssp. *dicoccoides* chromosome 2B disomic substitution line. They developed a linkage map of chromosome 2B, and mapped loci that inhibited threshability. Mapping of 58 markers that spanned a genetic distance of 79.5 cM on chromosome 2B using SSRs, SNP markers, and EST-derived primer sets revealed the threshability locus flanked by markers *Xwmc154* and *Xwmc25* at genetic distances of 0.4 and 1.9 cM, respectively. The gene at this locus was considered as Tg^{2B} and homoeologous to Tg^{2D} on 2DS because the marker *Xwmc25* was shown to be linked to Tg^{2D} as well (Nalam et al. 2007; Sood et al. 2009; Dvorak et al. 2012). Sood et al. (2009) assigned the location of the soft glume (*sog*) gene close to the centromere of chromosome $2A^{m}S$ of *T. monococcum.* The fact that *Tg* mapped to the distal regions of 2DS and 2BS ruled out the possibility that *sog* and *Tg* were homoeologous and suggests their diverse origin.

The evaluation of tetraploid 2B substitution lines indicated the epistatic control of Tg^{2B}, like Tg^{2D}, to *Q* on chromosome 5A (Faris et al. 2014a). It is also speculated that the difference in ploidy level may affect the gene expression of *Tg*. The hexaploid wheat cultivar, CS- *T. turgidum* ssp. *dicoccoides* substitution line containing TA106 chromosome 2B (CS106-2B developed by late E.R. Sears) was found to be as free-threshing as CS, which supported the non-epistatic control of Tg^{2B} to *Q* on 5A chromosome in the hexaploid background. On the contrary, Dvorak et al. (2012) reported the reduced threshability in hexaploid background due to gene(s) on 2BS. Another possibility is that Tg^{2B} in TA106 was disrupted by mutation or lost through gene-flow (Berkman et al. 2013; Dvorak et al. 2006; Luo et al. 2007), either of which could explain the free-threshing nature of the CS-2B substitution line.

Faris et al. (2014a) also suggested the possibility of factor(s) on chromosome 2A that confers a non-free-threshing phenotype in tetraploid backgrounds. This was supported by a non-free-threshing phenotype of 2A substitution lines of *T. turgidum* ssp. *dicoccoides*, and CS- *T. turgidum* ssp. *dicoccoides* substitution line containing TA106 chromosome 2A. A gene homoeologous to Tg^{2B} and Tg^{2D} on chromosome 2A could be responsible for inhibiting threshability in tetraploid accessions.

Faris et al. (2014b) evaluated a Ben (PI 596557) (*T. turgidum* ssp. *durum*) × cultivated emmer PI 41025 (*T. turgidum* ssp. *dicoccum)* wheat RIL population for QTLs associated with spike length, number of spikelets per spike, spike compactness, kernels per spike, grain weight per spike, thousand kernel weight, rachis fragility, and threshability. The group found a QTL associated with threshability on chromosome 2B, which corresponded well with the position of Tg^{2B} (Faris et al. 2014a). In both works of Faris et al. (2014a, b), the locus governing threshability was closely mapped to the SSR marker *Xwmc154* on 2B. Faris et al. (2014b)

observed the contribution of Tg^{2B} by PI 41025, indicating the mutation at Tg^{2B} must have happened during the evolution of non-free-threshing cultivated emmer to free-threshing durum or another fully domesticated tetraploid wheat.

Both works by Faris et al. (2014a) and Dvorak et al. (2012) provided a strong evidence of the presence of homoeologue of *Tg* on chromosome 2A. Two QTLs associated with threshability were mapped on chromosome 2A by Faris et al. (2014b) and the genetic position of one of them was similar to that of Tg^{2B}. Interestingly, the second QTL was associated with threshability and spike compactness, similar to Tg^{2B}.

Their study showed that cultivated emmer (PI 41025) possessed Tg^{2B} and possibly Tg^{2A} as well. Because seed of cultivated emmer is hulled and hard to thresh, it is likely to have the genotype $Tg^{2A}Tg^{2A}/Tg^{2B}Tg^{2B}/qq$. The mutations at all three loci must have happened during the course of evolution to give rise to the first free-threshing tetraploid wheat with the genotype $tg^{2A}tg^{2A}/tg^{2B}tg^{2B}/QQ$. It is probable to consider that a free-threshing tetraploid subspecies (Matsuoka and Nasuda 2004; Dvorak et al. 2012; Faris 2014; Faris et al. 2014a) must have been involved in amphiploidization event with *Ae. tauschii* to give rise to non-free-threshing hexaploid wheat due to the acquisition of Tg^{2D} from *Ae. tauschii* (McFadden and Sears 1946; Kerber and Rowland 1974). This non-free-threshing amphiploid must have mutated to tg^{2D} very rapidly to give rise to free threshing hexaploid wheat. This further corroborates the argument of genotype ($tg^{2A}tg^{2A}/tg^{2B}tg^{2B}/QQ$) of free-threshing tetraploid, because if it was not, then mutations at multiple loci would have been required, which would be expected to take a significant amount of time. Therefore, a single recessive mutation at Tg^{2D} gave rise to the fully domesticated *T. aestivum* ssp. *aestivum* with genotype $tg^{2A}tg^{2A}/tg^{2B}tg^{2B}/\ tg^{2D}tg^{2D}/QQ$ in relatively short amount of time. Further work is required to better understand the paralogous and orthologous genes

responsible for tough glumes and how they are involved in the complex genetic pathways to control the free-threshing character.

2.5. Molecular markers and genetic mapping in wheat

Molecular markers are DNA sequences that help to identify allelic variants and are associated with a certain location within the genome. The use of molecular markers has complemented conventional breeding methods, which would otherwise involve significant effort and resources in careful phenotypic selection. Its great advantage involves the elimination of plants with undesirable gene combinations at relatively early stages and expedites the selection of complex traits in a comparatively shorter time.

Over the years, polymorphism has been observed due to variations in the number of tandem repeats at certain loci, single nucleotide changes, or insertions or deletions of DNA segments. Simple sequence repeats (SSRs), or microsatellites, are DNA sequences consisting of short tandem repeats. High polymorphism levels, typically co-dominance, locus specificity, cost effectiveness and abundance have made SSRs widely-used markers. Single nucleotide polymorphism (SNPs) are highly abundant markers in any genome. They are identified by aligning the DNA sequences of multiple genotypes. The availability of the reference genome sequence of Chinese Spring (IWGSC 2018) has made it much easier and cost-effective to generate more SNP markers. These markers have made it possible to create high-density genetic linkage maps.

Mapping populations segregating for traits of interest and polymorphic molecular marker data helps in developing saturated genetic linkage maps. These high-density maps help in detection of QTLs controlling traits, understanding the evolution of genomes, and map-based cloning experiments.

2.6. Disease challenges in wheat production

With the intensive cultivation of wheat, various biotic constraints have emerged whereas plant immune systems have also evolved to resist attacks by pathogens. Pathogen invasion is estimated to cause reduction of approximately 14 % in yield capacity of crops resulting in losses of US$220 billion, annually (FAO 2017). It has been documented that early land plants were established via the interaction with symbiotic fungal associations, suggesting their co-evolution with microbes (Gehrig et al. 1996). Microbes invade plants for their colonization leading to their survival. Natural surface openings such as stomata, pores in the underside of leaf or root surfaces, serve as important entry sites for microbes. Once the cellulase-based plant cell wall has been crossed, pathogens are exposed to the host plasma membrane, where they encounter extracellular surface receptors that recognize pathogen-associated molecular patterns (PAMPs). PAMPs are microbial conserved features critical to the lifecycle of pathogens (Nurnberger et al. 2004, Zipfel and Felix 2005). Such features include lipopolysaccharides and flagellin of gram-negative bacteria or chitin and ergosterol in fungal cell walls. The N- and C-terminal regions of the flagellin protein of flagella is conserved and is recognized by many plant species as well as by mammalian innate immunity receptors (Underhill and Ozinsky 2002).

PAMPs are recognized by pathogen recognition receptors (PRRs) that are usually present in the plasma membrane of host cells. This first active response results in PAMP-triggered immunity (PTI), which prevents further infection by the pathogen (reviewed in Chisholm et al. 2006). Multiple PAMP signaling pathways like mitogen activated protein (MAP) kinase signaling, transcriptional induction of PTI associated genes, production of reactive oxygen species, and deposition of callose at the cell wall may or may not act together to activate defense. A conserved 22 amino acid peptide (flg22) corresponding to flagellin amino terminus upon

recognition by receptor FLS2 in *Arabidopsis* activates a complete MAP kinase cascade and WRKY transcription factors that halt the bacterial infection (Asia et al. 2002). FLS2 is a receptor-like kinase (RLK) consisting of extracellular leucine-rich repeats (LRRs) and an intracellular serine/threonine kinase domain (Gomez-Gomez and Boller 2000). Plants lacking FLS2 showed increased susceptibility to bacterial pathogens. Furthermore, it was shown that fls2 mutants when inoculated with various bacterial extracts containing PAMPs in addition to flagellin, showed reduced bacterial growth. This indicated that other PAMPs present in extracts were recognized by receptors other than FLS2 and supported the idea of convergence of multiple signaling pathways to elicit a defense response (Zipfel et al 2004). It was later shown that overexpression of WRKY results in decreased infection by both bacteria and fungi.

To escape PTI, pathogens evolved to evade recognition at the plasma membrane by secreting effector proteins that suppress resistance signaling of plants and is known as effector triggered susceptibility (ETS) (Zipfel 2009). Gram negative bacteria use the type 3 secretion system (TTSS) to deliver effectors, which was probably acquired via horizontal gene transfer or evolved from a flagellar apparatus. Fungal pathogens deliver their effectors via haustoria into the plant intercellular space (Mendgen and Hahn 2002; Whisson et al. 2007; Rafiqi et al. 2010, 2012). These effectors enhance pathogen virulence and enable them to survive and multiply in susceptible hosts by altering host physiology. These effectors remain unfolded until they enter their host and may contain prokaryotic chaperons or eukaryotic activators that help in their secretion in host environment (Akeda and Galan 2005). One such example is of *P. syringae* AvrRpt2 which is activated by eukaryotic cyclophilins like *Arabidopsis* ROC1 (Coaker et al. 2005). Some effector proteins like *Xanthomonas* AvrBs3 alter host cell transcription to fight against host PTI. These effector proteins contain a C-terminal nuclear localization signal (NLS)

and an acidic transcriptional activation domain (AAD) that serve as means to downregulate host defense mechanisms.

Pathogens also use means other than effectors to escape recognition by plant PRRs. *Magnaporthe oryzae* alters its cell wall decomposition by accumulating α-1,3-glucans at the surface of its cell wall, which prevents its decomposition by plant chitanses (Fujikawa et al. 2012). Other strategies adopted by fungi to escape host defense include subverting ROS damage by effector Pep1 of *U. maydis* in maize (Doehlemann et al. 2009; Hemetsberger et al. 2012), manipulating pH of infected tissue leading to host cell death, or inhibition of host proteases (reviewed in Rodriguez-Moreno et al. 2018).

As a response to ETS, plants developed a more specialized mechanism of direct or indirect recognition of effectors by using plant resistance (*R*) proteins, only after the entry of pathogen. This mechanism is known as effector-triggered immunity (ETI) (Jones and Dangl 2006; Zipfel 2009; Tsuda and Katagiri 2010) and results in cell death in the infected area through programmed cell death (PCD) or hypersensitive reaction (HR) (reviewed in Chisholm et al. 2006). Salicyclic acid (SA), jasmonic acid (JA), and ethylene dependent signaling are some important mechanisms associated with ETI against pathogens (Thomma et al. 1998, 2001; Glazebrook 2005).

The pairwise association of plant *R* genes and pathogen *Avr* genes led to the establishment of the gene-for-gene model (Flor 1956). An incompatible interaction occurs if either the resistance or avirulence gene is absent, leading the pathogen to escape recognition and then colonizing in the host. Several effectors produced by biotrophic pathogens and corresponding *R* genes have been cloned and characterized (Rafiqi et al. 2012). Several classes of *R*-genes have been identified and classified based on their protein domain organization. The

largest group of *R* genes include nucleotide binding site (NBS) and leucine-rich repeat (LRR) domains. The NBS domain consists of conserved motifs responsible for ATP/GTP binding and hydrolysis (Tameling et al. 2002) whereas LRRs are involved in protein-protein interactions (Kobe and Deisenhofer 1994). Examples would be *RPP2A* and *RPP2B* genes with NBS-LRR domains that confer resistance against *P. parasitica* in *Arabidopsis* (Sinapidou et al. 2004). The second class of R genes include receptor-like proteins (RLPs), receptor-like kinase (RLKs), and polygalacturonase-inhibiting proteins (PGIPs) (Chisholm et al. 2006). The tomato *Cf* gene, which confers resistance to leaf mold pathogen *C. fulvum* (Jones et al. 1994) is characteristic of extra-cytoplasmic LRR class of *R* genes.

Some necrotrophic fungal pathogens produce necrotrophic effectors (NEs), formerly referred to as host-selective toxins, that are important for pathogenicity (Scheffer and Livingston 1984; Wolpert et al. 2002). NE-producing nectrorophic specialist pathogens cause necrotrophic effector triggered susceptibility (NETS) (review by Friesen and Faris 2010; Liu et al. 2012; Shi et al. 2016), in opposition to ETI caused by biotrophs. In NETS, dominant host sensitivity genes recognize pathogen-produced NEs resulting in cell death and ultimately disease. The host response to the invading pathogen is much the same as in ETI caused by a biotroph, but because the pathogen is a necrotroph, it has the ability to feed and propogate on dying host tissue.

Recent studies of NE-host gene interactions have shown that typical disease resistance responses occur such as DNA laddering, heterochromatin condensation, cell shrinkage, induction of a hypersensitive reaction, oxidative burst and/or PR protein expression (Wolpert et al. 2002; Liu et al. 2012). This shows that a similar cascade of events occurs in both NETS and ETI. Even so, the effectors produced by *P. nodorum* and other necrotrophic pathogens are similar in structure and function as biotrophic effectors. One such NE is victorin secreted by *Cochliobolus*

victoriae when recognized by the oat susceptibility gene *Pc2* causes Victoria blight (Meehan and Murphy 1947). Interestingly, it was later found that the same gene also likely confers resistance to crown rust caused by *Puccinia coronata* in oats (Welsh et al. 1954). A homolog of *Pc2*, named as *LOV1* that provides victorin susceptibility in *Arabidopsis*, was then cloned by Lorang et al. (2007). There are studies in NETS systems showing the involvement of NBS-LRR domains along with other regions acting as bait to detect pathogen effectors (Sarris et al. 2016). *LOV1* encodes a coiled-coil-NBS-LRR (CC-NBS-LRR) protein and mediates responses involving induction of PR genes, production of phytoalexins, and HR-like cell death (Lorang et al. 2007). Two *P. nodorum*-wheat sensitivity genes have been cloned so far, namely *Tsn1* (Faris et al. 2010) and *Snn1* (Shi et al. 2016b) and contain Ser/Thr-NB-LRR and Ser/Thr domains, respectively. However, it is not yet known if these *P. nodorum*-wheat sensitivity genes were/are involved in recognition of biotroph-produced effectors that would lead to a resistance response. Nevertheless, these examples provide evidence to the subdual of resistance mechanism by necrotrophs to cause host susceptibility for their own benefit.

2.7. *Parastagonospora nodorum*

Parastagonospora [syn. anamorph: *Stagonospora*; teleomorph: *Phaeosphaeria*] *nodorum* (Berk.) syn. *Leptosphaeria nodorum* (Müll.) Quaedvleig, Verkley and Crous, belongs to Pleosporales class of fungi in Dothideomycetes order of Ascomycetes. Its asexual stage was first described as *Septoria nodorum* in 1850s by Miles Berkeley (Eyal et al. 1987). However, in 2001 it was moved to *Stagonospora* genus based on ITS sequence analysis (Goodwin and Zismann 2001). Based on sequence analysis of partial 28S nuclear ribosomal DNA (Quaedvlieg et al. 2013), and morphology of conidial spores and sexual stage, this necrotroph was moved to genus *Parastagonospora* and was renamed as *Parastagonospora nodorum*.

P. nodorum reproduces both asexually and sexually. Pseudothecia is the sexual fruiting body that carry ascospores born in asci (Eyal et al. 1987; Fitt et al. 1989), whereas pycinidia carry asexual spores called pycnidiospores. However, the primary source of disease inoculum is ascospores (Rapilly et al. 1973), which can be dispersed by wind (Solomon et al. 2006; see review by Han et al. 2007 and Oliver et al. 2012). Upon first infection, NEs are released through hyphae into the host cell. Chlorotic lesions are formed that eventually become lens shaped with brownish centers (Friesen and Faris 2010). The presence of pycnidia in lesions is a key feature of SNB (McMullen and Adhikari 2009). After 15-20 days of infection period, asexual spores (conidia) are released from pycnidia and splash dispersed to continue with the infection cycle. It has been shown that conidia are repeatedly produced from the same pycnidia each infection cycle and thereby, increasing the possibility of epidemics provided optimum weather conditions are met (Scharen 1966). The fungus can also survive in wheat straw or seeds for 2-3 years as overwintering structures (Scharen 1946).

P. nodorum was first reported as pathogen causing glume blotch (Weber 1922) in wheat in 1845 (Blaker 1978) in England. It also causes the serious foliar disease Septoria nodorum blotch (SNB) in wheat resulting in significant losses. By 1922, SNB affected countries included Italy, Sweden, Switzerland, Germany, France, Australia, and the US (Weber 1922). It has been shown to cause yield losses of 30% in the southeastern regions of the U.S. (Bhathal et al. 2013), 31% in Australia (Oliver et al. 2012; Bhathal et al. 2013), and 50% in Europe (Karjalainen et al. 1983). Currently, it is prevalent in the U.S., Canada, Western Australia, southern Germany, Switzerland, Latvia, Finland, and Norway (reviewed in Ficke et al. 2018). Because *P. nodorum* is a necrotroph, disease outbreaks accelerate towards the end of the growing season when senescing tissues are more abundant. Verreet et al. (1987) observed greater yield losses due to

infection of leaves than on wheat heads and probably due to reduced photosynthetic active leaf area. However, most studies agree that infection of both heads and leaves can cause yield loss of variable degrees depending on weather, field, and infection conditions. SNB can be managed in the field to some extent via crop rotation, fungicide treatments, and genetic resistance in the host.

The wheat-*P. nodorum* pathosystem has become a model system for NETS resulting from inverse gene-for gene interactions. To date, nine host sensitivity genes that interact with *P. nodorum* necrotrophic effectors have been characterized: SnToxA-*Tsn1* (Friesen et al. 2006, 2009; Liu et al. 2006; Zhang et al. 2009; Faris et al. 2010, 2011; Faris and Friesen 2009), SnTox1-*Snn1* (Liu et al. 2004a, b, 2012; Reddy et al. 2008; Shi et al. 2016b), SnTox2-*Snn2* (Friesen et al. 2007, 2009; Zhang et al. 2009), SnTox3-*Snn3-B1* (Friesen et al. 2008; Liu et al. 2009; Shi et al. 2016a), SnTox3-*Snn3-D1* (Zhang et al. 2011), SnTox4-*Snn4* (Abeysekara et al. 2009, 2012), SnTox5-*Snn5* (Friesen et al. 2012), SnTox6-*Snn6* (Gao et al. 2014), and SnTox7-*Snn7* (Shi et al. 2015).

2.7.1. SnToxA-*Tsn1*

The SnToxA-*Tsn1* is by far the most well characterized interaction in this pathosystem (Ciuffetti et al. 1997; Friesen et al. 2006; Faris et al. 2010). ToxA was first purified from *Pyrenophora tritici-repentis*, which causes the disease tan spot in wheat, and was designated as Ptr ToxA (Tomás and Bockus 1987; Balance et al. 1989). Homologues of the *ToxA* gene have been identified in three different species: *Pyrenophora tritici-repentis* (Tomás and Bockus 1987), *Parastagonospora nodorum* (Friesen et al. 2006), and *Bipolaris sorokiniana* which causes spot blotch, Helminthosporium leaf blight, and common root rot in wheat (McDonald et al. 2017). Friesen et al. (2006) identified higher nucleotide diversity in *P. nodorum*, and thereby concluded that *ToxA* likely originated in *P. nodorum* and was later horizontally transferred to *P. tritici-*

repentis. However, no haplotype of *B. sorokiniana ToxA* was detected in *P. nodorum*. Until the broader set of *B. sorokiniana* genomes are sequenced and analyzed, it cannot be stated with certainty about the actual donor of *ToxA* (reviewed in McDonald and Solomon 2018).

The ToxA gene encodes a 13.2 kDA mature peptide and has an RGD motif responsible for its internalization in host cells and its targeting to chloroplasts (Sarma et al. 2005). Approximately 24% of the global collection of *P. nodorum* isolates contain the *ToxA* gene (Friesen et al. 2006). *Ptr ToxA* was cloned by Balance et al. (1996) and Ciuffetti et al. (1997) and later *SnToxA* was cloned by Friesen et al. (2006). Sensitivity to ToxA is governed by the dominant *Tsn1* gene. *Tsn1* is located on chromosome arm 5BL of wheat (Faris et al. 1996).

Chromosome walking of BAC contig containing *Tsn1* delineated the gene to ~350-kb region. Out of the six genes that co-segregated with *Tsn1*, association mapping eliminated two of them. Mutant analysis indicated a mutation in a S/TPK-NBS-LRR-like gene and was later confirmed by genotyping 386 wheat cultivars. *Tsn1* is 10,581 bp in length and contains 8 exons. The coding region is 4473 bp long and codes for protein product of 1490 a.a. A total of 386 *Triticum* accessions were screened for presence of *Tsn1* and evaluation showed that *Tsn1* is present among B genome-containing tetraploid and hexaploid wheat species. Since, *Aegilops speltoides* (SS genome) is considered as the most closely related species of the B-genome progenitor and phylogenetic analysis also showed that *Tsn1* alleles of two *Ae. speltoides* were more divergent than *Triticum* accessions, it was concluded that *Tsn1* possibly originated in *Ae. speltoides* through gene-fusion event (Faris et al. 2010). Both Faris et al. (2010) and Manning and Ciuffetti (2005) has shown that *Tsn1* is not the receptor for ToxA but might be the one that monitors the receptor.

The SnToxA-*Tsn1* interaction was shown to be light dependent, cause disruption of host photosynthesis, and account for up to 95% of the disease variation (Faris and Friesen 2009). *Tsn1* contains S/T and NBS-LRR domains that are closely related to those of resistance genes. *Tsn1* has similarity to the barley stem rust *R* gene *Rpg1* (Brueggeman et al. 2002) and maize rust *R* gene *Rp3* (Webb et al. 2002; Faris et al. 2010), respectively. This further explains the ability of necrotrophic effectors to subvert ETI resistance mechanism to cause cell death in host.

2.7.2. SnTox1-*Snn1*

SnTox1-*Snn1* was the first inverse gene-for-gene interaction that was identified in the wheat-*P. nodorum* pathosystem (Liu et al. 2004a). SnTox1 is a protein that was partially purified from culture filtrate of isolate Sn2000 (Liu et al. 2004a). Heterologous expression of identified genes in *Pichia pastoris* and screening of differential lines narrowed down the search to single gene, SNOG_20078, in the annotated *P. nodorum* genome sequence. Infiltrations with culture filtrates containing SNOG_20078 produced necrosis on SnTox1-sensitive wheat lines, subsequently verifying SNOG_20078 as *SnTox1*. The SnTox1 protein contains 117 amino acids with a molecular weight of 10.3 kDA. The first 16 amino acids are predicted to be a signal peptide, and there are 16 cysteine residues in the mature protein (Liu et al. 2012). SnTox1 was found to be present in 85 % of the global collection of *P. nodorum* isolates and 11 protein isoforms were identified, suggesting strong diversifying selection presssure (Liu et al. 2012). Transcriptional analysis verified SnTox1 peak expression at 3DPI (Liu et al. 2012). Plant defense responses like oxidative burst, up-regulation of PR-genes, and DNA laddering were observed post SnTox1-*Snn1* interaction (Liu et al. 2012). Furthermore, Liu et al. (2012) observed that light was essential for penetration of pathogen inside the host cell apoplastic region.

The International Triticeae Mapping Initiative (ITMI) mapping population was used to map the corresponding dominant sensitivity gene *Snn1* to distal end of wheat chromosome arm 1BS (Liu et al. 2004a). Reddy et al. (2008) delineated *Snn1* to a 0.46 cM interval using wheat EST markers in high-resolution genetic map. Shi et al. (2016b) cloned *Snn1* using positional cloning and bioinformatic analysis of chromosome 1BS bacterial artificial chromosome (BAC)-based minimum tiling path (MTP) clones and validated by gene complementation experiments. *Snn1* was found to be member of the wall-associated kinase (WAK) class of plant receptor kinases. It is 3045 bp in length with three exons and coding sequence length of 2145 bp. Phylogenetic analysis revealed that *Snn1* belongs to a group of WAK genes that are specific to monocots. Mutations in the conserved domains including wall-associated receptor kinase galacturonan binding (GUB_WAK), epidermal growth factor-calcium binding (EGF_CA), and S/TPK domains resulted in loss of function and therefore, indicated their absolute requirement for recognition of SnTox1. Transcriptional analysis revealed that the gene was only expressed in leaves, and its expression levels decreased in the presence of light as was found with *Tsn1* (Faris et al. 2010). *Snn1* was also found to be down regulated upon its interaction with SnTox1 as opposed to expression pattern of SnTox1 in pathogen (Liu et al. 2012). Presence of functional *Snn1* alleles in cultivated emmer indicated its possible origin in the same and then was subsequently transferred to durum and bread wheat. Shi et al. (2016b) also studied induction of mitogen-activated protein kinase (*MAPK*) genes that are typically involved in PTI defense mechanisms. *TaMAPK3* was activated within 15 mins of disease inoculation and was up regulated for very short time as has been observed in PTI response (Tsuda et al. 2009). The Snn1 and SnTox1 proteins were shown to interact directly, indicating that Snn1 is the receptor for SnTox1 (Shi et al. 2016b).

2.7.3. SnTox2-*Snn2*

SnTox2 was the third necrotrophic effector that was partially purified and characterized after SnToxA and SnTox1. It was identified from culture filtrates of isolate Sn6 and its size was estimated to be between 3-10 kDA using ultra filtration (Friesen et al. 2007). The corresponding sensitivity gene *Snn2* was mapped on wheat chromosome arm 2DS using BR34 × Grandin (BG) RI population. The SnTox2-*Snn2* interaction was again found to be light dependent and explained up to 47% of the disease variation. The additive effects of *Snn2* and *Tsn1* sensitivity genes were identified in the same population by Friesen et al. (2007). Zhang et al. (2009) developed SSR and EST-STS based markers to saturate the 2D linkage map and delimited *Snn2* to a 4.0 cM interval by flanking markers *XTC253803* and *Xcfd51*.

2.7.4. SnTox3-*Snn3*

The SnTox3-*Snn3* is the fourth interaction to be identified in this pathosystem (Friesen et al. 2008). *SnTox3* was identified and cloned using purified active fractions (Liu et al. 2009) and is 693 bp with no introns. Similar to *ToxA*, *SnTox3* also encodes for pre-mature protein; and the size of the mature protein after cleavage of some amino acids residus from the N-terminal region is 17.88 kDA. Disease evaluation of the Br34 × Grandin (BG) population using multiple isolates suggested the role of epistatic and additive interactions amongst *P. nodorum* produced NEs. Friesen et al. (2008) showed that *Snn2* is epistatic to *Snn3,* and effects of *Snn3* are greatly minimized in the presence of *Snn2* and *Tsn1,* which is probably due to large additive effects of both NEs. The potential use of the same or different modes of action by NEs may act in epistatic or additive manners as proposed by Friesen et al. (2008). *SnTox3* was found to be absent in only 39.9% of 923 global field isolate samples. Winterberg et al. (2014) observed upregulation of PR

proteins, jasmonic acid pathway proteins and phenylpropanoid pathway proteins at 2 dpi followed by cell death at 3dpi.

SnTox3 is unique that it interacts with two homoeologous genes on wheat chromosomes 5B and 5D to cause disease and were designated as *Snn3-B1* and *Snn3-D1* (Zhang et al. 2011). Functional alleles of both genes were detected in diploid progenitors of wheat. Zhang et al. (2011) used an F_2 population derived from cross between LDN-TA2377 and BG220 that segregates for both SnTox3-*Snn3-B1* and SnTox3-*Snn3-D1* interactions. However, the SnTox3-*Snn3-D1* interaction showed much more severe necrosis and was epistatic to SnTox3-*Snn3-B1* (Zhang et al. 2011). The authors inferred the putative homoelogous relationship of *Snn3-B1* and *Snn3-D1* based on highly conserved marker order in both regions, and observation of functional alleles of both genes in the diploid progenitors (Zhang et al. 2011). A saturated genetic map of the *Snn3-D1* region was developed in *Aegilops tauschii* TA2377 × AL8/78 F_2 population with average density of one marker per 1.40 cM. High resolution mapping using 863 insensitive F_2 plants subsequently delineated *Snn3-D1* to 1.38 cM (Zhang et al. 2011). The SnTox3-*Snn3-B1* interaction accounted for 17% of disease variation in the BG population (Friesen et al. 2008). This interaction was first identified in RIL population derived from cross Br34 × Grandin and *Snn3-B1* was mapped 1.4 cM distal to *Xcfd20* on chromosome arm 5BS in RI lines (Friesen et al. 2008). Saturation mapping was done by Shi et al. (2016a) using two F_2 populations which were developed by crossing Sumai3 (sensitive to SnTox3) × BR34 (insensitive to SnTox3) (BS population) and Sumai3 × Chinese Spring-*T. turgidum* ssp. *dicoccoides* chromosome 5B disomic substitution line (CS-DIC 5B) (insensitive to SnTox3) (CS population). High resolution mapping was performed using the BS population due to 3-fold higher recombination rate than the CS population, and *Snn3-B1* was delimited to 1.5 cM interval flanked by markers *Xfcp654* and

Xfcp652 (Shi et al. 2016a). Mutant analysis identified 13 SnTox3-insensitive mutants with probable mutation in either *Snn3-B1* itself or other genes in the pathway required for compatible SnTox3- *Snn3-B1* interaction (Shi et al. 2016a). This work provided a basis for map-based cloning of both possible homoeologous genes. *Snn3-D1* is currently at gene complementation step to validate the identified gene as *Snn3-D1* (Faris et al. unpublished).

2.7.5. SnTox4-*Snn4*

Abeysekara et al. (2009) described the fifth wheat-*P. nodorum* interaction, which was designated as SnTox4-*Snn4*. SnTox4 was partially purified from the Swiss isolate Sn99CH1A7a and, like previously characterized *P. nodorum* NEs, it was also a protein of size between 10-30 kDA that required light to cause susceptibility in sensitive wheat lines. SnTox4 caused a less severe mottled necrotic reaction and accounted for as much as 41% of disease variation. The corresponding sensitivity gene, *Snn4,* was mapped on wheat chromosome arm 1AS using the Arina × Forno RI population developed by Paillard et al. (2003). *Snn4* was delineated to 2.5 cM interval flanked by *Xcfd58.1* on the proximal side and EST markers *XBG262267*/*XBG262975* on the distal side (Abeysekara et al. 2009).

2.7.6. SnTox5-*Snn5*

SnTox5-*Snn5* was the sixth necrotrophic effector-host gene interaction that was identified in wheat (Friesen et al. 2012). Culture filtrate of the Sn2000 fungal isolate was found to produce an NE other than SnToxA and was named as SnTox5. Infiltration of a tetraploid population derived from Lebsock (North Dakota durum variety) × *T. turgidum* ssp. *carthlicum* accession PI 94749 (LP749 population) (Chu et al. 2010) with Sn2000 culture filtrates led to the identification of two host sensitivity genes on chromosomes 5B and 4B. The 5B QTL corresponded to the *Tsn1* gene. No host sensitivity gene was previously reported on 4B, and therefore the sensitivity locus

on 4B was designated as *Snn5* (Friesen et al. 2012). When culture filtrate of the SnToxA-knockout isolate Sn2000K06-1 was used to infiltrate the same population, a 1 sensitive: 1 insensitive segregation ratio was observed indicating the role of single gene that was *Snn5*. Ultrafiltration experiments estimated the size of SnTox5 to be between 10-30 kDA. Like previously known NEs, SnTox5 is also a protein that requires light to interact with the corresponding sensitivity gene in the host. When the LP749 population was infiltrated with another *P. nodorum* isolate, Sn1501, which contains SnTox3 and SnTox5, it was found that a compatible SnTox5-*Snn5* interaction was epistatic to SnTox3-*Snn3*. The SnTox5-*Snn5* interaction explained up to 63% of the disease variation when no other interactions were segregating in the population.

2.7.7. SnTox6-*Snn6*

Culture filtrate of the *P. nodorum* isolate Sn6 was found to produce novel NE designated SnTox6, which was about 12 kDA in size (REF). The corresponding sensitivity gene, *Snn6,* was mapped on wheat chromosome arm 6AL using the ITMI population. *Snn6* was delineated to a 3.2 cM interval flanked by markers *XBE424987* and *XBE403326*. Again, SnTox6-*Snn6* was shown to be light dependent, and it explained 27% of the disease variation in the ITMI population.

2.7.8. SnTox7-*Snn7*

Shi et al. (2015) identified the ninth *P. nodorum*-NE interaction and designated it as SnTox7-*Snn7*. SnTox7 was identified in culture filtrates of *P. nodorum* isolate Sn6, and it was found to be a small protein of size less than 30 kDA. Light sensitive experiments showed that, unlike previously characterized interactions with exception of SnTox3-*Snn3*, this interaction was not completely light-dependent. It caused necrosis in sensitive wheat lines and explained as

much as 33% of the disease variation. The corresponding sensitivity gene was identified in the wheat cultivar Timstein and mapped to long arm of wheat chromosome 2D. It was delineated to a 2.7 cM interval and *Xcfd44* was found to co-segregate with *Snn7*. Shi et al. (2015) also showed that *Snn7* is relatively rare as compared to other sensitivity genes in wheat cultivars.

2.8. References

Abeysekara NS, Faris JD, Chao S, et al (2012) Whole-genome QTL analysis of *Stagonospora nodorum* blotch resistance and validation of the SnTox4-*Snn4* interaction in hexaploid wheat. Phytopathology 102:94–104. doi: 10.1094/PHYTO-02-11-0040

Abeysekara NS, Friesen TL, Keller B, Faris JD (2009) Identification and characterization of a novel host-toxin interaction in the wheat-*Stagonospora nodorum* pathosystem. Theor Appl Genet 120:117–126. doi: 10.1007/s00122-009-1163-6

Abramovitch RB, Kim YJ, Chen S, et al (2003) *Pseudomonas* type III effector AvrPtoB induces plant disease susceptibility by inhibition of host programmed cell death. EMBO J 22:60–69. doi: 10.1093/emboj/cdg006

Akeda Y, Galán JE (2005) Chaperone release and unfolding of substrates in type III secretion. Nature 437:911–915. doi: 10.1038/nature03992

Avni R, Nave M, Barad O, et al (2017) Wild emmer genome architecture and diversity elucidate wheat evolution and domestication. Science 357:93–97. doi: 10.1126/science.aan0032

Goodwin BS, Zismann VL (2001) Phylogenetic Analyses of the ITS region of ribosomal DNA reveal that *Septoria passerinii* from barley is closely related to the wheat pathogen *Mycosphaerella graminicola*. Mycologia 93:934-946. doi: 10.2307/3761758

Ballance GM, Lamari L, Bernier CC (1989) Purification and characterization of a host-selective necrosis toxin from *Pyrenophora tritici-repentis*. Physiol and Mol Plant Pathol 35:203–213. doi: 10.1016/0885-5765(89)90051-9

Ballance GM, Lamari L, Kowatsch R, Bernier CC (1996) Cloning, expression and occurrence of the gene encoding the *Ptr* necrosis toxin from *Pyrenophora tritici-repentis*. Mol Plant Pathol On-line

Bertsch F (1943) Der Dinkel. Landw Jahrbuch 92:241-252

Berkman PJ, Visendi P, Lee HC, et al (2013) Dispersion and domestication shaped the genome of bread wheat. Plant Biotechnol J 11:564–571. doi: 10.1111/pbi.12044

Bhathal JS, Loughman R, Speijers J (2003) Yield reduction in wheat in relation to leaf disease from yellow (tan) spot and *Septoria nodorum* blotch. Eur J Plant Pathol 109:435–443. doi: 10.1023/A:1024277420773

Blatter RHE, Jacomet S, Schlumbaum A (2004) About the origin of European spelt (*Triticum spelta* L.): allelic differentiation of the HMW Glutenin B1-1 and A1-2 subunit genes. Theor Appl Genet 108:360–367. doi: 10.1007/s00122-003-1441-7

Blatter RHE, Jacomet S, Schlumbaum A (2002) Spelt-specific alleles in HMW glutenin genes from modern and historical European spelt (*Triticum spelta* L.). Theor Appl Genet 104:329–337. doi: 10.1007/s001220100680

Bolton MD, Thomma BPHJ, Nelson BD (2006) *Sclerotinia sclerotiorum* (Lib.) de Bary: biology and molecular traits of a cosmopolitan pathogen. Mol Plant Pathol 7:1–16. doi: 10.1111/j.1364-3703.2005.00316.x

Borrill P, Harrington SA, Uauy C (2019) Applying the latest advances in genomics and phenomics for trait discovery in polyploid wheat. Plant J 97:56–72. doi: 10.1111/tpj.14150

Brueggeman R, Rostoks N, Kudrna D, et al (2002) The barley stem rust-resistance gene *Rpg1* is a novel disease-resistance gene with homology to receptor kinases. PNAS 99:9328–9333. doi: 10.1073/pnas.142284999

Whisson CS, Boevink CP, Moleleki L, et al (2007) A translocation signal for delivery of oomycete effector proteins into host plant cells. Nature 450:115–118. doi: 10.1038/nature06203

Chen QF, Yen C, Yang JL (1998) Chromosome location of the gene for brittle rachis in the Tibetan weedrace of common wheat. Genet Resour Crop Ev 45:407–410. doi: 10.1023/A:1008635208146

Chisholm ST, Coaker G, Day B, et al (2006) Host-microbe interactions: shaping the evolution of the plant immune response. Cell 124:803–814. doi: 10.1016/j.cell.2006.02.008

Chu CG, Chao S, Friesen TL, et al (2010) Identification of novel tan spot resistance QTLs using an SSR-based linkage map of tetraploid wheat. Mol Breeding 25:327–338. doi: 10.1007/s11032-009-9335-2

Ciuffetti LM, Tuori RP, Gaventa JM (1997) A single gene encodes a selective toxin causal to the development of tan spot of wheat. Plant Cell 9:135–144. doi: 10.1105/tpc.9.2.135

Coaker G, Falick A, Staskawicz B (2005) Activation of a phytopathogenic bacterial effector protein by a eukaryotic cyclophilin. Science 308:548–550. doi: 10.1126/science.1108633

Debernardi JM, Lin H, Chuck G, et al (2017) microRNA172 plays a critical role in wheat spike morphology and grain threshability. Development 144:1966-1975. doi: 10.1242/dev.146399

Doehlemann G, Linde K van der, Aßmann D, et al (2009) Pep1, a secreted effector protein of *Ustilago maydis*, is required for successful invasion of plant cells. PLoS Pathog. 5(2):e1000290. doi: 10.1371/journal.ppat.1000290

Dvorak J, Akhunov ED, Akhunov AR, et al (2006) Molecular characterization of a diagnostic DNA marker for domesticated tetraploid wheat provides evidence for gene flow from wild tetraploid wheat to hexaploid wheat. Mol Biol Evol 23:1386–1396. doi: 10.1093/molbev/msl004

Dvorak J, Deal KR, Luo MC, et al (2012) The origin of spelt and free-threshing hexaploid wheat. J Hered 103:426–441. doi: 10.1093/jhered/esr152

Endo TR, Gill BS (1996) The deletion stocks of common wheat. J Hered 87:295–307. doi: 10.1093/oxfordjournals.jhered.a023003

Eyal Z, Scharen AL, Prescott JM, et al (1987) The *septoria* diseases of wheat: concepts and methods of disease management. CIMMYT

Faris J, Anderson JA, Francl L, Jordahl J (1996) Chromosomal location of a gene conditioning insensitivity in wheat to a necrosis-inducing culture filtrate from *Pyrenophora tritici-repentis*. Phytopathology 86:459–463. doi: 10.1094/Phyto-86-459

Faris JD (2014) Wheat Domestication: Key to Agricultural Revolutions Past and Future. In: Tuberosa R, Graner A, Frison E (eds) Genomics of Plant Genetic Resources: Volume 1. Managing, sequencing and mining genetic resources. Springer Netherlands, Dordrecht, pp 439–464

Faris JD, Fellers JP, Brooks SA, et al (2003) A bacterial artificial chromosome contig spanning the major domestication locus *Q* in wheat and identification of a candidate gene. Genetics 164:311–321

Faris JD, Friesen TL (2009) Reevaluation of a tetraploid wheat population indicates that the *Tsn1*-ToxA interaction is the only factor governing *Stagonospora nodorum* blotch susceptibility. Phytopathology 99:906–912. doi: 10.1094/PHYTO-99-8-0906

Faris JD, Gill BS (2002) Genomic targeting and high-resolution mapping of the domestication gene *Q* in wheat. Genome 45:706–718

Faris JD, Zhang Q, Chao S, et al (2014a) Analysis of agronomic and domestication traits in a durum × cultivated emmer wheat population using a high-density single nucleotide polymorphism-based linkage map. Theor Appl Genet 127:2333–2348. doi: 10.1007/s00122-014-2380-1

Faris JD, Zhang Z, Chao S (2014b) Map-based analysis of the tenacious glume gene *Tg-B1* of wild emmer and its role in wheat domestication. Gene 542:198–208. doi: 10.1016/j.gene.2014.03.034

Faris JD, Zhang Z, Lu H, et al (2010) A unique wheat disease resistance-like gene governs effector-triggered susceptibility to necrotrophic pathogens. Proc Natl Acad Sci USA 107:13544–13549. doi: 10.1073/pnas.1004090107

Faris JD, Zhang Z, Rasmussen JB, et al (2011) Variable expression of the *Stagonospora nodorum* effector SnToxA among isolates is correlated with levels of disease in wheat. Mol Plant Microbe Interact 24:1419–1426. doi: 10.1094/MPMI-04-11-0094

Ficke A, Cowger C, Bergstrom G, et al (2018) Understanding yield loss and pathogen biology to improve disease management: *Septoria Nodorum* Blotch - A case study in wheat. Plant Dis. 102:696–707. doi: 10.1094/PDIS-09-17-1375-FE

Figueroa M, Hammond-Kosack KE, Solomon PS (2018) A review of wheat diseases- a field perspective. Mol Plant Pathol 19:1523–1536. doi: 10.1111/mpp.12618

Fitt BDL, McCartney HA, Walklate PJ (1989) The role of rain in dispersal of pathogen inoculum. Annu Rev Phytopathol 27:241–270. doi: 10.1146/annurev.py.27.090189.001325

Flor HH (1956) The complementary genetics systems in flax and flax rust. Adv. Genet. 8:29-54

Friesen TL, Chu C, Xu SS, et al (2012) SnTox5-*Snn5*: a novel *Stagonospora nodorum* effector-wheat gene interaction and its relationship with the SnToxA-*Tsn1* and SnTox3-*Snn3-B1* interactions. Mol Plant Pathol 13:1101–1109. doi: 10.1111/j.1364-3703.2012.00819.x

Friesen TL, Chu CG, Liu ZH, et al (2009) Host-selective toxins produced by *Stagonospora nodorum* confer disease susceptibility in adult wheat plants under field conditions. Theor Appl Genet 118:1489–1497. doi: 10.1007/s00122-009-0997-2

Friesen TL, Faris JD (2010) Characterization of the wheat-*Stagonospora nodorum* disease system: what is the molecular basis of this quantitative necrotrophic disease interaction?. Can J Plant Pathol 32:20–28. doi: 10.1080/07060661003620896

Friesen TL, Meinhardt SW, Faris JD (2007) The *Stagonospora nodorum*-wheat pathosystem involves multiple proteinaceous host-selective toxins and corresponding host sensitivity genes that interact in an inverse gene-for-gene manner. Plant J 51:681–692. doi: 10.1111/j.1365-313X.2007.03166.x

Friesen TL, Stukenbrock EH, Liu Z, et al (2006) Emergence of a new disease as a result of interspecific virulence gene transfer. Nature Genetics 38:953–956. doi: 10.1038/ng1839

Friesen TL, Zhang Z, Solomon PS, et al (2008) Characterization of the interaction of a novel *Stagonospora nodorum* host-selective toxin with a wheat susceptibility gene. Plant Physiol 146:682–693. doi: 10.1104/pp.107.108761

Fujikawa T, Sakaguchi A, Nishizawa Y, et al (2012) Surface α-1,3-glucan facilitates fungal stealth infection by interfering with innate immunity in plants. PLoS Pathog 8(8):e1002882. doi: 10.1371/journal.ppat.1002882

Gao Y, Faris JD, Liu Z, et al (2015) Identification and characterization of the SnTox6-*Snn6* interaction in the *Parastagonospora nodorum*-wheat pathosystem. Mol Plant Microbe Interact 28:615–625. doi: 10.1094/MPMI-12-14-0396-R

Gill BS, Li W, Sood S, et al (2007) Genetics and genomics of wheat domestication-driven evolution. Isr J Plant Sci 55:223–229. doi: 10.1560/IJPS.55.3-4.223

Glazebrook J (2005) Contrasting mechanisms of defense against biotrophic and necrotrophic pathogens. Annu Rev Phytopathol 43:205–227. doi: 10.1146/annurev.phyto.43.040204.135923

Gómez-Gómez L, Boller T (2000) *FLS2*: an LRR receptor-like kinase involved in the perception of the bacterial elicitor flagellin in *Arabidopsis*. Mol Cell 5:1003–1011.

Greenwood JR, Finnegan EJ, Watanabe N, et al (2017) New alleles of the wheat domestication gene *Q* reveal multiple roles in growth and reproductive development. Development 144:1959–1965. doi: 10.1242/dev.146407

Hane JK, Lowe RGT, Solomon PS, et al (2007) Dothideomycete–plant interactions illuminated by genome sequencing and EST analysis of the wheat pathogen *Stagonospora nodorum*. Plant Cell 19:3347–3368. doi: 10.1105/tpc.107.052829

Hemetsberger C, Herrberger C, Zechmann B, et al (2012) The *Ustilago maydis* effector Pep1 suppresses plant immunity by inhibition of host peroxidase activity. PLoS Pathog 8(5):e1002684. doi: 10.1371/journal.ppat.1002684

Huang S, Sirikhachornkit A, Su X, et al (2002) Genes encoding plastid acetyl-CoA carboxylase and 3-phosphoglycerate kinase of the *Triticum*/*Aegilops* complex and the evolutionary history of polyploid wheat. PNAS 99:8133–8138. doi: 10.1073/pnas.072223799

International Wheat Genome Sequencing Consortium (IWGSC) (2014) A chromosome-based draft sequence of the hexaploid bread wheat (*Triticum aestivum*) genome. Science 345(6194):1251788. doi: 10.1126/science.1251788

Jantasuriyarat C, Vales MI, Watson CJW, et al (2004) Identification and mapping of genetic loci affecting the free-threshing habit and spike compactness in wheat (*Triticum aestivum* L.). Theor Appl Genet 108:261–273. doi: 10.1007/s00122-003-1432-8

Jones JDG, Dangl JL (2006) The plant immune system. Nature 444:323–329. doi: 10.1038/nature05286

Jones DA, Thomas CM, Hammond-Kosack KE, et al (1994) Isolation of the tomato *Cf-9* gene for resistance to *Cladosporium fulvum* by transposon tagging. Science 266:789–793

Karjalainen R, Laitinen A, Juuti T (1983) Effects of *Septoria nodorum* Berk. on yield and yield components of spring wheat. Agr Food Sci 55:333–344. doi: 10.23986/afsci.72133

Kato K, Miura H, Sawada S (1999) QTL mapping of genes controlling ear emergence time and plant height on chromosome 5A of wheat. Theor Appl Genet 98:472–477. doi: 10.1007/s001220051094

Kato K, Sonokawa R, Miura H, et al (2003) Dwarfing effect associated with the threshability gene *Q* on wheat chromosome 5A. Plant Breeding 122:489–492. doi: 10.1111/j.1439-0523.2003.00886.x

Kerber ER, Dyck PL (1969) Inheritance in hexaploid wheat of leaf rust resistance and other characters derived from *Aegilops squarrosa*. Can J Genet Cytol 11:639–647. doi: 10.1139/g69-076

Kerber ER, Rowland GG (1974) Origin of the free threshing character in hexaploid wheat. Can J Genet Cytol 16:145–154. doi: 10.1139/g74-014

Kihara H (1944) Discovery of the DD-analyser, one of the ancestors of *Triticum vulgare* (abstr). Agric Hortic 19:889–890

Kimber G, Sears ER (1987) Evolution in the Genus *Triticum* and the Origin of Cultivated Wheat. In: Heyne EG (ed) Wheat and wheat improvement. 2nd edition. American Society of Agronomy, Madison, pp 154–164 doi: 10.2134/agronmonogr13.2ed.c6

Kobe B, Deisenhofer J (1994) The leucine-rich repeat: a versatile binding motif. Trends Biochem Sci 19:415–421

Krasileva KV, Vasquez-Gross HA, Howell T, et al (2017) Uncovering hidden variation in polyploid wheat. Proc Natl Acad Sci USA 114:E913–E921. doi: 10.1073/pnas.1619268114

Kuckuck H (1959) Neuere Arbeiten zur Entstehung der hexaploiden Kulturweizen. Z. Pflanzenzücht 41:205-226

Li W, Gill BS (2006) Multiple genetic pathways for seed shattering in the grasses. Funct Integr Genomics 6:300–309. doi: 10.1007/s10142-005-0015-y

Liu Z, Faris JD, Oliver RP, et al (2009) SnTox3 acts in effector triggered susceptibility to induce disease on wheat carrying the *Snn3* gene. PLoS Pathogens 5(9):e1000581. doi: 10.1371/journal.ppat.1000581

Liu Z, Friesen TL, Ling H, et al (2006) The *Tsn1*-ToxA interaction in the wheat-*Stagonospora nodorum* pathosystem parallels that of the wheat-tan spot system. Genome 49:1265–1273. doi: 10.1139/g06-088

Liu Z, Zhang Z, Faris JD, et al (2012) The cysteine rich necrotrophic effector SnTox1 produced by *Stagonospora nodorum* triggers susceptibility of wheat lines harboring *Snn1*. PLoS Pathogens 8(1):e1002467. doi: 10.1371/journal.ppat.1002467

Liu ZH, Faris JD, Meinhardt SW, et al (2004a) Genetic and physical mapping of a gene conditioning sensitivity in wheat to a partially purified host-selective toxin produced by *Stagonospora nodorum*. Phytopatholgy 94:1056–1060. doi: 10.1094/PHYTO.2004.94.10.1056

Liu ZH, Friesen TL, Rasmussen JB, et al (2004b) Quantitative Trait Loci analysis and mapping of seedling resistance to *Stagonospora nodorum* leaf blotch in wheat. Phytopathology 94:1061–1067. doi: 10.1094/PHYTO.2004.94.10.1061

Lombard V, Golaconda Ramulu H, Drula E, et al (2014) The carbohydrate-active enzymes database (CAZy) in 2013. Nucleic Acids Res 42:D490–D495. doi: 10.1093/nar/gkt1178

Lorang JM, Sweat TA, Wolpert TJ (2007) Plant disease susceptibility conferred by a "resistance" gene. PNAS 104:14861–14866. doi: 10.1073/pnas.0702572104

Luo MC, Yang ZL, You FM, et al (2007) The structure of wild and domesticated emmer wheat populations, gene flow between them, and the site of emmer domestication. Theor Appl Genet 114:947–959. doi: 10.1007/s00122-006-0474-0

MacKey J (1966) Species relationship in *Triticum*. Hereditas Supplement 2:237–276

MacKey J (1954) Neutron and x-ray Experiments in wheat and a revision of the speltoid problem. Hereditas 40:65–180

Manning VA, Ciuffetti LM (2005) Localization of Ptr ToxA produced by *Pyrenophora tritici-repentis* reveals protein import into wheat mesophyll cells. Plant Cell 17:3203–3212. doi: 10.1105/tpc.105.035063

Matsuoka Y, Nasuda S (2004) Durum wheat as a candidate for the unknown female progenitor of bread wheat: an empirical study with a highly fertile F1 hybrid with *Aegilops tauschii* Coss. Theor Appl Genet 109:1710–1717. doi: 10.1007/s00122-004-1806-6

McDonald MC, Ahren D, Simpfendorfer S, et al (2018) The discovery of the virulence gene ToxA in the wheat and barley pathogen *Bipolaris sorokiniana*. Mol Plant Pathol 19:432–439. doi: 10.1111/mpp.12535

McDonald MC, Solomon PS (2018) Just the surface: advances in the discovery and characterization of necrotrophic wheat effectors. Curr Opin Microbiol 46:14–18. doi: 10.1016/j.mib.2018.01.019

Mcfadden ES, Sears ER (1946) The origin of *Triticum spelta* and its free-threshing hexaploid relatives. J Hered 37:81–89. doi: 10.1093/oxfordjournals.jhered.a105590

Mcmullen M, Adhikari T (2009) Fungal leaf spot diseases of wheat: Tan Spot, *Stagonospora nodorum* blotch and *Septoria tritici* blotch. NDSU Extension Service, Fargo 1-6.

Mendgen K, Hahn M (2002) Plant infection and the establishment of fungal biotrophy. Trends Plant Sci 7:352–356

Meehan F, Murphy HC (1947) Differential Phytotoxicity of Metabolic By-Products of *Helminthosporium victoriae*. Science 106:270–271. doi: 10.1126/science.106.2751.270-a

Miller TE, Reader SM (1982) A major deletion of part of chromosome 5A of *Triticum aestivum*. Wheat Inf Serv 88: 10-12.

Mori N, Ohta S, Chiba H, et al (2013) Rediscovery of Indian dwarf wheat (*Triticum aestivum* L. ssp. *sphaerococcum* (Perc.) MK.) an ancient crop of the Indian subcontinent. Genet Resour Crop Evol 60:1771–1775. doi: 10.1007/s10722-013-9994-z

Muramatsu M (1963) Dosage effect of the spelta gene *Q* of hexaploid wheat. Genetics 48:469–482

Muramatsu M (1979) Presence of vulgare gene, *Q* in a dense-spike variety of *Triticum dicoccum* Schubl. Rep Plant Germplasm Inst Kyoto Univ 4:39–41

Muramatsu M (1986) The vulgare super gene, *Q*: its universality in durum wheat and its phenotypic effects in tetraploid and hexaploid wheats. Can J Genet Cytol 28:30–41. doi: 10.1139/g86-006

Nalam VJ, Vales MI, Watson CJW, et al (2007) Map-based analysis of genetic loci on chromosome 2D that affect glume tenacity and threshability, components of the free-threshing habit in common wheat (*Triticum aestivum* L.). Theor Appl Genet 116:135–145. doi: 10.1007/s00122-007-0653-7

Nesbitt M, Samuel D (1996) From staple crop to extinction? The archaeology and history of the hulled wheats. In: Proceedings of the First International Workshop on Hulled Wheats: 21-22 July 1995; Castelvecchio Pascoli, Tuscany, Italy. pp 41–100

Nilsson-Ehle H (1920) Multiple Allelomorphe Und Komplexmutationen Beim Weizen. Hereditas 1:277–311. doi: 10.1111/j.1601-5223.1920.tb02463.x

Nilsson-Ehle H (1917) Untersuchungen uber speltoid mutationen beim weizen. Botan Notiser 305–329

Nürnberger T, Brunner F, Kemmerling B, et al (2004) Innate immunity in plants and animals: striking similarities and obvious differences. Immunol Rev 198:249–266

Ogihara Y, Hasegawa K, Tsujimoto H (1994) High-resolution cytological mapping of the long arm of chromosome 5A in common wheat using a series of deletion lines induced by gametocidal (Gc) genes of *Aegilops speltoides*. Molec Gen Genet 244:253–259. doi: 10.1007/BF00285452

Oliver RP, Friesen TL, Faris JD, et al (2012) *Stagonospora nodorum*: from pathology to genomics and host resistance. Annu Rev Phytopathol 50:23–43. doi: 10.1146/annurev-phyto-081211-173019

Paillard S, Schnurbusch T, Winzeler M, et al (2003) An integrative genetic linkage map of winter wheat (*Triticum aestivum* L.). Theor Appl Genet 107:1235–1242. doi: 10.1007/s00122-003-1361-6

Percival J (1921) The wheat plant; a monograph. Duckworth, London.

Quaedvlieg W, Verkley GJM, Shin HD, et al (2013) Sizing up *Septoria*. Stud Mycol 75:307–390. doi: 10.3114/sim0017

Rafiqi M, Ellis JG, Ludowici VA, et al (2012) Challenges and progress towards understanding the role of effectors in plant–fungal interactions. Curr Opin Plant Biol 15:477–482. doi: 10.1016/j.pbi.2012.05.003

Rafiqi M, Gan PHP, Ravensdale M, et al (2010) Internalization of flax rust avirulence proteins into flax and tobacco cells can occur in the absence of the pathogen. Plant Cell 22:2017–2032. doi: 10.1105/tpc.109.072983

Rafiqi M, Ellis JG, Ludowici VA, et al (2012) Challenges and progress towards understanding the role of effectors in plant–fungal interactions. Curr Opin Plant Biol 15:477–482. doi: 10.1016/j.pbi.2012.05.003

Rapilly F, Foucault B, Lacazedieux J (1973) Studies on the inoculum of *Septoria nodorum* Berk. (*Leptosphaeria nodorum* Muller) agent of glume blotch of wheat. I. Ascospores. In: Annales de Phytopathologie. https://eurekamag.com/research/000/207/000207570.php.

Reddy L, Friesen T, Meinhardt S, et al (2008) Genomic Analysis of the *Snn1* locus on wheat chromosome arm 1BS and the identification of candidate genes. Plant Genome Journal 1(1):55-66. doi: 10.3835/plantgenome2008.03.0181

Rodriguez-Moreno L, Ebert M, Bolton M, et al (2017) Tools of the crook: Infection strategies of fungal plant pathogens. Plant J 93(4):664-674. doi: 10.1111/tpj.13810

Endo T, Mukai Y (1988) Chromosome mapping of a speltoid suppression gene of *Triticum aestivum* L. based on partial deletions in the long arm of chromosome SA. Jpn J Genet 63:501–505. doi: 10.1266/jjg.63.501

Sarma GN, Manning VA, Ciuffetti LM, et al (2005) Structure of *Ptr* ToxA: an RGD-containing host-selective toxin from *Pyrenophora tritici-repentis*. Plant Cell 17:3190–3202. doi: 10.1105/tpc.105.034918

Sarris PF, Cevik V, Dagdas G, et al (2016) Comparative analysis of plant immune receptor architectures uncovers host proteins likely targeted by pathogens. BMC Biology 14:8. doi: 10.1186/s12915-016-0228-7

Sax K (1922) Sterility in wheat hybrids. II. Chromosome behavior in partially sterile hybrids. Genetics 7:513–552

Scharen AL (1964) Environmental influences on development of glume blotch in wheat. Phytopathology 54:300-303

Scharen AL (1966) Cyclic production of pycnidia and spores in dead wheat tissue by *Septoria nodorum*. Phytopathology 56(5):580-581

Scheffer RP, Livingston RS (1984) Host-selective toxins and their role in plant diseases. Science 223:17–21. doi: 10.1126/science.223.4631.17

Shi G, Friesen T, Saini J, et al (2015) The Wheat Gene *Snn7* Confers Susceptibility on Recognition of the Necrotrophic Effector SnTox7. Plant Genome 8(2):1-10. doi: 10.3835/plantgenome2015.02.0007

Shi G, Zhang Z, Friesen TL, et al (2016a) Marker development, saturation mapping, and high-resolution mapping of the *Septoria nodorum* blotch susceptibility gene *Snn3-B1* in wheat. Mol Genet Genomics 291:107–119. doi: 10.1007/s00438-015-1091-x

Shi G, Zhang Z, Friesen TL, et al (2016b) The hijacking of a receptor kinase–driven pathway by a wheat fungal pathogen leads to disease. Science Advances 2(10):e1600822. doi: 10.1126/sciadv.1600822

Simonetti MC, Bellomo MP, Laghetti G, et al (1999) Quantitative trait loci influencing free-threshing habit in tetraploid wheats. Genet Resour Crop Ev 46:267–271. doi: 10.1023/A:1008602009133

Simons KJ, Fellers JP, Trick HN, et al (2006) Molecular characterization of the major wheat domestication gene *Q*. Genetics 172:547–555. doi: 10.1534/genetics.105.044727

Sinapidou E, Williams K, Nott L, et al (2004) Two TIR:NB:LRR genes are required to specify resistance to Peronospora parasitica isolate Cala2 in Arabidopsis. Plant J 38:898–909. doi: 10.1111/j.1365-313X.2004.02099.x

Singh HB, Anderson E, Pal BP (1957) Studies in the genetics of *Triticum vavilovi* Jakub. Agron J 49:4–11. doi: 10.2134/agronj1957.00021962004900010002x

Singh MP (1969) Some Radiation Induced Changes at '*Q*' Locus in Bread Wheat. Caryologia 22:119–126. doi: 10.1080/00087114.1969.10796330

Solomon PS, Waters ODC, Jörgens CI, et al (2006) Mannitol is required for asexual sporulation in the wheat pathogen *Stagonospora nodorum* (glume blotch). Biochem J 399:231–239. doi: 10.1042/BJ20060891

Sood S, Kuraparthy V, Bai G, et al (2009) The major threshability genes soft glume (*sog*) and tenacious glume (*Tg*), of diploid and polyploid wheat, trace their origin to independent mutations at non-orthologous loci. Theor Appl Genet 119:341–351. doi: 10.1007/s00122-009-1043-0

Swaminathan MS (1963) Induced mutations at the *Q* locus in relation to the phylogeny of hexaploid *Triticum* species. Proc XI Int Cong Genet The Hague. https://eurekamag.com/research/014/077/014077778.php

Tameling WIL, Elzinga SDJ, Darmin PS, et al (2002) The tomato R gene products I-2 and MI-1 are functional ATP binding proteins with ATPase activity. Plant Cell 14:2929–2939

Thomma BP, Eggermont K, Penninckx IA, et al (1998) Separate jasmonate-dependent and salicylate-dependent defense-response pathways in Arabidopsis are essential for resistance to distinct microbial pathogens. PNAS USA 95:15107–15111

Thomma BP, Penninckx IA, Cammue BP, et al (2001) The complexity of disease signaling in *Arabidopsis*. Curr Opin Immunol 13:63–68. doi: 10.1016/S0952-7915(00)00183-7

Tomás A and Bockus W (1987) Cultivar-specific toxicity of culture filtrates of *Pyrenophora tritici-repentis*. Phytopathology 77:1337-1340

Tsuda K, Katagiri F (2010) Comparing signaling mechanisms engaged in pattern-triggered and effector-triggered immunity. Curr Opin Plant Biol 13:459–465. doi: 10.1016/j.pbi.2010.04.006

Tsuda K, Sato M, Stoddard T, et al (2009) Network properties of robust immunity in plants. PLoS Genetics 5:e1000772. doi: 10.1371/journal.pgen.1000772

Tsujimoto H, Noda K (1990) Deletion mapping by gametocidal genes in common wheat: position of speltoid suppression (*Q*) and β-amylase (*β-Amy-A2*) genes on chromosome 5A. Genome 33:850–853. doi: 10.1139/g90-128

Tsujimoto H, Noda K (1989) Structure of chromosome 5A of wheat speltoid mutants induced by the gametocidal genes of *Aegilops speltoides*. Genome 32:1085–1090. doi: 10.1139/g89-558

Underhill DM, Ozinsky A (2002) Toll-like receptors: key mediators of microbe detection. Curr Opin Immunol 14:103–110

Verreet JA, Hoffmann GM, Amberger A (1987) Auswirkungen der Infektion durch Septoria nodorum in verschiedenen Entwicklungsstadien des Weizens auf die Produktionsleistung. Z. Pflanzenkr. Pflanzeschultz 94:283-300

Watanabe N, Ikebata N (2000) The effects of homoeologous group 3 chromosomes on grain colour dependent seed dormancy and brittle rachis in tetraploid wheat. Euphytica 115:215–220. doi: 10.1023/A:1004066416900

Watanabe N, Sugiyama K, Yamagishi Y, et al (2002) Comparative telosomic mapping of homoeologous genes for brittle rachis in tetraploid and hexaploid wheats. Hereditas 137:180–185. doi: 10.1034/j.1601-5223.2002.01609.x

Webb CA, Richter TE, Collins NC, et al (2002) Genetic and Molecular Characterization of the Maize *rp3* Rust Resistance Locus. Genetics 162:381–394

Weber GF (1922) *Septoria* diseases of cereals. Phytopathology 12:537-285

Welsh JN, Peturson B, Machacek JE (1954) Associated inheritance of reaction to races of crown rust, *Puccinia coronate avenae* Erikss., and to Victoria blight, *Helminthosporium victoriae* M. and N., in oats. Can J. Botany 32:55-68

Winterberg B, Du Fall LA, Song X, et al (2014) The necrotrophic effector protein SnTox3 re-programs metabolism and elicits a strong defence response in susceptible wheat leaves. BMC Plant Biology 14:215. doi: 10.1186/s12870-014-0215-5

Wolpert TJ, Dunkle LD, Ciuffetti LM (2002) Host-selective toxins and avirulence determinants: what's in a name? Annu Rev Phytopathol 40:251–285. doi: 10.1146/annurev.phyto.40.011402.114210

Yan Y, Hsam SLK, Yu JZ, et al (2003) HMW and LMW glutenin alleles among putative tetraploid and hexaploid European spelt wheat (*Triticum spelta* L.) progenitors. Theor Appl Genet 107:1321–1330. doi: 10.1007/s00122-003-1315-z

Zhang Z, Friesen TL, Simons KJ, et al (2009) Development, identification, and validation of markers for marker-assisted selection against the *Stagonospora nodorum* toxin sensitivity genes *Tsn1* and *Snn2* in wheat. Mol Breeding 23:35–49. doi: 10.1007/s11032-008-9211-5

Zhang Z, Friesen TL, Xu SS, et al (2011) Two putatively homoeologous wheat genes mediate recognition of SnTox3 to confer effector-triggered susceptibility to *Stagonospora nodorum*. Plant J 65:27–38. doi: 10.1111/j.1365-313X.2010.04407.x

Zipfel C (2009) Early molecular events in PAMP-triggered immunity. Curr Opin Plant Biol 12:414–420. doi: 10.1016/j.pbi.2009.06.003

Zipfel C, Felix G (2005) Plants and animals: a different taste for microbes? Curr Opin Plant Biol 8:353–360. doi: 10.1016/j.pbi.2005.05.004

Zipfel C, Robatzek S, Navarro L, et al (2004) Bacterial disease resistance in *Arabidopsis* through flagellin perception. Nature 428:764–767. doi: 10.1038/nature02485

Shifting the limits in wheat research and breeding using a fully annotated reference genome | Science. http://science.sciencemag.org/content/361/6403/eaar7191. Accessed 22 Dec 2018

RefSeq v1.0 URGI / Latest news / News / Home - IWGSC. https://www.wheatgenome.org/News/Latest-news/RefSeq-v1.0-URGI. Accessed 13 Jan 2019

3. THE ORIGIN OF *TRITICUM AESTIVUM* SSP. *SPELTA* IRANIAN TYPE AND ITS RELATIONSHIP TO COMMON WHEAT

3.1. Abstract

Several critical mutations for domestication occurred in wheat that enabled early farmers to efficiently harvest the grain. These mutations caused abolishment of spikelet shattering, softening of glumes, reduction of spike length, more spikelets per spike, toughness of rachis, and larger and free-threshing seeds. The genes known as *Q* and *Tg* (tenacious glume) are responsible for the free-threshing character of modern domesticated wheat. However, one subspecies of hexaploid wheat, *Triticum aestivum* ssp. *spelta* Iranian type, has tough glumes and non-free-threshing seed, but has been shown to carry the free-threshing *Q* allele. Therefore, to identify genetic factors that control the free-threshing character and other domestication related traits, I evaluated a population of 74 recombinant inbred lines derived from a cross between Chinese Spring and an Iranian type accession of *Triticum aestivum* ssp. *spelta*. The identification of a quantitative trait locus (QTL) associated with seed threshability on chromosome 2A in the region known to harbor the Tg^{2A} gene and an inactive tg^{2D} allele on chromosome 2D supported the hypothesis of Iranian spelta being formed through a more recent hybridization event between free-threshing hexaploid wheat and emmer wheat. Phylogenetic analysis of Iranian spelta accessions along with other free- and non-free-threshing wheats using full-length *Q* gene sequences corroborated this finding. QTL associated with other agronomic traits were identified on multiple chromosomes, including a QTL on 5D that had pleiotropic effects on days to heading, kernels per spike, and grain weight, which was likely due to the vernalization gene, *Vrn-D1*. Findings from this research will help to address the questions regarding evolution of

hexaploid wheat and will further our understanding of the regulatory and functional nature of genes governing the critical threshability trait in wheat.

3.2. Introduction

Modern day bread wheat (*Triticum aestivum* ssp. *aestivum* L., 2*n* = 6*x* = 42, AABBDD genomes) evolved from two allopolyploidization events, several mutations that helped in the acquisition of free-threshability and domestication related genes, and interspecific gene flow (see review, Faris 2014). The first allopolyploidization event occurred about a half million years ago (Huang et al. 2002; Chalupska et al. 2008) and involved a hybridization between the wild diploid wheat, *T. urartu* Tumanian ex Gandylian (2*n* = 2*x* = 14, AA genome) as the A genome donor (Dvorak et al. 1993) and a species similar to *Aegilops speltoides* Tausch (2*n* = 2*x* = 14, SS genome) (related but distinct form) as the B genome donor (Dvorak and Zhang 1990; Blake et al. 1999; Huang et al. 2002; Chalupska et al. 2008; Salse et al. 2008). As the result of this event, the tetraploid wheat *T. turgidum* ssp. *dicoccoides* Thell (2*n* = 4*x* = 28, AABB genomes) known as wild emmer came into existence. Then a second amphiploidization took place about 8,000 years ago, (Nesbitt and Samuel 1996; Huang et al. 2002) and involved hybridization between a different AB genome tetraploid subspecies of *T. turgidum* and the diploid goatgrass *Aegilops tauschii* Coss. (2*n* = 2*x* = 14, DD genome) (Kihara 1944; McFadden and Sears 1946), which resulted in the allohexaploid *T. aestivum* L. (2*n* = 6*x* = 42, AABBDD genomes).

Domestication was initiated through mutations in genes that conferred the brittle rachis trait (*Br)* on chromosomes 2A (Peng et al. 2003; Peleg et al. 2011; Thanh et al. 2013), 3A and 3B (Watanabe and Ikebata 2000; Nalam et al. 2006; Li and Gill 2006; Thanh et al. 2013; Avni et al. 2017) of wild emmer, which led to a type with a non-brittle rachis. This was a critical transition for early farmers because it abolished the natural seed dispersal mechanism, which allowed them

to more efficiently harvest the grains. This and other changes gave rise to the AB tetraploid subspecies *T. turgidum* ssp. *dicoccum*, commonly known as cultivated emmer wheat (*T. turgidum* ssp. *dicoccum* L., $2n = 4x = 28$, AABB genome). However, cultivated emmer wheat still had a fragile (but non-brittle) rachis and the seed was non-free threshing and hulled. These traits were due to the *q* gene on chromosome arm 5AL (Muramatsu 1979; Faris and Gill 2002; Simons et al. 2006) and tenacious glume (*Tg*) genes on chromosome arms 2AS and 2BS (Simonetti et al. 1999; Faris et al. 2014a, b).

The *Q* gene has pleiotropic effects on numerous traits including glume shape and tenacity, spike length, rachis fragility, ear emergence time, and plant height (see Faris et al. 2005 for review). It is a member of the *APETALA2* (*AP2*) class of transcription factors (Faris et al. 2003; Simons et al. 2006) and regulated by the microRNA miR172 (Debernardi et al. 2017). A mutation in the miR172 binding site of *q* led to inhibition of miR172 activity and increased expression of the gene, resulting in the *Q* allele (Debernardi et al. 2017). This mutation exists in all domesticated tetraploid and hexaploid wheat cultivars and confers the free-threshing character. Both wild and cultivated emmer wheats contain the *q* allele. Because the mutation only occurred once (Simons et al. 2006), it likely occurred in the tetraploid that was involved in the amphiploidization event to give rise to hexaploid wheat, leading to the presence of the *Q* allele in both durum and bread wheat types.

Tg is responsible for tough glumes that adhere strongly to the grains. Early cytogenetic studies along with recent molecular mapping studies have corroborated the position of Tg^{2D} on short arm of chromosome 2D (Kerber and Rowland 1974; Jantasuriyarat et al. 2004; Nalam et al. 2007; Sood et al. 2009). Using wild emmer, Simonetti et al. (1999) were the first to show that a putative homoeoallele of Tg^{2D} existed on 2BS in tetraploid wheat. Faris et al. (2014a) showed

more conclusively through comparative mapping that a Tg^{2D} homoeolog on 2BS in wild emmer inhibited threshability. Faris et al. (2014b) evaluated a Ben (*T. turgidum* ssp. *durum*) × cultivated emmer PI 41025 (*T. turgidum* ssp. *dicoccum)* wheat RIL population and found QTL associated with threshability on chromosome arms 2AS and 2BS, which were considered Tg^{2A} and Tg^{2B}. This was the first study to show that cultivated emmer has the genotype $Tg^{2A}Tg^{2A}/Tg^{2B}Tg^{2B}/qq$. Therefore, mutations in all three genes occurred to give rise to modern free-threshing durum wheat, and also in the Tg^{2D} gene from *Ae. tauschii* to form today's common bread wheat.

Other hybridization events that occurred after wheat domestication also took place among some subspecies. A cross between hexaploid club wheat (*T. aestivum* ssp. *compactum*) and cultivated emmer gave rise to European spelta (*T. aestivum* ssp. *spelta*, $2n = 6x = 42$, AABBDD genomes), which is non-free threshing due to acquisition of the *q* allele from cultivated emmer (Bertsch 1943; MacKey 1966; Blatter et al. 2002, 2004; Yan et al. 2003). Another form of spelta wheat is Iranian spelta (Kuckuck 1959), which was found growing in northern regions of Iran and other Middle East regions (Kuckuck 1964). It was once assumed to be more primitive than European spelta, but Luo et al. (2000) showed that, whereas European spelta has the *q* allele, Iranian spelta possesses the *Q* allele. The presence of the free-threshing *Q* allele in Iranian spelta was subsequently confirmed by Simons et al. (2006).

Even though it carries the free-threshing *Q* allele, Iranian spelta has tough glumes and non-free-threshing seed, suggesting it possesses other genes epistatic to *Q* that prohibit the expression of the free-threshing trait. Dvorak et al. (2012) used marker analysis to suggest that Iranian spelta may possess Tg^{2A} and/or Tg^{2B}, which could be responsible for the lack of the free-threshing trait. Here, I conducted molecular mapping and QTL analyses in a common wheat × Iranian spelta biparental population to identify the genetic loci associated with threshability, and

to quantify their effects. I also evaluated the population for other agronomic traits such as days to heading, spike length, kernels per spike, plant height, grain weight, and spikelets per spike to identify potentially useful allelic variation derived from Iranian spelta. In addition, I sequenced *Q* from different Iranian and European spelta lines to identify its phylogenetic position on the tree.

3.3. Material and methods

3.3.1. Plant material

A recombinant inbred line (RIL) population was developed from a cross between two hexaploid landraces, Chinese Spring and the *T. aestivum* ssp. *spelta* Iranian type accession P503 (Luo et al. 2000), the latter which was obtained from Prof. Jan Dvorak, University of California-Davis. Chinese Spring carries the *Q* and *tg* alleles and is fully free-threshing. Despite carrying the free-threshing *Q* allele (Luo et al. 2000; Simons et al. 2006), P503 has tough glumes and non-free-threshing seed. Therefore, to study the gene(s) responsible for suppression of free-threshing traits, RILs were developed from a single F_2 plant using the single-seed descent method and were bulked at the F_7 generation. This population consisting of 74 lines will be subsequently referred to as the CSP population.

3.3.2. Phenotyping

The CSP population along with its parents were phenotyped for agronomic and domestication-related traits including days to heading (DTH), spike length (SL), kernels per spike (KPS), grain weight per spike (GWS), plant height (HT), spikelets per spike (SPS), and threshability (THR). A total of seven replicates of the CSP population together with CS and P503 were grown in a completely randomized design (CRD) for three greenhouse seasons (2 replicates each for Fall 2016 and Spring 2017, and 3 replicates for Fall 2017). RILs were grown in 6″ clay

pots with one plant per pot to represent a single experimental unit. Each pot contained Metro Mix 902 soil (Hummert International, Earth City, MO) supplemented with fertilizer. Greenhouse conditions were maintained at 21˚C with a photoperiod of 16 hours.

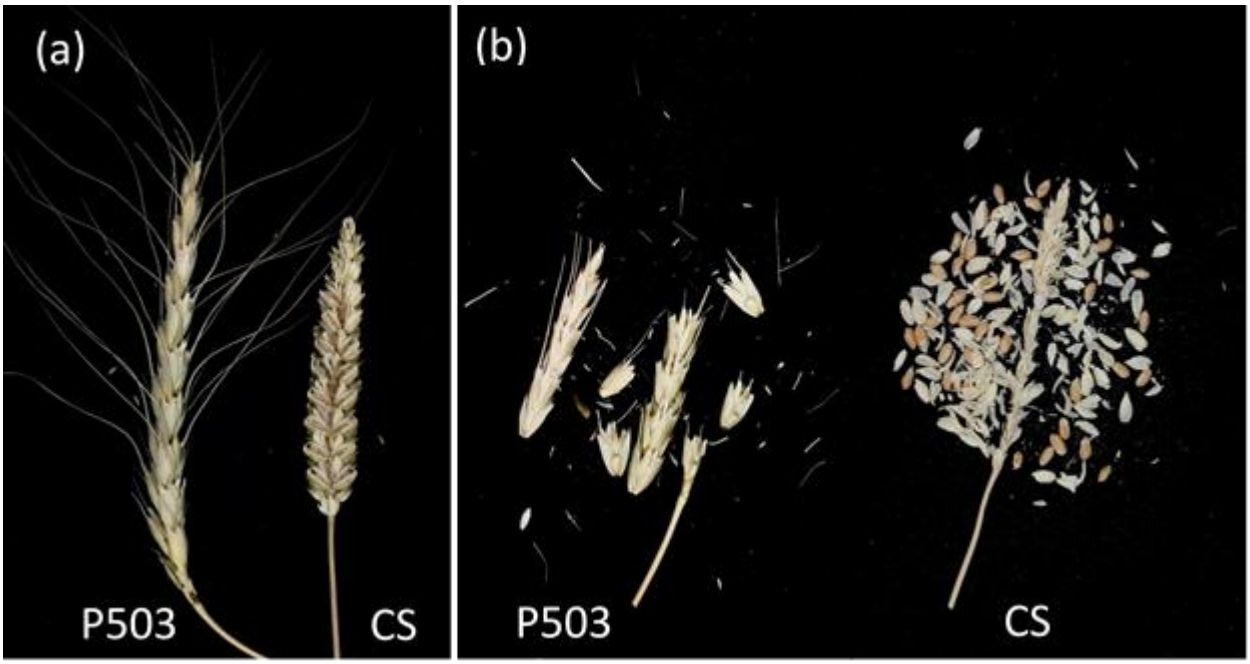

Figure 3.1. Spikes of Chinese Spring and Triticum aestivum ssp. spelta Iranian type accession P503 before threshing (a) and after threshing (b).

DTH was recorded as the number of days between seed sowing and the complete emergence of the first head. Plant height (in centimeters) of matured plants was measured before harvesting. It was measured from the base of the plant to tip of the tallest spike excluding the awns. Spike morphology and threshability were evaluated after spikes were harvested and dried at 32 ˚C for 3-4 days to ensure all spikes were moisture free. Mature spikes and seeds from both parents are presented in Figure 3.1. Four main spikes from each RIL were used to measure SL, KPS, GWS, SPS, and THR as described in Faris et al. (2014a). For spike length, a ruler was used to measure the length from the base of the first spikelet to the tip of the most terminal spikelet excluding the awns. KPS and GWS were measured after pooling seeds from all four threshed spikes and then dividing the number by 4. Spikelets were counted to determine spikelets per

spike (SPS). Each spike was hand-threshed and scored for threshability by placing it on a corrugated rubber mat lying on a bench and rubbed with a wooden block covered with the same rubber material back and forth across the spike one time. The rate of threshability of each spike was recorded on a 1-4 scale as described in Faris et al. (2014a), where 1 = completely free-threshing with release of almost all seeds from hulls; 2 = mostly free-threshing with < 50% of seeds remaining hulled; 3 = somewhat difficult to thresh with > 50% of seed remaining hulled; and 4 = difficult to thresh with most of the seeds remaining attached to hulls.

3.3.3. Statistical analysis

Phenotypic data from four main spikes were averaged to derive means for SL, KPS, GWS, SPS, and THR. This was done separately for all seven replicates. Bartlett's test for homogeneity of error variances (Snedecor and Cochran 1989) was performed using replicates within and among the three greenhouse seasons using PROC GLM in the SAS program version 9.4 (SAS institute 2013). Overall mean RIL scores were calculated for all traits from homogenous experiments and/or replicates and used for further analysis. Fisher's least significant difference (LSD) was performed at $\alpha = 0.05$ to calculate significant differences among means of the RILs for each trait. Trait value range, standard deviation, and histograms representing the distribution of data were generated using means of each trait. A correlation matrix was also calculated to study the relationship among different traits.

3.3.4. Genotyping and linkage map construction

DNA from the parents and the CSP population was extracted as described by Faris et al. (2000). The extracted DNA pellet was dissolved in 50 μL of TE buffer and quantified using a Nanodrop spectrophotometer ND-1000. DNA samples were then diluted to approximately 200 ng/μL using distilled water.

Molecular markers including simple sequence repeats (SSRs) and single nucleotide polymorphism (SNPs) were used to develop genetic linkage maps in the CSP population. SSRs were chosen from previously published maps obtained from the GrainGenes database (https://wheat.pw.usda.gov/GG3/) and approximately 4-6 polymorphic markers were targeted to map on each wheat chromosome. Polymerase chain reaction (PCR) amplifications was performed in 10 μL reactions and amplified PCR products were resolved on 6% polyacrylamide gels, stained with GelRed stain, and scanned on a Typhoon FLA 9500 variable mode laser imager (GE Healthcare Life Sciences, Piscataway, NJ).

The 90K iSelect Assay BeadChip (Wang et al. 2014) comprising of approximately 90,000 SNPs was used for SNP genotyping of the CSP population. SNP allele clustering and genotype calling was performed with GenomeStudio Polyploid Clustering v1.0 software as described in its Module v1.0 Software Guide. Accuracy for these clusters was validated visually, and incorrect SNP clusters were removed manually. SNPs that followed a biallelic segregation pattern and whose location corresponded well with consensus map by Wang et al. (2014) were selected for map construction. SNP data along with polymorphic SSR data were combined to construct genetic linkage maps of the 21 chromosomes.

Linkage maps were assembled using the program MapDisto v.1.8 (Lorieux 2012). Genetic distances were calculated using the Kosambi mapping function (Kosambi 1944) and markers were grouped using the 'find groups' command with a logarithm of odds (LOD) threshold of 3.0 and maximum recombination frequency of 0.3. The command 'order sequence' which uses sum of adjacent frequencies (SARF) was used to establish the initial marker order. The best order of marker loci was determined by using 'check inversions', 'ripple order', and 'drop locus' commands.

3.3.5. QTL analysis

I identified genomic regions associated with the phenotypic traits by regressing phenotypic means against the genotypic data. Quantitative trait loci (QTLs) analysis was performed using QGene v 4.3.10 (Joehanes and Nelson 2008). Multiple interval mapping (MIM) was used to identify QTLs significantly associated with the traits under investigation. The coefficient of determination (R^2) was used to indicate the amount of variation explained by the QTL. A critical LOD threshold of 3.5 at $P \geq 0.05$ for whole genome analysis was determined using permutation test with 1000 iterations.

3.3.6. Phylogenetic analysis

The full-length genomic sequence of *Q* was obtained from the wheat lines listed in Table 3.1 to determine variation in *Q*/*q* alleles. The *Q* gene was PCR-amplified and sequenced in three overlapping fragments using gene-specific primers (Table 3.2) as described by Simons et al. (2006). Two independent PCR reactions for each fragment were performed to identify PCR errors. PCR amplicons were electrophoresed on 1% agarose gels for 60 minutes at 90 V. The amplified fragment was excised from the gel and purified using the Wizard ® SV gel and PCR Clean Up System from Promega (Madison, WI). The purified product from fragment 2 was ligated to a cloning vector from Qiagen PCR cloning kit (QIAGEN, Hilden, Germany) because of its larger size, and transformed into NEB 5-α competent *E. coli* cells (New England Biolabs, Ipswich, MA). Product insert was confirmed with M13 primers in positive colonies. Selected colonies were then cultured in 2.5 mL liquid LB media with carbenicillin for 12-16 hours. Plasmid DNA was extracted from cells using the QIAprep spin Miniprep kit (QIAGEN, Hilden, Germany) and sent for sequencing. The amplicons were sent for sequencing by Sanger approach to Eurofins MWG Operon (Louisville, KY).

Table 3.1. *Triticum* accessions deployed in phylogenetic analysis using *Q*/*q* genomic sequences

Accession name	PI/CItr	Ploidy	Genus	Species	Subspecies	*Q*/*q* alleles
TA2801	NA	4X	*Triticum*	*turgidum*	*carthlicum*	*Q*
Bobwhite	PI 520554	6X	*Triticum*	*aestivum*	*aestivum*	*Q*
ND495	NA	6X	*Triticum*	*aestivum*	*aestivum*	*Q*
TA2601	NA	6X	*Triticum*	*aestivum*	*compactum*	*Q*
NA	CItr 191826	4X	*Triticum*	*turgidum*	*polonicum*	*Q*
Langdon	NA	4X	*Triticum*	*turgidum*	*durum*	*Q*
Chinese Spring	CItr 14108	6X	*Triticum*	*aestivum*	*aestivum*	*Q*
Renan	PI 564569	6X	*Triticum*	*aestivum*	*aestivum*	*Q*
NA	PI 466995	4X	*Triticum*	*turgidum*	*dicoccoides*	*q*
16-1	NA	4X	*Triticum*	*turgidum*	*dicoccoides*	*q*
TA106	NA	4X	*Triticum*	*turgidum*	*dicoccoides*	*q*
69Z99.7	PI 355459	4X	*Triticum*	*turgidum*	*dicoccoides*	*q*
Tdom19	CItr 14621	4X	*Triticum*	*turgidum*	*dicoccoides*	*q*
DN2378	PI 361862	6X	*Triticum*	*aestivum*	*macha*	*q*
TA704	NA	2X	*Triticum*	*urartu*		*q*
Iranian spelta	PI 572914	6X	*Triticum*	*aestivum*	*spelta*	*Q*
Iranian spelta	PI 367199	6X	*Triticum*	*aestivum*	*spelta*	*Q*
Iranian spelta Sears P503	NA	6X	*Triticum*	*aestivum*	*spelta*	*Q*
Iranian spelta	PI 572915	6X	*Triticum*	*aestivum*	*spelta*	*Q*
European spelta	PI 266848	6X	*Triticum*	*aestivum*	*spelta*	*q*
European spelta	PI 272573	6X	*Triticum*	*aestivum*	*spelta*	*q*
European spelta (Sears)	NA	6X	*Triticum*	*aestivum*	*spelta*	*q*
European spelta	PI 338367	6X	*Triticum*	*aestivum*	*spelta*	*q*
European spelta TA2603	NA	6X	*Triticum*	*aestivum*	*spelta*	*q*
European spelta	PI 378469	6X	*Triticum*	*aestivum*	*spelta*	*q*
European spelta	PI 348483	6X	*Triticum*	*aestivum*	*spelta*	*q*
European spelta	PI 286060	6X	*Triticum*	*aestivum*	*spelta*	*q*
European spelta	PI 348189	6X	*Triticum*	*aestivum*	*spelta*	*q*
European spelta	PI 355651	6X	*Triticum*	*aestivum*	*spelta*	*q*
European spelta	PI 585008	6X	*Triticum*	*aestivum*	*spelta*	*q*

Table 3.2. List of primers for targeting *Q*-gene fragments

Target site	Primers	Sequences (5' to 3')	Annealing temperature (°C)	Fragment size (bp)
Q-gene (fragment 1)	AP5P.11-3	GCCCTCGCAGCCCGCGGCCACCGCGCTCCCA	68	805
	AP2.8R	CGCGGCCAAATCGGGGCAAAGGAATTCAAACGA		
Q-gene (fragment 2)	Wap2.2F	CACTGGATAATTTCTTCAGGTGGTTTCGACACTGC	68	1906
	AP2.15R	ACATGGAACCTTAATTTCAGGAACGAACTTGTCG		
Q-gene (fragment 3)	AP2.16F	CTGCTTGGTGCGCTGCTCCACCAGCTTACTGAAA	72	1081
	AP45.1R	CAGAAGGCCCAACGGTTAACGCAACAATGGC		

Sequencing reads were assembled using the software Sequencher v4.8. Multiple sequence alignments were generated using MUSCLE (Edgar 2004) in MEGA v7.0.26 (Tamura et al. 2013) software. The phylogenetic tree was constructed with the neighbor joining method using the p-distance model with pairwise-deletion option in MEGA. Confidence values for branch nodes were calculated using 1000 bootstraps.

3.4. Results

3.4.1. Linkage maps

A total of 8457 SNPs and 19 SSRs were mapped in the CSP RIL population revealing 949 unique loci and resulting in genetic linkage maps that spanned 2,360 cM giving an average density of 2.5 cM/locus (Table 3.3). The B genome was the most polymorphic with 4,545 markers that detected 438 loci spanning 826.4 cM making it the most dense at 1.9 cM/locus. The D genome was the least polymorphic with a total of 398 markers detecting 100 loci that spanned 522.5 cM and a density of only 5.2 cM/locus. Although the A genome had fewer markers than the B genome, it had the most recombination with a total length of 1,011.2 cM.

Of the 8,476 markers used in this study, 95 (1.1%) had segregation ratios that deviated significantly ($P < 0.05$) from the expected 1:1 ratio (Table 3.3). Markers with distorted ratios

occurred on all chromosomes with the exception of chromosomes 1D, 3D, 4B, 4D, and 5A. The D genome contained the highest percentage of distorted markers at 2.0%.

Table 3.3. Summary of linkage groups and genome mapping parameters for the CSP population

Chromosome	SSR	SNP	Total markers	Loci	Length (cM)	cM/loci	Number of distorted markers	% distorted markers
1A	1	504	505	87	167.8	1.9	6	1.2
1B	4	754	758	54	114.9	2.1	5	0.7
1D	1	84	85	15	20.8	1.4	0	0.0
2A	1	778	779	34	105.8	3.1	2	0.3
2B	8	945	953	83	138.0	1.7	9	0.9
2D	1	110	111	20	72.1	3.6	1	0.9
3A	0	389	389	53	159.7	3.0	10	2.6
3B	0	627	627	62	128.9	2.1	1	0.2
3D	0	87	87	7	22.8	3.3	0	0.0
4A	0	440	440	44	140.0	3.2	5	1.1
4B	0	230	230	39	83.2	2.1	0	0.0
4D	0	9	9	9	35.6	4.0	0	0.0
5A	1	342	343	79	176.6	2.2	0	0.0
5B	2	650	652	82	142.3	1.7	16	2.5
5D	0	18	18	13	141.6	10.9	2	11.1
6A	0	481	481	31	74.3	2.4	4	0.8
6B	0	751	751	55	96.3	1.8	17	2.3
6D	0	29	29	20	133.9	6.7	2	6.9
7A	0	596	596	83	187.0	2.3	8	1.3
7B	0	574	574	63	122.8	1.9	4	0.7
7D	0	59	59	16	95.8	6.0	3	5.1
A genome	3	3530	3533	411	1011.2	2.5	35	0.9
B genome	14	4531	4545	438	826.4	1.9	52	1.1
D genome	2	396	398	100	522.5	5.2	8	2.0
Total	19	8457	8476	949	2360.1	2.5	95	1.1

3.4.2. Trait analysis

Homogeneity of error of variances was observed among all seven replicates for DTH from the three seasons (Table 3.4). DTH ranged from 76.0 to 146.0 for the CSP RILs with a population mean of 104.0 days (Figure 3.2; Table 3.5). P503 took 72.2 days longer to head than CS, suggesting CS is responsible for reduced DTH.

Table 3.4. Bartlett's test of homogeneity of score variance for the agronomic traits

Trait	Pr > ChiSq
DTH	0.25
SL	0.86
KPS[a]	0.30
KPS[b]	0.30
KPS[c]	0.34
GWS	0.09
HT[c]	0.23
SPS	0.61
THR	0.68

days to heading (*DTH*), spike length (*SL*), kernels per spike season 1 (*KPS*^{a}), kernels per spike season 2 (*KPS*^{b}), kernels per spike season 3 (*KPS*^{c}), grain weight per spike (*GWS*), plant height season 2- rep2 (*HT*^{b2}), plant height season 3 (*HT*^{c}), spikelets per spike (*SPS*), and threshability (*THR*)

Error variances were homogenous for all seven replicates of the three seasons for SL (Table 3.4), and overall RIL means were used for further analysis. CS and P503 had average SL of 8.2 and 9.8 cm, respectively, and the CSP population had a mean of 9.1 cm (Figure 3.1, 3.2; Table 3.5). The range of population varied from 7.0 to 10.9 cm.

Replicates for KPS were homogenous within each season (Table 3.4), but they were not homogeneous among seasons (data not shown). Therefore, the means among replicates for each season were evaluated separately and designated as KPS^{a} (Fall 2016), KPS^{b} (Spring 2017), and KPS^{c} (Fall 2017). On average, CS had 37.1, 41.3, and 49.5 KPS whereas P503 had 15.8, 16.3, and 14.0 KPS, respectively, for KPS^{a}, KPS^{b}, and KPS^{c} (Figure 3.2; Table 3.5). RILs had mean values of 23.7, 27.5, and 31.1 with ranges from 3.3-51.5, 11.0-41.0, and 12.0-48.0 for KPS^{a}, KPS^{b}, and KPS^{c}, respectively.

Error variances for GWS were homogenous for all three seasons (Table 3.4), and overall RIL means were therefore used for further analysis. GWS means ranged from 0.4 to 1.5 g with a population mean of 0.9 g (Figure 3.2; Table 3.5). CS and P503 had GWS means of 1.2 g and 0.5 g, respectively. Higher grain weight was most likely due to greater KPS in CS.

Bartlett's test showed homogeneity of variances among all replicates of the three seasons for SPS (Table 3.4). Therefore, the RIL means calculated from all seven replicates were used in further analysis. CS had 23.8 SPS, and P503 had 17.0, whereas the population mean was 19.2 and the range was 15.0-22.0 (Figure 3.2; Table 3.5).

Error variances for HT were homogenous only for replicates within season 3 (Table 3.4). Therefore, replicates for seasons 1 and 2, and the average of season 3 replicates were all analyzed separately. They will be hereafter referred to as HT^{a1}, HT^{a2}, HT^{b1}, HT^{b2}, and HT^{c}. Population means of HT^{a1}, HT^{a2}, HT^{b1}, HT^{b2}, and HT^{c} were 112.1 cm, 113.6 cm, 109.2 cm, 110.7 cm, and 122.2 cm, respectively (Figure 3.2, 3.3; Table 3.5). HT values for CS and P503 was measured as 105.0 cm and 124.0 cm; 132.5 cm and 126.0 cm; 95.0 cm and 137.2 cm; 112 cm and 136.7 cm; and 130.7 cm and 145.2 cm, respectively, and from the population ranges were 76.0 to 150.0 cm; 61.5 to 156.5 cm; 70.0 to 140.0 cm; 87 to 142 cm; and 59.4 to 149.7 cm, respectively.

Table 3.5. Parental and population means, population range, standard deviation, and LSD (P < 0.05) for the agronomic traits

Trait	Mean			Population range	Standard deviation	LSD (0.05)
	Chinese spring	P503	Population			
DTH	83.8	156.0	104.0	76.0 - 146.0	18.8	10.7
SL	8.2	9.8	9.1	7.0 - 10.9	1.2	0.8
KPS[a]	37.1	15.8	23.7	3.3 - 51.5	11.6	14.8
KPS[b]	41.0	17.1	27.5	11.0 - 41.0	8.9	12.7
KPS[c]	48.0	14.0	31.1	12.0 - 48.0	9.9	11.3
GWS	1.2	0.5	0.9	0.4 - 1.5	0.4	0.3
Ht[a1]	105.0	124.0	112.1	76.0 - 150.0	17.3	-
Ht[a2]	132.5	126.0	113.6	61.5 - 156.5	18.9	-
Ht[b1]	95.0	137.2	109.2	70.0 - 140.0	13.8	-
Ht[b2]	112.0	136.7	110.7	87.0 - 142.0	15.5	-
Ht[c]	130.7	145.2	122.2	59.4 - 149.7	18.8	23.8
SPS	23.8	17.0	19.2	15.0 - 22.0	2.4	2.1
THR	1.0	4.0	2.6	1.0 - 4.0	0.9	0.6

days to heading (*DTH*), spike length (*SL*), kernels per spike season 1 (KPS^a), kernels per spike season 2 (KPS^b), kernels per spike season 3 (KPS^c), grain weight per spike (*GWS*), plant height season 1- rep1 (HT^{a1}), plant height season 1- rep2 (HT^{a2}), plant height season 2- rep1 (HT^{b1}), plant height season 2- rep2 (HT^{b2}), plant height season 3 (HT^c), spikelets per spike (*SPS*), and threshability (*THR*)

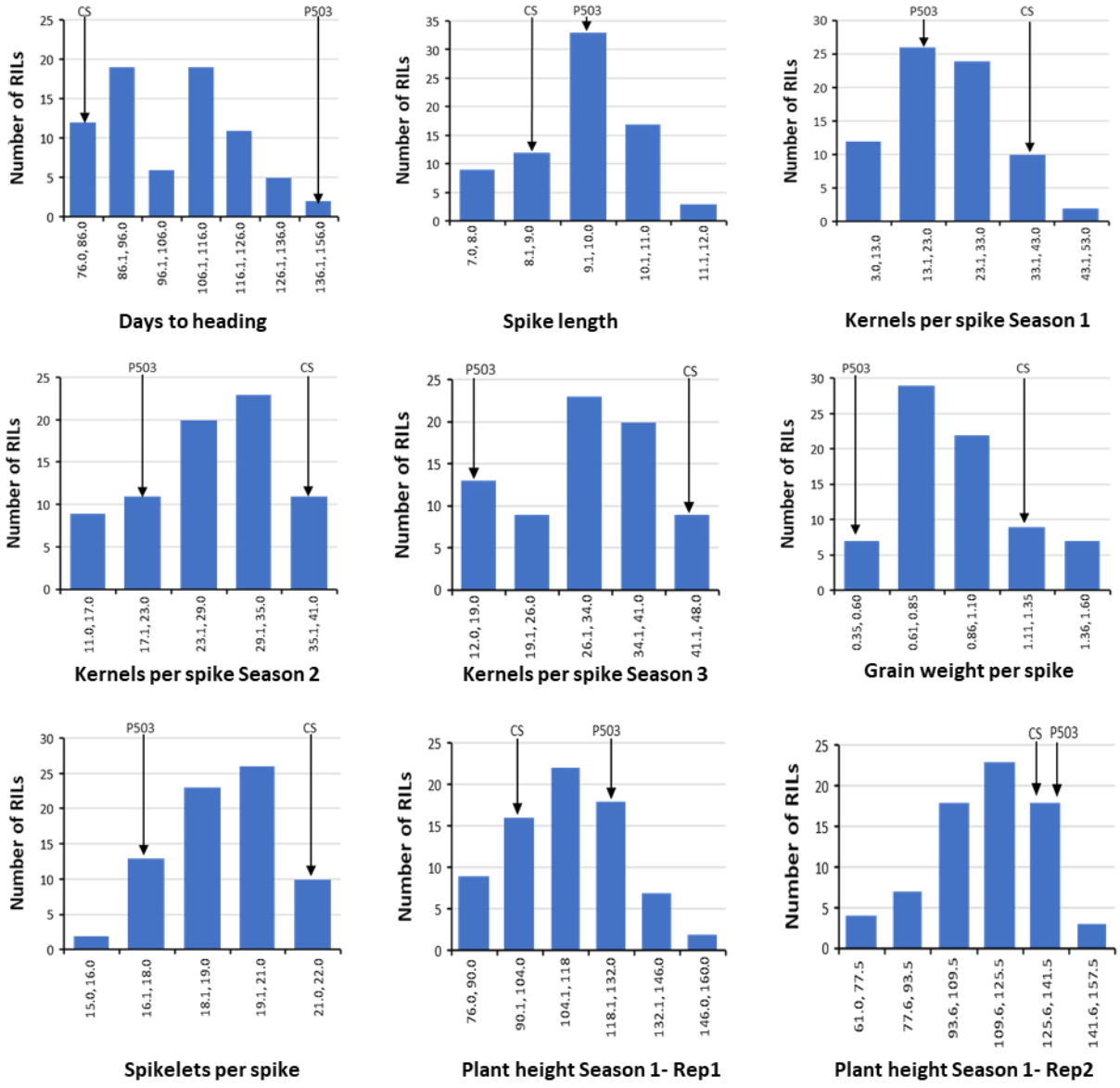

Figure 3.2. Histograms of the six phenotypic traits evaluated including days to heading (*DTH*), spike length (*SL*), kernels per spike season 1 (KPS^a), kernels per spike season 2 (KPS^b), kernels per spike season 3 (KPS^c), grain weight per spike (*GWS*), spikelets per spike (*SPS*), plant height season 1- rep1 (HT^{a1}), and plant height season 1- rep2 (HT^{a2}). Mean trait values of three seasons were used for all traits except for kernels per spike and plant height.

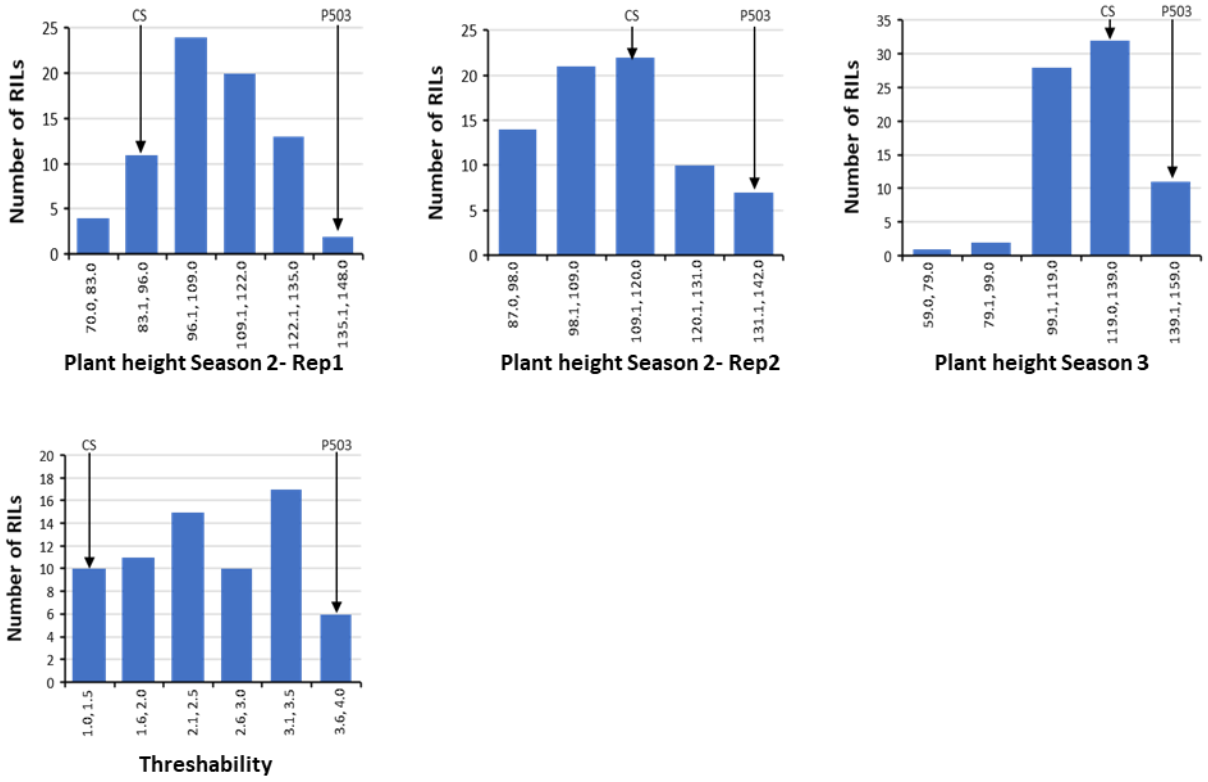

Figure 3.3. Histograms of the two phenotypic traits evaluated including plant height season 2-rep1 (HT^{b1}), plant height season 2- rep2 (HT^{b2}), plant height season 3 (HT^{c}), and threshability (*THR*) (continued). Mean trait values of three seasons were used for all traits except for kernels per spike and plant height.

Seed of the Iranian spelta parent P503 was non-free threshing and therefore given a threshing score of 4, whereas CS had completely free threshing seeds and had a score of 1 (Figure 3.1, Table 3.5). The Iranian spelta spikes disarticulated along the rachis, leaving a segment of the rachis attached behind a completely intact spikelet. This is known as barrel (B)-type disarticulation. The CSP population range of 1-4 (Figure 3.3) clearly indicated that alleles from P503 conferred the non-free threshing trait. The population mean was 2.6, suggesting that multiple genes derived from P503 likely contributed to making threshing difficult.

Correlation coefficients, as presented in Table 3.6, were calculated using Pearson correlation procedure in SAS. DTH was negatively correlated with SL, KPS, GWS, and SPS. SL

was positively correlated with all traits under study. KPS and GWS showed the highest positive correlation with SPS, and with each other. SL and GWS had slightly weaker positive association with HT. THR was positively correlated with SL, indicating longer spikes were harder to thresh.

Table 3.6. Pearson Correlation Coefficients between the mean values of agronomic traits

Trait	DTH	SL	KPS^{a}	KPS^{b}	KPS^{c}	GWS	HT^{a1}	HT^{a2}	HT^{b1}	HT^{b2}	HT^{c}	SPS	THR
DTH	1												
SL	-0.29**	1											
KPS^{a}	-0.54***	0.34**	1										
KPS^{b}	-0.44***	0.37***	0.49***	1									
KPS^{c}	-0.63***	0.35**	0.67***	0.56***	1								
GWS	-0.64***	0.50***	0.80***	0.61***	0.82***	1							
HT^{a1}	-0.07	0.17	0.41***	0.26*	0.38***	0.40***	1						
HT^{a2}	0.03	-0.03	0.11	-0.13	-0.14	-0.11	0.16	1					
HT^{b1}	0.03	-0.15	-0.06	0.07	-0.05	-0.06	-0.06	0.22	1				
HT^{b2}	0.05	0.26*	-0.04	0.22	0.21	0.21	0.38***	-0.13	0.04	1			
HT^{c}	0.03	0.34**	0.01	0.05	0.25*	0.22*	0.35**	-0.25	-0.1	0.56***	1		
SPS	-0.44***	0.40***	0.42***	0.35**	0.32**	0.43***	0.19	0.16	-0.1	-0.08	-0.11	1	
THR	0.07	0.27**	0.07	0.01	-0.05	0.01	0.01	0.17	-0.1	-0.05	0.16	-0.02	1

*$P \leq 0.05$, **$P \leq 0.01$, ***$P \leq 0.001$
days to heading (*DTH*), spike length (*SL*), kernels per spike season 1 (*KPS^{a}*), kernels per spike season 2 (*KPS^{b}*), kernels per spike season 3 (*KPS^{c}*), grain weight per spike (*GWS*), plant height season 1- rep1 (*HT^{a1}*), plant height season 1- rep2 (*HT^{a2}*), plant height season 2- rep1 (*HT^{b1}*), plant height season 2- rep2 (*HT^{b2}*), plant height season 3 (*HT^{c}*), spikelets per spike (*SPS*), and threshability (*THR*)

3.4.3. QTL analysis

QTL analysis revealed a total of eight QTLs with LOD ≥ 3.5. These QTLs revealed genomic regions involved in the control of seven traits.

For DTH, a major QTL was detected on the long arm of chromosome 5D (Figure 3.4, Table 3.7). This QTL, designated as *QEet.fcu-5D*, had a LOD value of 22.1 and explained of 67% of the phenotypic variation. P503 contributed longer heading times for this QTL in the population.

SL was controlled by a QTL on chromosome 1A, designated as *QEl.fcu-1A* (Figure 3.4, Table 3.7). It had an LOD value of 3.5 and explained 11.7% of the phenotypic variation. Effects for increased SL were contributed by P503.

Table 3.7. Quantitative trait loci associated with domestication-related traits in the Chinese Spring × P503 (CSP) recombinant inbred population

Trait	QTL	Position (cM)	LOD	$R^2 \times 100$	Marker interval	Additive effects[a]
DTH	*QEet.fcu-5D*	84	22.1	67.0	*IWB17912-IWB35901*	-14.69
SL	*QEl.fcu-1A*	40	3.5	11.7	*IWB30674-IWB28824*	-0.40
KPS[a]	*QKps.fcu-5D*	84	3.6	19.3	*IWB17912-IWB35901*	5.10
KPS[b]	*QKps.fcu-5D*	84	7.9	34.1	*IWB17912-IWB35901*	4.60
	QKps.fcu-6A	10	3.8	10.8	*IWB24996-IWB77829*	-4.30
KPS[c]	*QKps.fcu-5D*	80	8.1	34.1	*IWB30701-IWB63558*	5.77
GWS	*QGws.fcu-5D*	84	6.3	32.4	*IWB17912-IWB35901*	0.15
HT[a1]	*QHt.fcu-7D*	165	5.3	22.1	*IWB52359-IWB184416*	-9.13
HT[b2]	*QHt.fcu-6A*	120	4.3	18.1	*IWB43142*	-5.89
	QHt.fcu-7A	108	4.5	20.7	*IWB74447*	-5.96
HT[c]	*QHt.fcu-6A*	118	4.1	18.6	*IWB22698-IWB77861*	-6.30
SPS	*QSpn.fcu-7A*	112	6.3	30.2	*IWB452-IWB78282*	0.86
THR	*QFt.fcu-2A*	8	5.1	20.0	*IWB63394-IWB12412*	-0.43

days to heading (*DTH*), spike length (*SL*), kernels per spike season 1 (*KPS*^{a}), kernels per spike season 2 (*KPS*^{b}), kernels per spike season 3 (*KPS*^{c}), grain weight per spike (*GWS*), plant height season 1- rep1 (*HT*^{a1}), plant height season 1- rep2 (*HT*^{a2}), plant height season 2- rep1 (*HT*^{b1}), plant height season 2- rep2 (*HT*^{b2}), plant height season 3 (*HT*^{c}), spikelets per spike (*SPS*), and threshability (*THR*)

[a] A negative number value indicates that a higher value for a given trait is derived from P503 and a positive number indicates that a higher value for the trait is derived from Chinese Spring

Two QTLs, designated as *QKps.fcu-5D* and *QKps.fcu-6A* on chromosomes 5D and 6A, respectively, were associated with KPS (Figure 3.4, Table 3.7). The 5D QTL was significant for all three seasons (KPS[a], KPS[b] and KPS[c]) with LOD values of 3.6, 7.9, and 8.1 and accounting for 19.3, 34.1 and 34.1% of the phenotypic variation, respectively. The effects for increased KPS were conferred by CS. *QKps.fcu-6A* was only detected in the second season, and it had an LOD

value of 3.8. It explained 10.8% of the variation, and effects for increased seed number were contributed by P503.

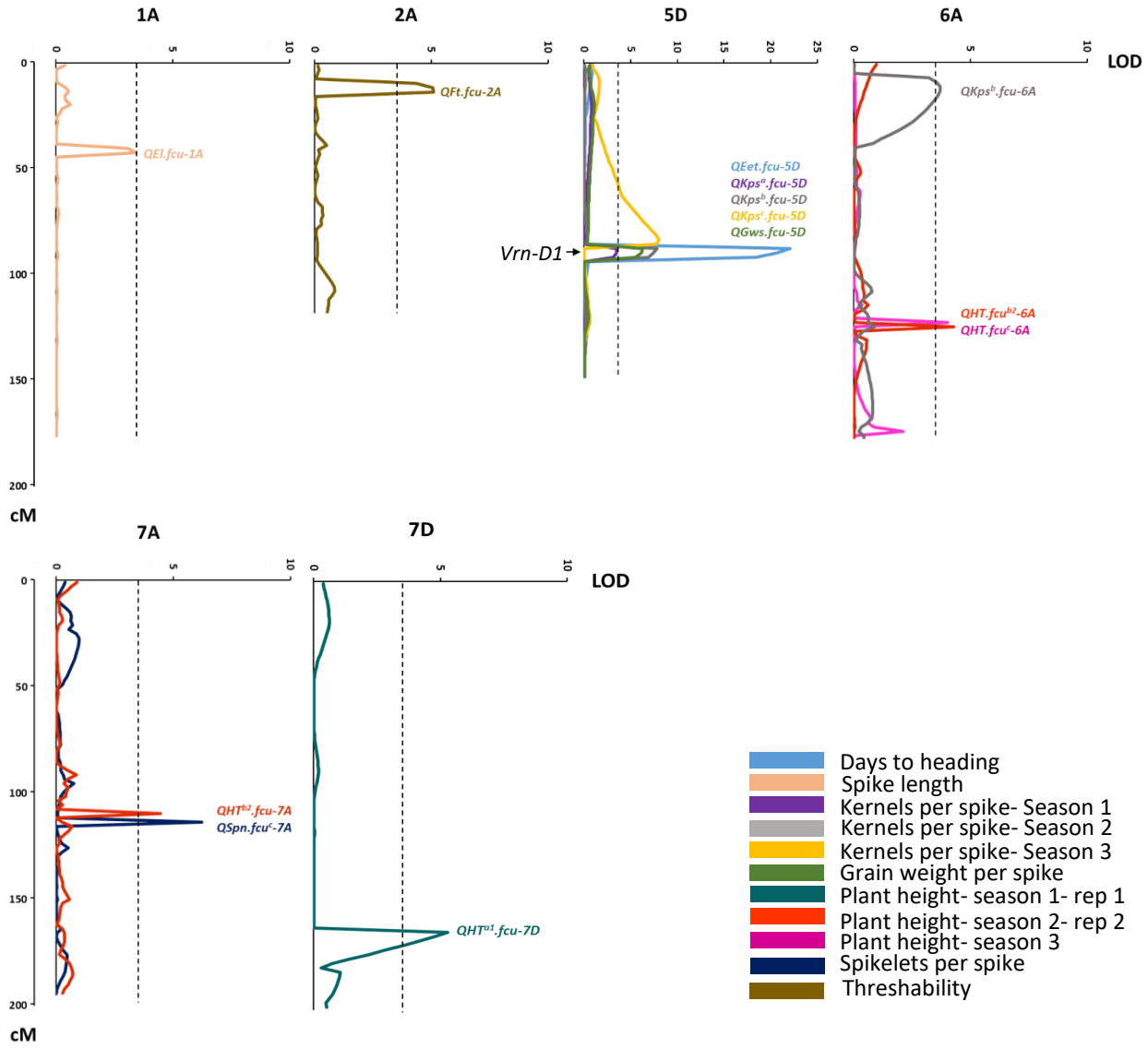

Figure 3.4. Graphical representation of eight QTL located on six different chromosomes of the hexaploid wheat genome associated with a total of seven agronomic and domestication traits evaluated in the CSP population. The approximate position of *Vrn-D1* is indicated by an arrow.

One QTL was associated with GWS and located in the marker interval *IWB17912-IWB35901* on chromosome 5D (Figure 3.4, Table 3.7). This QTL was designated as *QGws.fcu-5D,* and it had an LOD value of 6.3 and explained 32.4% of the variation. As for KPS, the effects for increased GWS were contributed by CS.

For HT, no significant QTLs were identified for replicate 2 of season 1 (HT^{a2}) and replicate 1 of season 2 (HT^{b1}). However, one QTL on chromosome 7D (*QHt.fcu-7D*) for HT^{a1} and two QTLs on chromosome 6A (*QHt.fcu-6A*), and 7A (*QHt.fcu-7A*) for HT^{b2} with LOD score of 5.3, 4.3, and 4.5, respectively were detected (Figure 3.4, Table 3.7). These three QTLs explained 22.1, 18.1, and 20.7% of the phenotypic variation in the CSP population. Effects for increased HT were derived from P503 for all three QTLs. *QHt.fcu-6A* was also associated with HT in season 3 where it had an LOD of 4.1 and explained 18.6% of the variation and again effects were derived from P503.

One QTL associated with SPS was identified on chromosome 7A and was designated *QSpn.fcu-7A* (Figure 3.4, Table 3.7). *QSpn.fcu-7A* had an LOD value of 6.3 and explained 30.2% of the phenotypic variation. An increase in SPS was conferred by CS.

For threshability, one QTL was detected on chromosome arm 2AS (Figure 3.4, Table 3.7), and was designated as *QFt.fcu-2A.* This QTL had an LOD score of 5.1 and explained 20% of the variation in threshability. As expected, the effects for threshing difficulty were contributed by the Iranian spelta parent, P503.

3.4.4. Phylogenetic analysis

Sequencing and alignment of *Q*/*q* alleles from European and Iranian accessions provide additional evidence that the former has *q* whereas the latter has the *Q* allele. Observation of the miRNA172 binding site motif showed that all Iranian type speltas harbored a thymine at position

3139 bp, which confers the *Q* allele, as opposed to a cytosine which confers the *q* allele as was observed in the European type speltas (Figure 3.5). Phylogenetic analysis of *Q* from 30 accessions (Genbank accession numbers provided in Appendix) including diploid, tetraploid, and hexaploid wheat species (Figure 3.6) showed that Iranian spelta accessions clustered with cultivated hexaploid and tetraploid species whereas European spelta accessions clustered with *q* containing wheat species. *T. turgidum* ssp. *dicoccoides* fell into a different clade indicating a more diverse origin relative to other wheat species included in the tree.

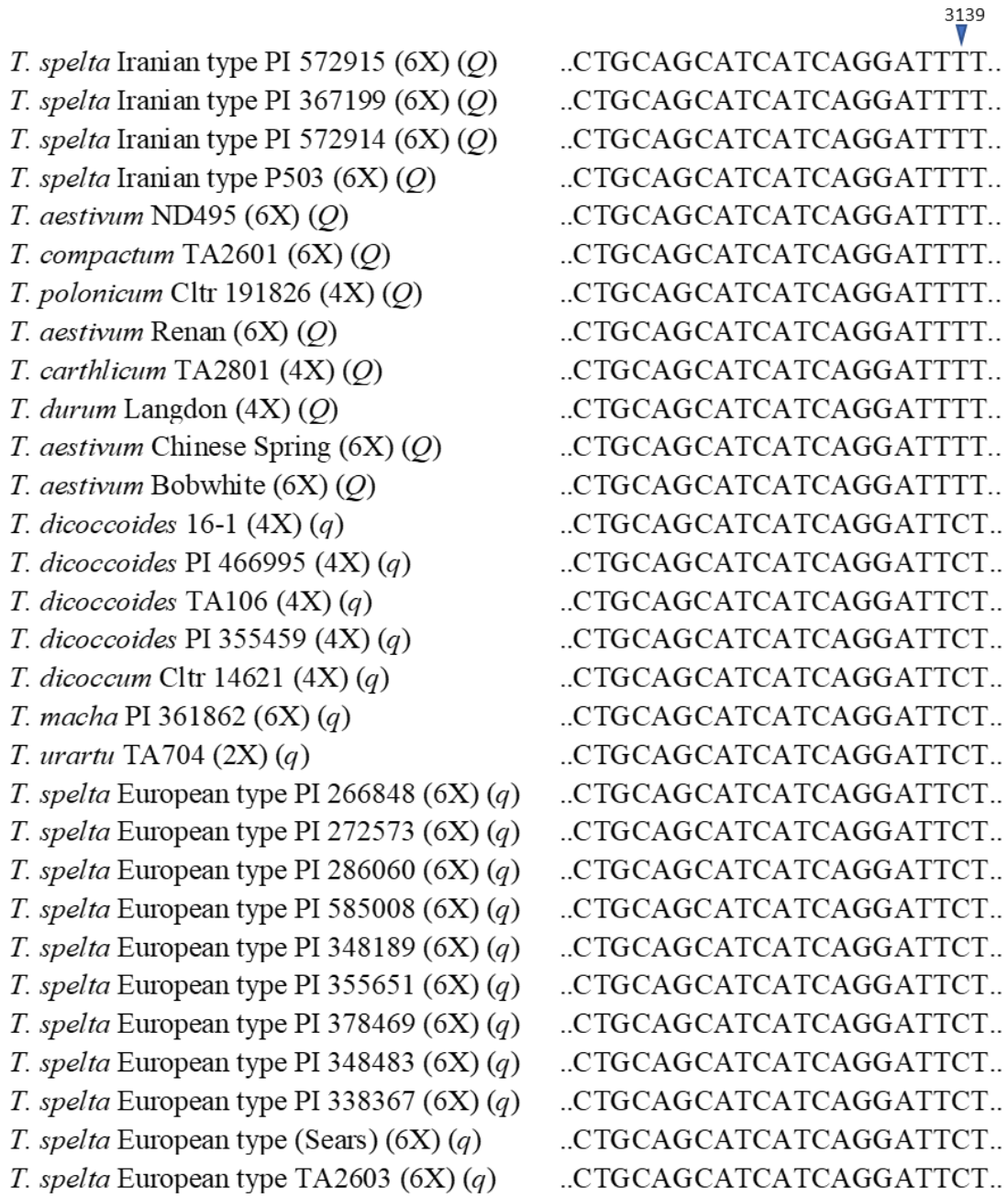

Figure 3.5. The location of critical SNP difference in miR172 binding site that distinguishes *Q* from *q* genotypes. The number at the top of arrow represent position of mutation based on genomic sequence of *Q* in Chinese Spring.

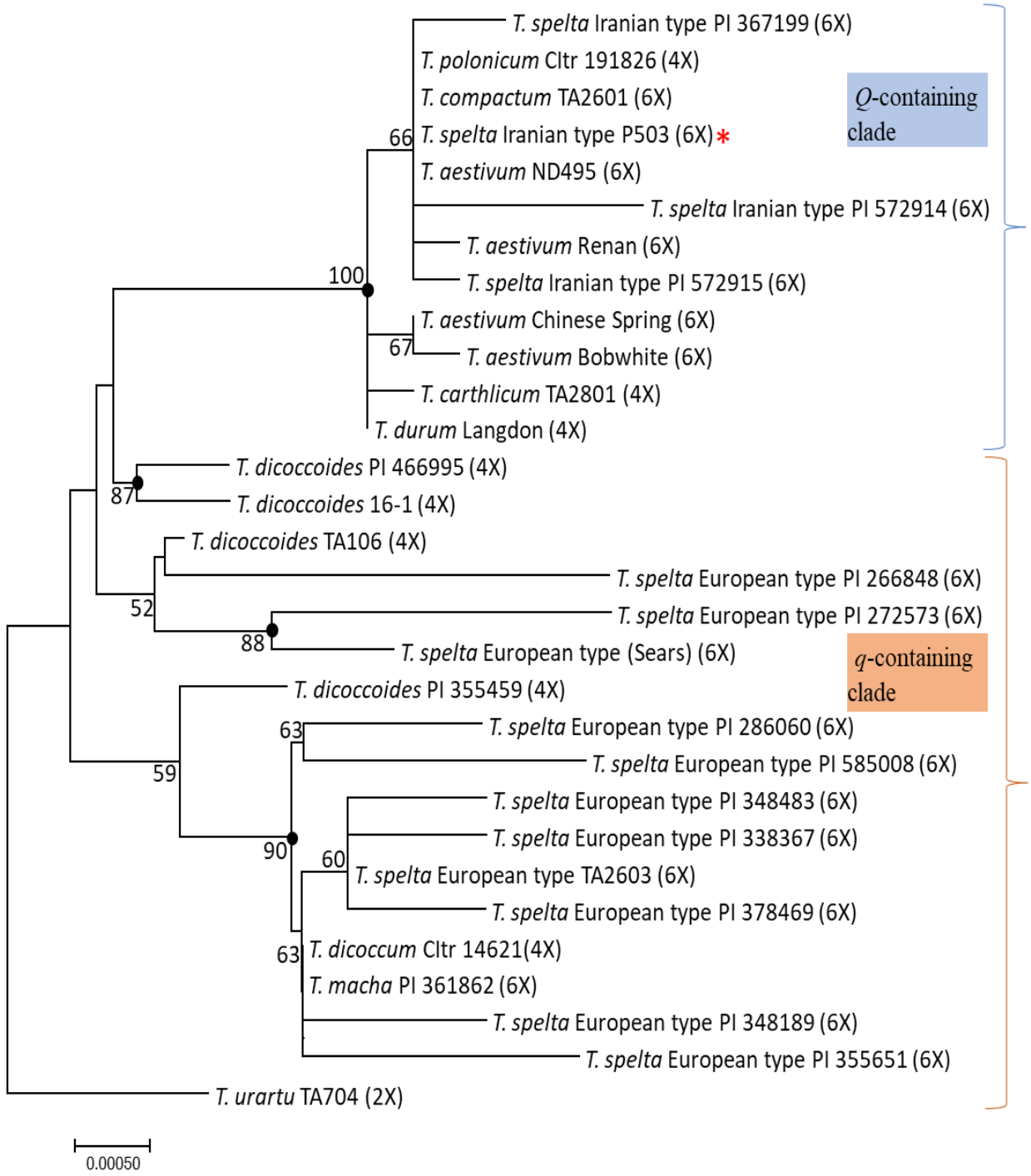

Figure 3.6. Phylogenetic tree of 30 genotypes based on the genomic sequence of the *Q* gene. The ploidy level of each genotype is indicated in parenthesis. Bootstrap values (%) > 50% are shown. Dots indicate nodes supported by bootstrap values > 70% and by strict consensus maximum parsimony tree. *Q* and *q*-containing clades are represented by blue and orange colour, respectively. Iranian spelta P503 is represented by star.

3.5. Discussion

3.5.1. Days to heading

The major difference between spring and winter wheat is their requirement of vernalization to initiate flowering to achieve reproductive success. Therefore, it plays a crucial role in favoring different varieties to adapt to diverse environmental conditions by modulating flowering time. In the CSP population, I identified a QTL on chromosome 5D with major effects for days to heading, and P503 contributed longer heading time for this QTL in the population. It is likely that the effects of *QEet.fcu-5D* are due to the *Vrn-D1* gene (Pugsley 1971; Law et al. 1976), which is known to be on the long arm of chromosome 5D in the same vicinity.

3.5.2. Plant height

Transgressive segregants were observed for all replicates along with broad variation in the population. Comparable results were previously reported for this trait (Kato et al. 1999; Klahr et al. 2007; Wu et al. 2010; Gang et al. 2011; and Cui et al. 2011).

Three QTLs on chromosomes 6A, 7A, and 7D were associated with plant height. The 6A QTL (*QHt.fcu-6A*) was common between replicate 2 of season 2 and average of season 3 replicates. It mapped to a position similar to that of the reduced height gene *Rht18* based on the locations of common markers (Konzak 1987, 1988; Tang 2015; Ford et al. 2018). *QHt.fcu-7A* was in a marker interval similar to that of *QPH.caas-7AL* as reported by Gao et al. (2015), and *QHt.fcu-7D* may be the same as that reported by Griffiths et al. (2012) based on the observation that both are near the centromere. Additionally, both 7A and 7D QTLs were experiment-specific, possibly due to minor G × E interactions.

3.5.3. Spike morphology

SL, KPS, GW, and SPS are the spike components that ultimately play key roles in determining grain yield. Spike length was controlled by a QTL on chromosome 1A (*QEl.fcu-1A*) that was in a position comparable to one reported by Marza et al. (2006) and Ma et al. (2007).

QKps.fcu-5D had large effects on KPS and was significant in all three seasons. This genomic region was also associated with grain weight. Such pleiotropic effects of this region are presumably controlled by *Vrn-D1,* which is known to have a strong influence on spike morphology traits (Kato et al. 2000).

The second QTL associated with KPS, *QKps.fcu-6A,* mapped in a position similar to *QChl-10.caas-6AS,* a QTL associated with chlorophyll content at 10 days post anthesis, which was reported by Gao et al. (2015). A study conducted by Yildirim et al. (2011) showed a positive correlation between chlorophyll SPAD reading and grain yield determined by grain number. Therefore, it is possible that kernel number is indirectly related with chlorophyll content. *QKps.fcu-6A* could also be the same QTL reported by Heidari et al. (2011) for grain yield. However, SNP markers were not used by Heidari et al. (2011) for genotyping, and therefore a definitive conclusion cannot be made regarding the same.

The QTL *QSpn.fcu-7A* for spikelets per spike is in a position similar to one reported by Zhai et al. (2016). *TaMOC1-7A* might be the gene underlying *QSpn.fcu-7A* and is already known to be associated with spikelet number in common wheat (Zhang et al. 2015). MOC1 is the orthologous gene in tomato (*Lateral suppressor Ls*), Arabidopsis (*LATERAL SUPPRESSOR LAX*) and rice (*MONOCULM 1 MOC1*) that regulate axillary meristem (AM) initiation and outgrowth, and spikelets are produced by AMs. *TaMOC1*, the wheat ortholog of rice *MOC1,* encodes a protein that is localized in the nucleus with transcriptional activation function.

TaMOC1-7A HapH is one such haplotype that might be associated with wheat domestication and Chinese wheat breeding history based on evolutionary analysis (Zhang et al. 2015).

3.5.4. Seed threshability

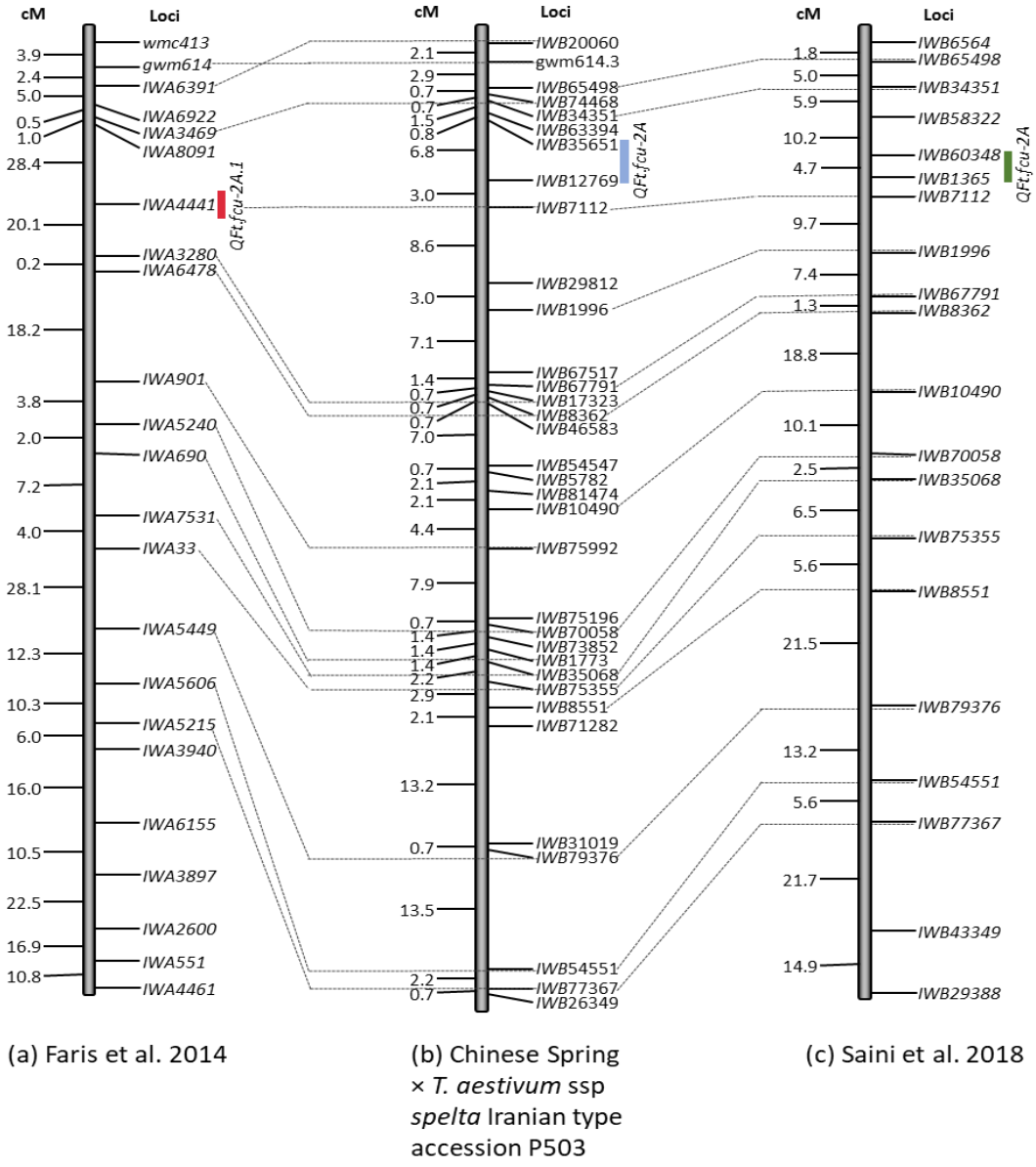

Figure 3.7. Marker comparison of the chromosome 2A QTL associated with threshability with previously reported QTLs in the *Tg*^{2A} locus region. The chromosome 2A genetic linkage map developed in a) Ben × PI 41025 RIL population using 9k SNPs and microsatellites, b) Chinese Spring × *Triticum aestivum* ssp. *spelta* Iranian type accession P503 RIL population using 90k SNPs and microsatellites, and c) Rusty × PI 193883 RIL population using 90k SNPs and microsatellites. The genetic distances in centimorgans (cM) are shown along the left side of map and markers are shown along the right. The dotted lines connect the common markers among three genetic maps. The genetic location of the *Tg*^{2A} QTL is shown in indicated by red (a), blue (b), and green (c) rectangles in genetic maps- a, b, and c, respectively.

The genes *Q* and *Tg* are known to be responsible for the free-threshing character of wheat. In absence of *Q*, *Tg* is expected to confer the non-free-threshing character in *T. spelta* and similar results were found in this research. The QTL on chromosome 2A had large effects on threshability. Comparisons of markers with Faris et al. (2014a) and Saini et al. (2018) (Figure 3.7) indicate that the effects at *QFt.fcu-2A* were due to the Tg^{2A} allele. Additionally, a second QTL on chromosome arm 2BS was detected in two replicates with LOD > 3.5 and in third replicate with LOD < 3.5 (data not shown). This experiment-specific QTL explained up to 15.5% of the phenotypic variation and peaked at marker *wmc154*, and therefore corresponded well with Tg^{2B} locus (Faris et al. 2014a). However, probably due to some genetic factors in the background and/or small population size, effects of this QTL were minimized. Previously, minor QTLs on chromosome 3A and 2A proximal to the Tg^{2A} locus were reported by Faris et al. (2014a); 4D and 5D were reported by Katkout et al. (2014); 6A, 6D, and 7B by Jantasuriyarat et al. (2004); 4A, 4B, and 7B by Peleg et al. (2011); and 6B by Simmonetti et al. (1999). However, in the CSP population, no QTLs were observed on these chromosomes.

Both Faris et al. (2014a) and Saini et al. (2018) reported Tg^{2A} and Tg^{2B} loci along with the *Q* locus to control threshability in tetraploid populations derived from crosses between durum wheat and cultivated emmer (*T. turgidum* ssp. *dicoccum*) accessions. Although QTLs underlying *Tg* loci reported in both studies are in similar locations as detected in this work, R^2 values varied among the three populations. In the BP025 population (Faris et al. 2014a), Tg^{2B} explained 17.2% of the variation and Tg^{2A} explained 5.7%, whereas in the RP883 population (Saini et al. 2018), Tg^{2A} had more substantial effects explaining 22.5% and Tg^{2B} explained only 6.7%. Our study had relatable results to Saini et al. (2018) and showed Tg^{2A} explained 20% of the phenotypic variation, whereas Tg^{2B} was not significant. This difference in effects at *Tg* loci might be because

that *Q* is not segregating in CSP population, difference in ploidy level, or due to some other genetic factors.

3.5.5. Evolution of Iranian spelta

Given the importance of wheat to humankind, the understanding of its origin and evolution is of concern. It has been reported with genetic evidence that European spelta evolved from hybridization between *T. aestivum* ssp. *compactum* and cultivated emmer (Bertsch 1943; MacKey 1966; Blatter et al. 2002, 2004; and Yan et al. 2003). However, the origin of Iranian spelta has always been controversial due to its small and sporadically existed population in medieval times, and two scenarios of its origin have been debated. Some researchers believe Iranian spelta to be the first amphiploid ancestral to modern day wheat, but archaeological evidence support the claim that it evolved later from free threshing hexaploid wheat.

Presence of the *Q* allele in P503 makes it clear that one of its parents would have had the free-threshing *Q* allele. Iranian spelta could be the first amphiploid in scenario one (Figure 3.8), and could have resulted from the hybridization of a *Q*-containing cultivated emmer wheat with *Ae. tauschii*. Although cultivated emmer is considered to be a *q*-containing subspecies of *T. turgidum*, a few accessions have been found to contain the *Q* allele (Muramatsu 1979; J. Faris, personal communication), which they may have acquired through recent gene-flow events. The resulting amphiploid would have had the *Q* allele and semi-tough glumes due to *Tg* alleles at A and/or B and D genomes. The amphiploid would have had to undergo rapid mutation in the Tg^{2D} gene to give genotype $Tg^{2A}Tg^{2A}/Tg^{2B}Tg^{2B}/tg^{2D}tg^{2D}/Q^{5A}Q^{5A}$, which would resemble that of P503. However, if this were the case then mutations in Tg^{2A} and Tg^{2B} would have had to happen to give rise to fully free threshing hexaploid, which would be expected to take considerable time. The absence of remains of spelta before the occurrence of free-threshing hexaploid make this

scenario unlikely. Moreover, the phylogenetic tree structure (Figure 3.6) argues against this scenario because Iranian spelta did not form a clade intermediate to *Q*- and *q*-containing accessions, but instead clustered close to the other *Q*-containing accessions.

A second scenario would be the more recent hybridization of a free-threshing hexaploid with cultivated or wild emmer (Figure 3.8). The resulting amphiploid would have Tg^{2A} and/or Tg^{2B}, tg^{2D}, and *Q*, which would resemble the P503 genotype. This hypothesis agrees well with Dvorak et al. (2012) where the group reported the presence of inactive tg^{2D} alleles in 5 out of 6 Asian spelta accessions. Moreover, based on the archaeological evidence, remains of spelta wheat were dated 1000 years later than the occurrence of free-threshing ssp. *aestivum* from 8th-9th millennium BP in the Near East (Feldman 2001). Faris (2014) also suggested that the cultivation of free-threshing wheat was followed by hulled hexaploids and speculated that, like European spelta, Iranian spelta could be a secondary derivative. The absence of ancestral hulled hexaploids might be due to its lack of advantage over cultivated emmer (Feldman 2001). Likewise, my phylogenetic tree results (Figure 3.6) support scenario 2, considering Iranian spelta did not form an intermediate clade between *Q*- and *q*-containing accessions. Although my results strongly suggest that Iranian spelta is not the primitive form of free-threshing hexaploid wheat, more work is needed to confirm these results including the evaluation of more Iranian spelta accessions, more extensive phylogenetic analyses based on genome-wide sequences, and cloning and analyses of the *Tg* genes.

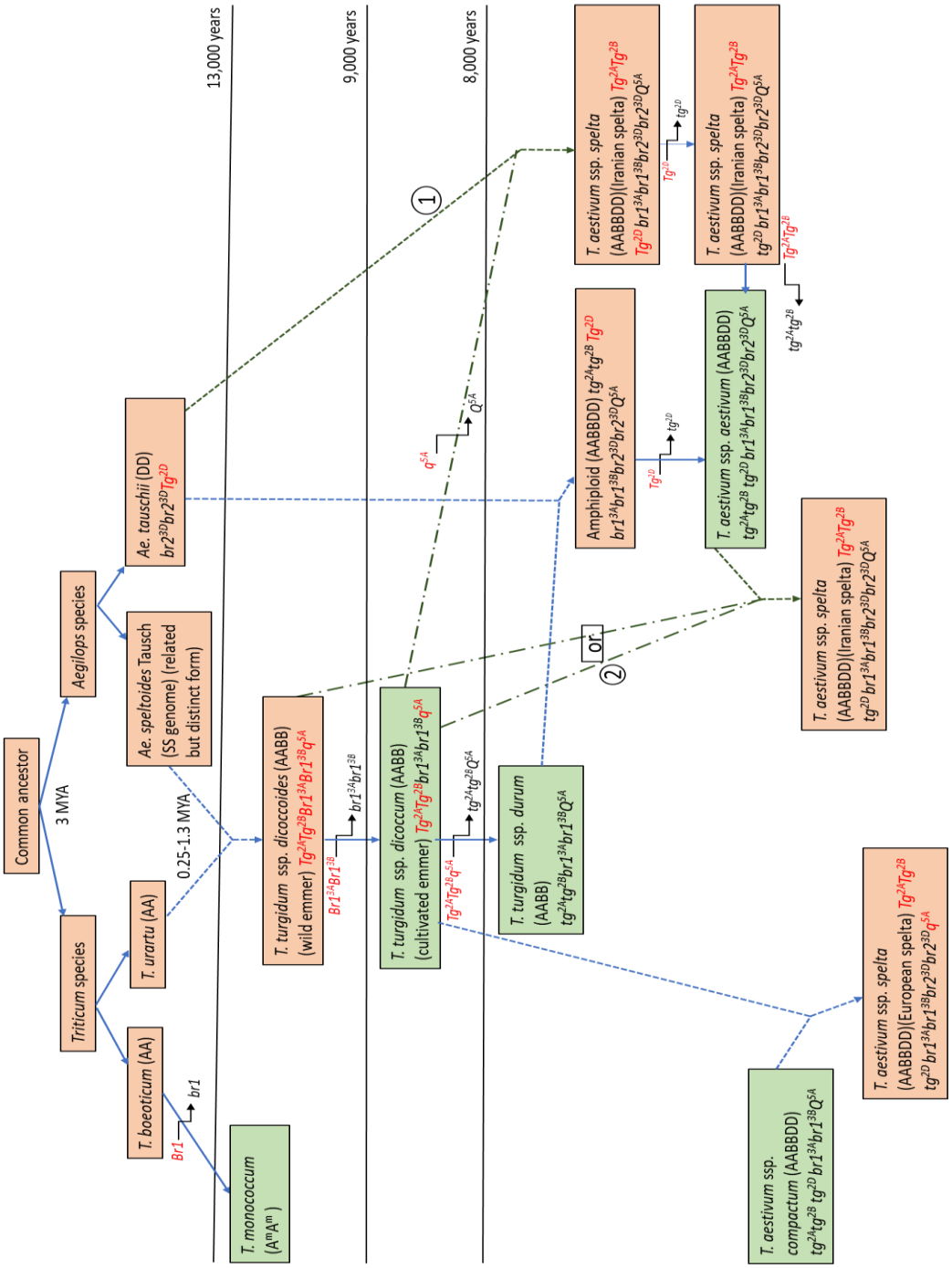

Figure 3.8. Model representing two hypothetical scenarios for the evolution of Iranian spelta. The pre-domestication and domesticated alleles for brittle rachis (*Br*), tenacious glume (*Tg*), and non-free-threshing (*q*) are shown in red and black font color, respectively. Scenario 1, indicates that *Q*-containing emmer hybridized with *Ae. tauschii* to give rise to amphiploid that mutated rapidly at Tg^{2D} locus to give $Tg^{2A}Tg^{2A}Tg^{2B}Tg^{2B}tg^{2D}tg^{2D}Q^{5A}Q^{5A}$ genotype that resembles P503 phenotype. Scenario 2, in which free-threshing hexaploid wheat hybridizes with cultivated/wild emmer to form Iranian spelta.

3.6. References

Avni R, Nave M, Barad O, et al (2017) Wild emmer genome architecture and diversity elucidate wheat evolution and domestication. Science 357:93–97. doi: 10.1126/science.aan0032

Bertsch F (1943) Der Dinkel. Landw Jahrbuch 92:241-252

Blake NK, Lehfeldt BR, Lavin M, et al (1999) Phylogenetic reconstruction based on low copy DNA sequence data in an allopolyploid: the B genome of wheat. Genome 42:351–360

Blatter RHE, Jacomet S, Schlumbaum A (2004) About the origin of European spelt (*Triticum spelta* L.): allelic differentiation of the HMW Glutenin B1-1 and A1-2 subunit genes. Theor Appl Genet 108:360–367. doi: 10.1007/s00122-003-1441-7

Blatter RHE, Jacomet S, Schlumbaum A (2002) Spelt-specific alleles in HMW glutenin genes from modern and historical European spelt (Triticum spelta L.). Theor Appl Genet 104:329–337. doi: 10.1007/s001220100680

Cavanagh CR, Chao S, Wang S, et al (2013) Genome-wide comparative diversity uncovers multiple targets of selection for improvement in hexaploid wheat landraces and cultivars. PNAS 110:8057–8062. doi: 10.1073/pnas.1217133110

Chalupska D, Lee HY, Faris JD, et al (2008) *Acc* homoeoloci and the evolution of wheat genomes. PNAS 105:9691–9696. doi: 10.1073/pnas.0803981105

Cui F, Li J, Ding A, et al (2011) Conditional QTL mapping for plant height with respect to the length of the spike and internode in two mapping populations of wheat. Theor Appl Genet 122:1517–1536. doi: 10.1007/s00122-011-1551-6

Debernardi JM, Lin H, Faris JD, et al (2017) microRNA172 plays a critical role in wheat spike morphology and grain threshability. Development 144:1966-1975. doi: 10.1242/dev.146399

Dvorak J, Deal KR, Luo MC, et al (2012) The origin of spelt and free-threshing hexaploid wheat. J Hered 103:426–441. doi: 10.1093/jhered/esr152

Dvorak J, Terlizzi P di, Zhang HB, et al (1993) The evolution of polyploid wheats: identification of the A genome donor species. Genome 36:21–31. doi: 10.1139/g93-004

Dvorak J, Zhang HB (1990) Variation in repeated nucleotide sequences sheds light on the phylogeny of the wheat B and G genomes. PNAS U S A 87:9640–9644

Edgar RC (2004) MUSCLE: multiple sequence alignment with high accuracy and high throughput. Nucleic Acids Res 32:1792–1797. doi: 10.1093/nar/gkh340

Faris J, Simons K, Zhang Z, et al (2005) The wheat super domestication gene *Q*. Wheat Inf Serv 100:129–148

Faris JD (2014) Wheat Domestication: Key to Agricultural Revolutions Past and Future. In: Tuberosa R, Graner A, Frison E (eds) Genomics of Plant Genetic Resources: Volume 1. Managing, sequencing and mining genetic resources. Springer Netherlands, Dordrecht, pp 439–464

Faris JD, Fellers JP, Brooks SA, et al (2003) A bacterial artificial chromosome contig spanning the major domestication locus *Q* in wheat and identification of a candidate gene. Genetics 164:311–321

Faris JD, Gill BS (2002) Genomic targeting and high-resolution mapping of the domestication gene *Q* in wheat. Genome 45:706–718

Faris JD, Haen KM, Gill BS (2000) Saturation mapping of a gene-rich recombination hot spot region in wheat. Genetics 154:823–835

Faris JD, Zhang Q, Chao S, et al (2014a) Analysis of agronomic and domestication traits in a durum × cultivated emmer wheat population using a high-density single nucleotide polymorphism-based linkage map. Theor Appl Genet 127:2333–2348. doi: 10.1007/s00122-014-2380-1

Faris JD, Zhang Z, Chao S (2014b) Map-based analysis of the tenacious glume gene *Tg-B1* of wild emmer and its role in wheat domestication. Gene 542:198–208. doi: 10.1016/j.gene.2014.03.034

Feldman M, Bonjean A, Angus W (2001) The Origin of cultivated wheat. The Origin of Cultivated Wheat In the Wheat Book 1–56

Ford B, Foo E, Sharwood RE, et al (2018) *Rht18* Semi-Dwarfism in wheat is due to increased expression of GA 2-oxidaseA9 and lower GA content. Plant Physiol 177:168-180. doi: 10.1104/pp.18.00023

Gao F, Wen W, Liu J, et al (2015) Genome-Wide linkage mapping of QTL for yield components, plant height and yield-related physiological traits in the Chinese wheat cross Zhou 8425B/Chinese Spring. Front Plant Sci 6:1099. doi: 10.3389/fpls.2015.01099

Griffiths S, Simmonds J, Leverington M, et al (2012) Meta-QTL analysis of the genetic control of crop height in elite European winter wheat germplasm. Molecular Breeding 29:159–171. doi: 10.1007/s11032-010-9534-x

Heidari B, Sayed-Tabatabaei BE, Saeidi G, et al (2011) Mapping QTL for grain yield, yield components, and spike features in a doubled haploid population of bread wheat. Genome 54:517–527. doi: 10.1139/g11-017

Huang S, Sirikhachornkit A, Su X, et al (2002) Genes encoding plastid acetyl-CoA carboxylase and 3-phosphoglycerate kinase of the *Triticum*/*Aegilops* complex and the evolutionary history of polyploid wheat. PNAS 99:8133–8138. doi: 10.1073/pnas.072223799

Jantasuriyarat C, Vales MI, Watson CJW, et al (2004) Identification and mapping of genetic loci affecting the free-threshing habit and spike compactness in wheat (*Triticum aestivum* L.). Theor Appl Genet 108:261–273. doi: 10.1007/s00122-003-1432-8

Joehanes R, Nelson JC (2008) QGene 4.0, an extensible Java QTL-analysis platform. Bioinformatics 24:2788–2789. doi: 10.1093/bioinformatics/btn523

Katkout M, Kishii M, Kawaura K, et al (2014) QTL analysis of genetic loci affecting domestication-related spike characters in common wheat. Genes Genet Syst 89:121-131. doi: 10.1266/ggs.89.121

Kato K, Miura H, Sawada S (2000) Mapping QTLs controlling grain yield and its components on chromosome 5A of wheat. Theor Appl Genet 101:1114–1121. doi: 10.1007/s001220051587

Kato K, Miura H, Sawada S (1999) QTL mapping of genes controlling ear emergence time and plant height on chromosome 5A of wheat. Theor Appl Genet 98:472–477. doi: 10.1007/s001220051094

Kerber ER, Rowland GG (1974) Origin of the free threshing character in hexaploid wheat. Can J Genet Cytol 16:145–154. doi: 10.1139/g74-014

Kihara H (1944) Discovery of the DD-analyser, one of the ancestors of *Triticum vulgare* (abstr). Agric Hortic 19:889–890

Klahr A, Zimmermann G, Wenzel G, et al (2007) Effects of environment, disease progress, plant height and heading date on the detection of QTLs for resistance to Fusarium head blight in an European winter wheat cross. Euphytica 154:17–28. doi: 10.1007/s10681-006-9264-7

Konzak CF (1987) RhtGenes. Ann. Wheat Newsletter 33:174-175.

Konzak CF (1988) Genetic analysis, genetic improvement and evaluation of induced semi-dwarf mutants in wheat. Semidwarf Cereal Mutants and Their Use in Cross-Breeding III Research Coordination Meeting, December, 16-20, 1985 77–94

Kosambi DD (1943) The estimation of map distances from recombination values. Ann Eugen 12:172–175. doi: 10.1111/j.1469-1809.1943.tb02321.x

Kuckuck H (1959) Neuere Arbeiten zur Entstehung der hexaploiden Kulturweizen. Z. Pflanzenzücht 41:205-226

Kuckuck H (1959) On the findings of *Triticum spelta* L. in Iran and on the arising of *Triticum aestivum*-types through crossing of different Spelta-types. In: Wheat Inform Serv Kyoto. https://eurekamag.com/research/014/129/014129580.php. Accessed 20 Dec 2018

Kuckuck H (1960) Über das Vorkommen von *Triticum spelta* im Iran, mit einem Beitrag zur Entwicklung der hexaploiden Kulturweizen. Berichte der 2 Kongress Eucarpia Köln 27-34

Kuckuck H (1964) Experimentelle Untersuchungeb zur Entstehung der Kulturweizen. I. Die variation des iranischen Speltzweizen und seine genetischen Bezeihungen zu *Triticum aestivum* ssp. *vulgare* (Vill., Host) Mac Key, ssp. *spelta* (L.) Thell. und ssp, *macha* (Dek. et Men.) Mac Key mit einem Beitrag zur Genetik des *Spelta*-Komplexes, Z Pflanzenzucht 51:94-140

Law CN, Worland AJ, Giorgi B (1976) The genetic control of ear-emergence time by chromosomes 5A and 5D of wheat. Heredity 36:49–58. doi: 10.1038/hdy.1976.5

Li W, Gill BS (2006) Multiple genetic pathways for seed shattering in the grasses. Funct Integr Genomics 6:300–309. doi: 10.1007/s10142-005-0015-y

Liu G, Xu S, Ni Z, et al (2011) Molecular dissection of plant height QTLs using recombinant inbred lines from hybrids between common wheat (*Triticum aestivum* L.) and spelt wheat (*Triticum spelta* L.). Chin Sci Bull 56:1897–1903. doi: 10.1007/s11434-011-4506-z

Lorieux M (2012) MapDisto: fast and efficient computation of genetic linkage maps. Mol Breeding 30:1231–1235. doi: 10.1007/s11032-012-9706-y

Luo MC, Yang ZL, Dvořák J (2000) The *Q* locus of Iranian and European spelt wheat. Theor Appl Genet 100:602–606. doi: 10.1007/s001220050079

Ma Z, Zhao D, Zhang C, et al (2007) Molecular genetic analysis of five spike-related traits in wheat using RIL and immortalized F2 populations. Mol Genet Genomics 277:31–42. doi: 10.1007/s00438-006-0166-0

MacKey J (1966) Species relationship in Triticum. Hereditas 2:237–276

Marza F, Bai GH, Carver BF, Zhou WC (2006) Quantitative trait loci for yield and related traits in the wheat population Ning7840 x Clark. Theor Appl Genet 112:688–698. doi: 10.1007/s00122-005-0172-3

Mcfadden ES, Sears ER (1946) The origin of *Triticum spelta* and its free-threshing hexaploid relatives. J Hered 37:81–89. doi: 10.1093/oxfordjournals.jhered.a105590

Muramatsu M (1979) Presence of vulgare gene, *Q*, in a dense-spike variety of *Triticum dicoccum* Schubl. Rep Plant Germplasm Inst Kyoto Univ 4:39–41

Nalam VJ, Vales MI, Watson CJW, et al (2007) Map-based analysis of genetic loci on chromosome 2D that affect glume tenacity and threshability, components of the free-threshing habit in common wheat (*Triticum aestivum* L.). Theor Appl Genet 116:135–145. doi: 10.1007/s00122-007-0653-7

Nesbitt M, Samuel D (1996) From staple crop to extinction? The archaeology and history of the hulled wheats. In: Proceedings of the First International Workshop on Hulled Wheats: 21-22 July 1995; Castelvecchio Pascoli, Tuscany, Italy. pp 41–100

Peleg Z, Fahima T, Korol AB, et al (2011) Genetic analysis of wheat domestication and evolution under domestication. J Exp Bot 62:5051–5061. doi: 10.1093/jxb/err206

Peng J, Ronin Y, Fahima T, et al (2003) Domestication quantitative trait loci in *Triticum dicoccoides*, the progenitor of wheat. PNAS 100:2489–2494. doi: 10.1073/pnas.252763199

Pugsley A (1971) A genetic analysis of spring-winter habit of growth in wheat. Aust J Agr Res 22:21-31. doi: 10.1071/AR9710021

Salse J, Bolot S, Throude M, et al (2008) Identification and characterization of shared duplications between rice and wheat provide new insight into grass genome evolution. Plant Cell 20:11–24. doi: 10.1105/tpc.107.056309

Simonetti MC, Bellomo MP, Laghetti G, et al (1999) Quantitative trait loci influencing free-threshing habit in tetraploid wheats. Genet Resour Crop Evol 46:267–271. doi: 10.1023/A:1008602009133

Simons KJ, Fellers JP, Trick HN, et al (2006) Molecular characterization of the major wheat domestication gene *Q*. Genetics 172:547–555. doi: 10.1534/genetics.105.044727

Snedecor GW, Cochran WG (1980) Statistical methods, 7th ed. Ames, Iowa : Iowa State University Press

Sood S, Kuraparthy V, Bai G, et al (2009) The major threshability genes soft glume (*sog*) and tenacious glume (*Tg*), of diploid and polyploid wheat, trace their origin to independent mutations at non-orthologous loci. Theor Appl Genet 119:341–351. doi: 10.1007/s00122-009-1043-0

Tamura K, Stecher G, Peterson D, et al (2013) MEGA6: Molecular Evolutionary Genetics Analysis Version 6.0. Mol Biol Evol 30:2725–2729. doi: 10.1093/molbev/mst197

Tang T (2016) Physiological and genetic studies of an alternative semi-dwarfing gene *Rht18* in wheat. PhD thesis, University of Tasmania

Thanh PT, Vladutu CI, Kianian SF, et al (2013) Molecular genetic analysis of domestication traits in emmer wheat. I: Map Construction and QTL Analysis using an F2 Pupulation. Biotechnol Biotechnol Equip 27:3627–3637. doi: 10.5504/BBEQ.2013.0008

Wang S, Wong D, Forrest K, et al (2014) Characterization of polyploid wheat genomic diversity using a high-density 90,000 single nucleotide polymorphism array. Plant Biotechnol J 12:787–796. doi: 10.1111/pbi.12183

Watanabe N, Ikebata N (2000) The effects of homoeologous group 3 chromosomes on grain colour dependent seed dormancy and brittle rachis in tetraploid wheat. Euphytica 115:215–220. doi: 10.1023/A:1004066416900

Wu X, Wang Z, Chang X, et al (2010) Genetic dissection of the developmental behaviours of plant height in wheat under diverse water regimes. J Exp Bot 61:2923–2937. doi: 10.1093/jxb/erq117

Yan Y, Hsam SLK, Yu JZ, et al (2003) HMW and LMW glutenin alleles among putative tetraploid and hexaploid European spelt wheat (*Triticum spelta* L.) progenitors. Theor Appl Genet 107:1321–1330. doi: 10.1007/s00122-003-1315-z

Yıldırım M, KILIÇ H, Kendal E, Karahan T (2011) Applicability of chlorophyll meter readings as yield predictor in durum wheat. J Plant Nutr 34:151–164. doi: 10.1080/01904167.2011.533319

Zhai H, Feng Z, Li J, et al (2016) QTL Analysis of spike morphological traits and plant height in winter wheat (*Triticum aestivum* L.) using a high-density SNP and SSR-based linkage map. Front Plant Sci 7:. doi: 10.3389/fpls.2016.01617

Zhang B, Liu X, Xu W, et al (2015) Novel function of a putative *MOC1* ortholog associated with spikelet number per spike in common wheat. Sci Rep 5:12211. doi: 10.1038/srep12211

SAS Institute (2011) SAS/STAT 9.3 User's Guide. SAS Instiute Inc., Cary, NC

4. SATURATION MAPPING OF THE *PARASTAGONOSPORA NODORUM SNN5* SUSCEPTIBILITY GENE IN WHEAT

4.1. Abstract

Parastagonospora nodorum is a filamentous ascomycete that produces multiple necrotrophic effectors that play significant roles in host cell death when recognized by corresponding wheat sensitivity genes. This system follows an inverse gene-for-gene interaction to cause severe foliar disease on wheat. The SnTox5-*Snn5* interaction was first identified in a tetraploid doubled haploid population derived from Lebsock (sensitive) and PI 94749 (insensitive) (LP749), and *Snn5* was mapped on the short arm of chromosome 4B. In this study, I used the LP749 population to develop a saturated map of the *Snn5* region on chromosome 4B of wheat. Multiple resources were used for marker design, and two co-segregating markers were found. Additionally, flanking markers that were developed delineated *Snn5* to 2.8 cM interval. The physical distance between the *Snn5*-flanking markers was 1.38 Mb and a total of 16 putative genes were found within the interval based on reference genome annotations. Markers developed in this study will further facilitate marker-assisted selection and eventual positional cloning of *Snn5*.

4.2. Introduction

Pathogens invade the plant interior and colonize themselves for their own survival. Plants evolved their first layer of immunity against these pathogens by recognizing pathogen-associated molecular patterns (PAMPs) via plant recognition receptors (PRRs) (Jones and Dangl 2006). PAMPs are microbial conserved features critical for survival of pathogen, and PRRs are host cell receptors often present in plasma membrane that recognize PAMPs to initiate pathogen triggered immunity (PTI) (reviewed in Chisholm et al. 2006). However, pathogens escaped PTI by

secreting effector proteins, but plants subsequently developed a second layer of defense referred to as effector-triggered immunity (ETI), which involves direct or indirect recognition of effectors by plant resistance (*R*) proteins resulting in programmed cell death (Jones and Dangl 2006; Zipfel 2009; Tsuda and Katagiri 2010). ETI is a well-studied mechanism in biotrophs but less is known about its mechanism in plants against necrotrophs, which feed on dead or dying tissue.

Parastagonospora [syn. *anamorph*: Stagonospora; *teleomorph*: *Phaeosphaeria*] *nodorum* (Berk.) syn. *Leptosphaeria nodorum* (Müll.) Quaedvleig, Verkley and Crous, belongs to Pleosporales class of fungi in Dothideomycetes order of Ascomycetes. It is a necrotroph that derives energy from dead host tissue to complete its life cycle (reviewed by Friesen and Faris 2010) and causes Septoria nodorum blotch (SNB). It was first reported as a pathogen that caused glume blotch on wheat in 1845 in England (Blaker 1978). Recent studies have shown that necrotrophic effectors (NEs) are secreted by these pathogens, and when recognized by host-specific genes cause similar events as in ETI. However, the host response including cell death is advantageous to the pathogen because it is a necrotroph (Oliver and Solomon 2010). This inverse gene-for-gene relationship is referred to as necrotrophic effector-triggered susceptibility (NETS) (Friesen and Faris 2010; Oliver et al. 2012; Liu et al. 2012).

So far, nine *P. nodorum* NE-wheat sensitivity gene interactions have been characterized: SnToxA-*Tsn1* (Friesen et al. 2006, 2009; Liu et al. 2006; Zhang et al. 2009; Faris et al. 2010, 2011; Faris and Friesen 2009), SnTox1-*Snn1* (Liu et al. 2004a, b, 2012; Reddy et al. 2008; Shi et al. 2016a), SnTox2-*Snn2* (Friesen et al. 2007, 2009; Zhang et al. 2009), SnTox3-*Snn3-B1* (Friesen et al. 2008; Liu et al. 2009; Shi et al. 2016b), SnTox3-*Snn3-D1* (Zhang et al. 2011), SnTox4-*Snn4* (Abeysekara et al. 2009, 2012), SnTox5-*Snn5* (Friesen et al. 2012), SnTox6-*Snn6* (Gao et al. 2014), SnTox7-*Snn7* (Shi et al. 2015). *SnToxA*, *SnTox1*, and *SnTox3* have been cloned

from the pathogen and *Tsn1* and *Snn1* have been cloned in wheat. *Tsn1* contains protein kinase, nucleotide binding (NB) and leucine-rich repeat (LRR) domains (Faris et al. 2010), whereas *Snn1* belongs to WAK family of receptor kinases (Shi et al. 2016b). The cloning of these genes has shown the presence of characteristic disease-resistance gene domains in host sensitivity genes and demonstrated *P. nodorum*'s ability to hijack host resistance molecular pathway to cause susceptibility.

Because of wheat's world wide importance as a food crop, knowing the chromosomal location of genes with detrimental effects is important for its adaptation to disease infested regions. One such effector-host gene interaction, SnTox5-*Snn5*, was identified in a tetraploid population and mapped on long arm of chromosome 4B of wheat. An F_2 population derived from same parents confirmed the dominant nature of the *Snn5* sensitivity gene. This interaction explained 63% of the variation in disease when segregating alone in the population, and the disease severity was much higher when either combined with SnToxA-*Tsn1* or SnTox3-*Snn3-B1* (Friesen et al. 2012). SnTox5 was found to be a fairly heat stable protein with estimated size between 10-30 kDA (Friesen et al. 2012). Similar to other known effectors, a compatible SnTox5-*Snn5* interaction was shown to be dependent on light.

A dense molecular map is a pre-requisite to clone a gene using a map-based approach. The benefit of a dense linkage map is in its usage for screening multiple mapping populations to locate important segregating genes. The objectives of this study were to develop a saturated genetic linkage map of the *Snn5* region and to develop markers suitable for marker-assisted selection against *Snn5*.

4.3. Material and methods

4.3.1. Plant materials

A doubled haploid (DH) population was derived from a cross between Lebsock and the *T. turgidum* ssp. *carthlicum* accession PI 94749 (Chu et al. 2010) (hereafter referred to as LP749 population). Lebsock is a North Dakota durum wheat variety and previous results have shown that it is sensitive to SnTox5. PI 94749 was originally obtained from USDA-ARS National Small Grain Research Facility, National Small Grain Collection, Aberdeen, ID and is insensitive to SnTox5 (Friesen et al. 2012). LP749 is a tetraploid population that consists of 146 DH lines and was used for mapping newly developed markers to saturate the *Snn5* region. All plants were grown in the greenhouse with average temperature of 21°C and with 16-h photoperiod.

4.3.2. Necrotrophic effector bioassays

Culture filtrates (CF) of *P. nodorum* isolates Sn2000K06-1 and Sn99CH1A7a were prepared according to Friesen and Faris (2012). Infiltration of differential lines along with the parents Lebsock and PI 94749 was done using filter-sterilized CF to ensure the presence of SnTox5. All differential and parental lines were planted in small cones, each having three seeds of same line. Approximately 25 ul of active CF was infiltrated using a 1 ml needless syringe into the fully expanded second leaf of each plant. The infiltration boundary was marked with a marker and plants were kept in a growth chamber at 21˚C with a 16-hour photoperiod. Plants were scored at 3 days post infiltration and were marked as sensitive or insensitive depending on presence or absence of necrosis.

4.3.3. Marker development and molecular mapping

Previously published wheat genetic and physical maps (Song et al. 2005; Roder et al. 1998; Sourdille et al. 2004; Somers et al. 2004; Torada et al. 2006; Xu et al. 2008) were scanned

to find SSRs that were previously reported to map to chromosome arm 4BL. Second, consensus maps based on SNP markers from the 9K (Cavanagh et al. 2013) and 90K arrays (Wang et al. 2014) were downloaded and used as queries in BLASTn searches of wheat chromosome 4B reference sequences (IWGSC 2017) at https://urgi.versailles.inra.fr/blast/. Friesen et al. (2012) reported the location of *Snn5* locus to be distal to the deletion breakpoint 4BL-5-0.86. SNPs that had low-copy hits on 4BL were converted to allele-specific STARP markers by designing the asymmetrically modified allele-specific (AMAS) and reverse primers according to the method described by Long et al. (2017).

Third, the entire 4B chromosome sequence of the durum cultivar Svevo (https://d-data.interomics.eu/node/1) was downloaded and trimmed to identify the genomic region distal to the 4BL-5 (fraction 0.86) breakpoint. The Svevo genome sequence was chosen because Svevo is a tetraploid and its reference genome is available online (https://d-data.interomics.eu/node/1). A total of 138 SSRs, 47 gene-specific primers, 64 repeat junction marker (RJM) (You et al. 2010) (https://probes.pw.usda.gov/RJPrimers/) and repeat junction-junction marker (RJJM) (You et al. 2010) (https://probes.pw.usda.gov/RJPrimers/) were designed to further saturate the *Snn5*-containing region. Gene-specific markers were designed using gene sequences located between genomic positions 637,245,310 and 640,729,297 bp of Svevo using Primer 3 (Rozen and Skaletsky 2000) and along with other markers were tested for polymorphism between the parents.

Fourth, a predicted gene (TraeCS4B02G343100) with sequence similarity to the *Snn3-D1* gene (Faris et al. unpublished) was located at position 636,916,138-636,918,886 bp of chromosome arm 4BL in the CS reference sequence (IWGSC 2017). Blastn with *Snn3-D1* as query sequence gave two hits on TraeCS4B02G343100. These two hits were at positions

636,918,219-636,918,462 and 636,917,881-636,918,088, and showed the two genes shared as much as 71% similarity along the coding regions. Seventeen gene-specific markers spanning the full *Snn3-D1* like gene were designed using Primer 3 (Rozen and Skaletsky 2000) and were checked for polymorphism between the parents. A dominant polymorphic marker was developed and later converted to a co-dominant marker by sequencing the region. All newly designed markers with their forward and reverse sequence are listed in Table 4.1.

Table 4.1. Markers developed for molecular mapping of *Snn5*

Marker type	Marker designation	F primer	R primer	Source[a]	Start position[b]	End position[c]
SSR	*fcp739*	TGTCCGTGTTCTTTGTTCTGA	TTCGTTTGCTGGTATTTTACGA	IWGSC 2017	563664331	563664621
STARP	*fcp740*	GCAACAGGAACCAGCTATGACTCGAAGTGTTGAGATCAGTTT	TCACCCTTGGTCAGGTCAGA	90K SNP	579100013	579100137
		GACGCAAGTGAGCAGTATGACTCGAAGTGTTGAGATCAACTC				
STARP	*fcp741*	GCAACAGGAACCAGCTATGACGTGTTGCTAATCACGAGATCTA	TGGTAACACCGACAATGGCT	90K SNP	594872695	594872895
		GACGCAAGTGAGCAGTATGACGTGTTGCTAATCACGAGACATG				
STARP	*fcp742*	GCAACAGGAACCAGCTATGACCTACAGTTTTTGGCATGTTCC	CGCGCTTACTAATCACCGTC	90K SNP	609513071	609513271
		GACGCAAGTGAGCAGTATGACCTACAGTTTTTGGCATGCCCT				
STARP	*fcp743*	GCAACAGGAACCAGCTATGACGTCAAAATTACAAGCAATCGTAC	TGCAAAATCCATGTGTCCAAATCT	90K SNP	611505762	611505829
		GACGCAAGTGAGCAGTATGACGTCAAAATTACAAGCAATCACAT				
STARP	*fcp744*	GCAACAGGAACCAGCTATGACGAACCACCGCATAAGGCTA	TTCCTGTGGTAACGCAACTTGG	90K SNP	612214519	612214614
		GACGCAAGTGAGCAGTATGACGAACCACCGCATAAGAATG				
STARP	*fcp745*	GCAACAGGAACCAGCTATGACTATGAGCGAATCCGGCCTT	AGCCTCAGGAACTAGGATAATGG	90K SNP	613150370	613150570
		GACGCAAGTGAGCAGTATGACTATGAGCGAATCCGGTTTC				
SSR	*fcp746*	CTGGGTACTGACTAAATGCAA	CAATTACTTCTCGGAATGTTG	IWGSC 2017	617849208	617849362
SSR	*fcp747*	CATTCGACCCCTGCATAGTTA	GTTGCAGGTCTAGTCGCTTTG	CNR ITB 2017	638070884	638071062
SSR	*fcp748*	TGTTTCATTCAATTCGCTTCAT	GGTCATCCACTTGAGGGAAAT	CNR ITB 2017	618846178	618845762
SSR	*fcp749*	CCGACAATACAAAACTTCAAAGG	CCCTTGGTGTTGAGGGTTTAT	IWGSC 2017	632512678	632512887
SSR	*fcp750*	TTTTCTCACAGTTCGGGTGTT	CCTACACGTAGCTCTGCCACT	CNR ITB 2017	637245270	637245480
SSR	*fcp751*	GCAGGTTGCAAGCAATCTTAG	CGCCTCCTGCTACCTCTATTT	CNR ITB 2017	636664782	636664929
SSR	*fcp752*	CGTAGAGAGGGGAGAAACATC	CGGTGTTGATGGTTTATACAAG	CNR ITB 2017	636109141	636109308
SSR	*fcp753*	CCCTAATTTTGCACACCAACA	AGGAGGAAGAAGCAGAAGCAG	CNR ITB 2017	636908831	636909042
SSR	*fcp754*	ACTGCATGCTGGAGTTCACTT	ACCCCAAAGCCTACACATAGC	CNR ITB 2017	637245310	637245457
SSR	*fcp755*	ACTGCATGCTGGAGTTCACTT	ACCCCAAAGCCTACACATAGC	CNR ITB 2017	637245310	637245457
SSR	*fcp756*	CTGCTGCCTCAGATCACAAG	TGCAGGTGATGAATGCTGAC	CNR ITB 2017	638623993	638624150
SSR	*fcp757*	CTTCCTCCTCCTCGGTATCC	CGCCTCTCCTCTGTTTTGAG	CNR ITB 2017	640480730	640480879
SSR	*fcp758*	TCTGGGAATCCTAGCACGAC	TGGGTTTCTCCTTTGTCTCAA	CNR ITB 2017	640729297	640729446

Table 4.1. Markers developed for molecular mapping of *Snn5* (continued)

Marker type	Marker designation	F primer	R primer	Source[a]	Start position[b]	End position[c]
SSR	*fcp759*	TCCTACAAGTGGGAAGCCATT	TCACACGAGGAAGAAGGAGAA	CNR ITB 2017	640977589	640978251
SSR	*fcp760*	AGGAGGGATGCTTGTAACCAC	TGATCGCATCATCACAACAAT	CNR ITB 2017	641150191	641150326
InDel	*fcp761*	ATACACGTCGATATGTCCTTCCTT	CGGGGATAAGTTCACTTCAGTATT	IWGSC 2017	636917017	636917213
SSR	*fcp762*	GTCAGGCCATGTTCGTGTAGT	GAGCTGCCTCATGTGAAACTT	IWGSC 2017	637344574	637344772
STARP	*fcp763*	GCAACAGGAACCAGCTATGACACCATCACCAGAAAGCTTTC	TCTGGGGTGACGAAGATGAC	90K SNP	638116020	638116220
		GACGCAAGTGAGCAGTATGACACCATCACCAGAAAGCCCTT				
STARP	*fcp764*	GCAACAGGAACCAGCTATGACGGACCGAATCCTCGCCA	GTGGCGATGCTGGTTCAAAG	90K SNP	638115851	638116043
		GACGCAAGTGAGCAGTATGACGGACCGAATCCTCATCG				
STARP	*fcp765*	GCAACAGGAACCAGCTATGACCAAGTGATTCTTCATCTCCA	TCAATGGTTGCTGCCAGTTC	90K SNP	638116145	638116345
		GACGCAAGTGAGCAGTATGACCAAGTGATTCTTCATCCTCG				
SSR	*fcp766*	CCCGCACAGTTCTTTTCCT	GGGGACTGGGGAGGAGAT	CNR ITB 2017	643899153	643899304
STARP	*fcp767*	GCAACAGGAACCAGCTATGACCCATCAATTGTGCCACC	TGGAGGATGATCAACCGAGC	90K SNP	645318820	645318920
		GACGCAAGTGAGCAGTATGACCCATCAATTGTGCTGCT				
STARP	*fcp768*	GCAACAGGAACCAGCTATGACCATTTCAGCTAAGCAAATACG	TCGCGTCGTGAAAAAGAACG	90K SNP	644785484	644785584
		GACGCAAGTGAGCAGTATGACCATTTCAGCTAAGCAAACCCA				
SSR	*fcp769*	TCAGGGTCTCCTCGTCCTC	TTTGTAGCCAACCGACTTGAC	CNR ITB 2017	649184824	649184974
SSR	*fcp770*	CCTCGTACCCGCACACAG	CTAGCGGAAGCAGCAGAAGT	CNR ITB 2017	651665469	651665637
SSR	*fcp771*	CGTGCGCCATTACTGTATTTT	GGTGTGCCATTAGTAGTGTTGC	CNR ITB 2017	652193720	652193878
SSR	*fcp772*	CCAAGCGAAGACCTACATCAA	CCTGGTCATAGTGCCAAAAAT	CNR ITB 2017	654118789	654118939
SSR	*fcp773*	TCGGTCTTGCGATAAAAGTTG	TCCACCTTTGAATTGTGTGTG	CNR ITB 2017	656527697	656527860
SSR	*fcp774*	GCGTGTGCTCGTTCTCTTTTA	ACGAGAGCTCGAGGAGGAG	IWGSC 2017	625963650	625963900

[a]90K SNP source: https://wheat.pw.usda.gov/cgi-bin/graingenes/report.cgi?class=mapdata;name=Wheat_2014_90KSNP;show=map;
CNR ITB 2017: https://www.interomics.eu/durum-wheat-genome
IWGSC 2017: https://urgi.versailles.inra.fr/jbrowseiwgsc/

[b, c] The start and end position are in respect to the reference genome from where marker was designed. Marker position for 90K SNPs were obtained from IWGSC 2017 reference genome

4.3.4. Genotyping and linkage map construction

DNA from the parents, the LP749 population, and F_2 plants was extracted as described by Faris *et al*. (2000). The extracted DNA pellet was dissolved in 50 μL of TE buffer and quantified using a Nanodrop spectrophotometer ND-8000. DNA samples were then diluted to approximately 200 ng/μL using distilled water.

Polymerase chain reaction (PCR) amplifications were performed in 10 μL volumes consisting of 200 ng of template DNA, 1X PCR buffer, 1.5 mM $MgCl_2$, 0.125 nM dNTPs, 4 pmol of each primer and 1 unit of Taq DNA polymerase. The PCR conditions were 94˚C for 5 mins, followed by 35 cycles of 94˚C for 30 s, touchdown annealing temperature of 61˚C to 56˚C for 30 s, and 72˚C for 90 s, followed by a final extension of 72˚C for 7 mins. The amplified PCR products were resolved on 6% polyacrylamide gels, stained with GelRed stain, and scanned on a Typhoon FLA 9500 variable mode laser imager (GE Healthcare Life Sciences, Piscataway, NJ).

Linkage maps were assembled using the program MapDisto v.1.8 (Lorieux 2012). Genetic distances were calculated using the Kosambi mapping function (Kosambi 1943) and markers were grouped using the 'find groups' command with a logarithm of odds (LOD) threshold of 3.0 and maximum recombination frequency of 0.3. The command 'order sequence' which uses sum of adjacent frequencies (SARF) was used to establish the initial marker order. The best order of marker loci was determined by using 'check inversions', 'ripple order', and 'drop locus' commands.

4.3.5. BLAST similarity searches

The genomic sequence corresponding to the interval between markers that flanked *Snn5* was obtained from both Chinese Spring (https://urgi.versailles.inra.fr/jbrowseiwgsc/) and Svevo (https://www.interomics.eu/durum-wheat-genome) reference sequences. High confidence genes

from CS were used as queries in tblastx searches of the National Centre for Biotechnology Information (NCBI) non-redundant database (http://www.ncbi.nlm.gov/). A significant match was called when there was at least 40% amino acid identity and an *e*-value of less than e-11 (Lu and Faris 2006). In addition, searches were limited to the Poaceae family to avoid exceeding computation time allowed for single searches on NCBI. For Svevo, sequences between flanking markers were downloaded and subjected to annotation using the TriAnnot (http://urgi.versailles.inra.fr/triannot/) bioinformatics pipeline to find high confidence genes. Again, these genes were searched using tblastx with the same criteria as mentioned above to find the putative corresponding protein.

4.4. Results

4.4.1. Saturation mapping of *Snn5*

All markers were tested for polymorphism between parents Lebsock and PI 94749. All mapped markers are shown in Figure 4.1. From previously published chromosome 4B maps (Song et al. 2005; Roder et al. 1998; Sourdille et al. 2004; Somers et al. 2004; Torada et al. 2006; Xu et al. 2008), *barc1054* mapped on short arm of chromosome 4B, *gwm6* mapped 4.2 cM distal to *Snn5* and *hbg211* mapped on to terminal end of long arm of chromosome 4B. These three SSRs were mapped in this study in addition to 23 SSRs that were previously mapped and published by Chu et al. (2010) and Friesen et al. (2012).

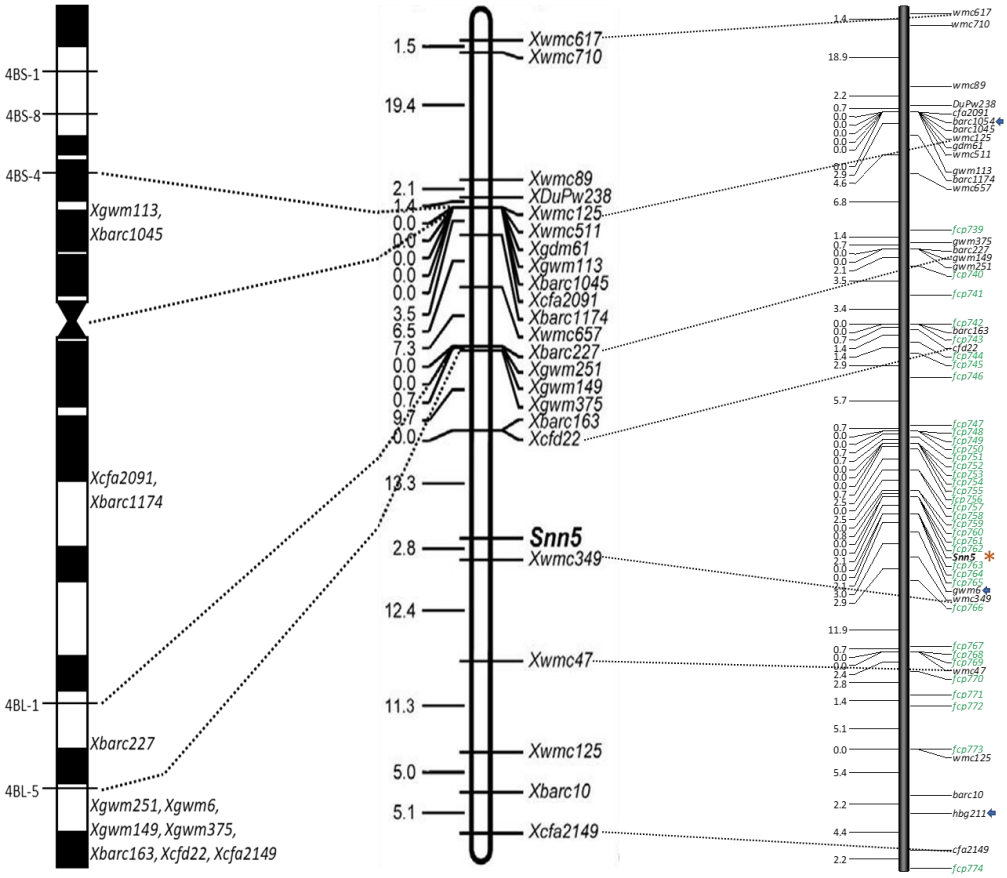

Figure 4.1. Map-based analysis of *Snn5*. Left: Physical map of chromosome 4B; Middle: Low-resolution map constructed in the Lebsock × PI 94749 DH population consisting of 146 lines (Friesen et al. 2012); and right: Saturated map constructed in the same population. centiMorgan distances between markers are indicated to the left of the maps and marker loci to the right. Markers marked by blue arrow are the SSRs mapped in this study. Markers in green represent the new markers designed in this study. The dashed lines connect the same marker mapped in different maps.

Previously, a total of 11 STARP markers were mapped to chromosome arm 4BL (Faris et al. unpublished). Of them, *fcp740* to *fcp745* mapped proximal to *Snn5* at distances ranging from 27.6 cM to 17.2 cM, whereas *fcp763*, *fcp764*, *fcp765*, *fcp767*, and *fcp768* mapped distal to *Snn5*. Three co-segregating STARP markers, *fcp763*, *fcp764*, and *fcp765*, mapped 2.1 cM distal to *Snn5*. *fcp767* and *fcp768* mapped 22.1 cM and 22.8 cM distal to *Snn5*, respectively.

In addition, 64 RJM and RJJM, and 64 gene-specific primer sets for predicted genes were designed. *fcp761* is the gene specific marker for possible homolog of *Snn3-D1* gene on long arm

of chromosome 4B and was found to co-segregating with *Snn5*. The remaining 127 primer sets were either monomorphic or amplified genomic regions other than the targeted region on chromosome 4B.

A total of 138 SSR primer pairs were designed and checked for polymorphism between parents. Of these, 24 (17%) detected loci on 4BL, and *fcp762* was found to co-segregate with *Snn5* (Figure 4.1). SSRs *fcp759* and *fcp760* mapped 0.7 cM proximal to *Snn5* and were therefore closer to *Snn5* than the STARP markers *fcp763, fcp764* and *fcp765*, which mapped 2.1 cM distal to the gene. *fcp739* mapped 31.9 cM proximal to *Snn5* and SSRs *fcp746* to *fcp758* mapped at a distances ranging from 14.3 cM to 3.2 cM proximal to *Snn5*. *fcp766* and *fcp769* to *fcp774* mapped 10.2 cM and 22.8 cM to 48.8 cM distal to *Snn5*, respectively. The genetic map of LP749 was expanded from 102 cM to 118.3 cM.

4.5. Discussion

Parastagonospora nodorum is a necrotrophic specialist pathogen that interacts with wheat in an inverse gene-for-gene manner as opposed to gene-for-gene as Flor (1956) described for biotrophic pathogens. To gain understanding of the molecular mechanisms involved in these host-pathogen interactions, it is necessary to clone the genes from both pathogen and host. The development of saturated genetic maps and reliable molecular markers that are tightly linked to the genes of interest are the first steps towards map-based cloning. Here, I demonstrate the saturation mapping of host sensitivity gene *Snn5* that recognizes necrotrophic effector SnTox5 to result in susceptibility in wheat.

Chu et al. (2010) presented the first genetic map of chromosome 4B in the LP749 population, which harbored 21 SSR markers. The genetic length was 102.3 cM with an average density of 4.9 cM per marker. Friesen et al. (2012) later added three additional markers and

mapped *Snn5* 2.8 cM proximal to *wmc349* on long arm of chromosome 4B. In this study, I added 36 new co-dominant markers along with three SSRs from previously published maps with a focus on saturating the *Snn5* region. The addition of these markers improved the overall average marker density of the map to 1.6 cM per marker. I found two markers, *fcp761* and *fcp762*, that cosegregated with *Snn5*. The markers *fcp759*, *fcp760*, *fcp763*, *fcp764*, and *fcp765* together delineated *Snn5* to 2.8 cM interval.

In a study conducted by Schnurbusch et al. (2003), the group identified two QTLs on chromosome arms 3BS and 4BL for glume blotch resistance. An RI population was derived from the cross between Swiss winter wheat cultivars Arina and Forno and field trials were performed under natural infestation. A 4BL QTL was mapped in the marker interval *gwm251-gwm6*, which corresponds to the location of *Snn5*. The same population was used by Abeysekara et al. (2009) to map *P. nodorum* leaf blotch sensitivity genes using Swiss isolate Sn99Ch1A7a. This group identified a major QTL on chromosome arm 1AS that coincided with *Snn4* and minor QTLs on chromosomes 2A and 3A, indicating that the leaf blotch QTLs did not coincide with glume blotch. In our study, I used the same Sn99Ch1A7a isolate for screening sensitivity to SnTox5 and found strong necrosis on the SnTox5 differential line LP29, whereas no reaction on Arina and Forno wheat cultivars. Therefore, the 4BL glume blotch QTL reported by Schnurbusch et al. (2003) was not likely due to the *Snn5*-SnTox5 interaction.

It is well known that higher recombination occurs in certain regions of the genome referred to as recombination hot-spots (Shiroishi et al. 1993; Smith 1994; Lichten and Goldman 1995). By comparing physical maps with recombination-based maps, Gill et al. (1996) found higher recombination rate in gene-rich regions relative to gene-poor regions. Furthermore, they found kb/cM estimates ranged from 118 kb for gene-rich regions to 22,000 kb for gene poor

regions. Sourdille et al. (2003) identified a recombination hot-spot in deletion bin 4BL5-0.86-1.00 using a doubled haploid mapping population derived from the French variety Courtot (Ct) and Chinese Spring (CS). This region was reported to be located distally between genetically unlinked loci *XksuH11-4B* and *Xcdo1312-4B*. Although the hot-spot markers were distal to the *Snn5*-containing region, it is possible that region was shifted due to different mapping population or poor coverage of chromosome 4B with only 29 microsatellites in the CSCt population. However, there is also a possibility of the *Snn5* region having another hot spot because of its high recombination rate. The orientation of markers and their physical distances in CS and Svevo indicates high recombination in the *Snn5* region (Figure 4.2). Recombination hot spots are expected to be highly decondensed as compared to proximal heterochromatic areas that contain repetitive DNA (Faris et al. 2000). With help of mapped markers, *Snn5* was narrowed to a 1.38 Mb segment with a physical to genetic distance ratio of ~492 kb/cM. Faris et al. (2000) identified a hot spot on chromosome 5B and with use of molecular markers, the group reported physical to genetic distance ratio to be <200 kb/cM which is about 22-fold higher than the genomic average. Faris et al. (2003) also reported the physical to genetic distance of ~330 kb/cM across BAC contig spanning *Q* locus in wheat. Given the estimates of physical to genetic distance ratio in recombination hot spots, the *Snn5* locus may reside in one as well.

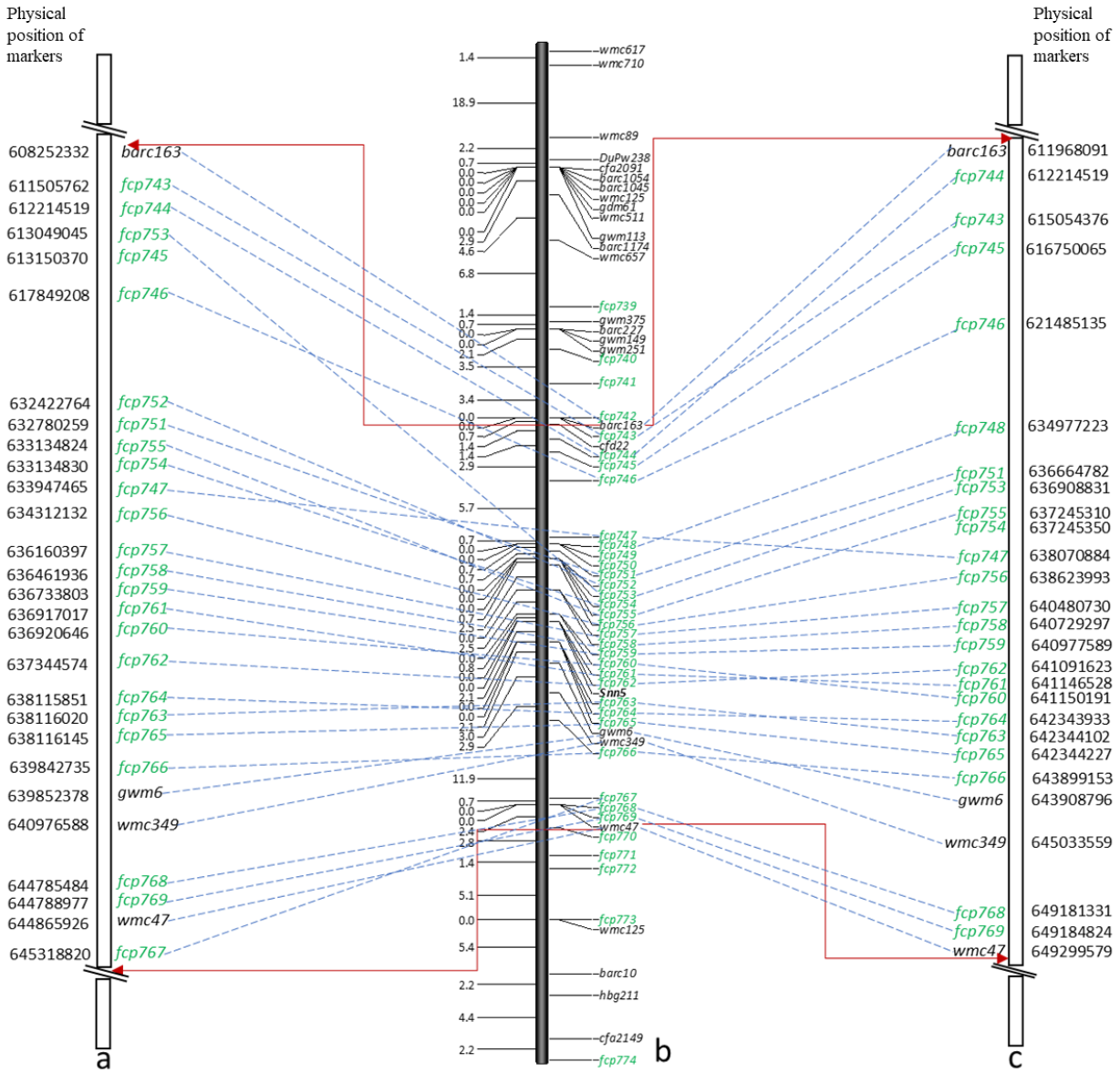

Figure 4.2. Comparative mapping of the *Snn5* saturated genetic map with the sequenced genomes of Chinese Spring and Svevo. a) physical order of markers in Chinese Spring (IWGSC 2018); b) saturated map constructed in the Lebsock × PI 94749 DH population consisting of 146 lines; c) physical order of markers in durum cultivar Svevo (CNR ITB 2017). Markers in green represent new markers designed in this study. The red lines mark the zoomed-out region used for comparison. The dashed blue lines connect the same marker mapped in physical and genetic map.

The availability of reference genome sequences enabled me to identify candidate genes (Table 4.2) for *Snn5* on chromosome arm 4BL. The genomic sequence residing between flanking markers *fcp759* and *fcp764* was analyzed to find high confidence genes. In the CS reference

genome (http://wheat-urgi.versailles.inra.fr/Seq-Repository), the interval was positioned between 636,733,803 to 638,115,851 bp and in Svevo (http://d-data.interomics.eu) it was between 640,977,589 to 642,343,933 bp. A total of 16 genes were found within the interval and 8 genes were common between Chinese Spring and Svevo (Figure 4.3). One candidate gene with locus ID TraeCS4B02G343100 had similarity to the serine/threonine-protein domain of protein kinases. TraeCS4B02G343100 shares sequence similarity with *Snn3-D1* (Faris et al. unpublished) and *fcp761* is the gene-specific marker that was designed from TraeCS4B02G343100 and co-segregates with *Snn5* in the saturated map. *Tsn1* is a *P. nodorum*-wheat sensitivity gene that has Ser/Thr-NB-LRR domains (Faris et al. 2010) and *Snn1* is aother sensitivity gene that was identified to be member of wall-associated kinase (WAK) that also contains a Ser/Thr domain (Shi et al. 2016b). In tomato, *Pto* is a resistance gene that encodes for a Ser/Thr kinase and is required along with the NB-LRR protein Prf to activate defense and confer resistance to *Pseudomonas syringae* strains carrying avrPto (Martin et al. 1993). Another example is the Arabidopsis *PBS1* gene, which is a Ser/Thr kinase that is required for the function of the *RPS5 NB-LRR* gene (Swiderski and Innes 2001). Protein kinases result in the activation of transcription factors that further help in defense mechanisms as well. Given the history of *P. nodorum* NEs to subvert the plant defense mechanism as observed in the SnToxA-*Tsn1* and SnTox1-*Snn1* interactions, which result in cell death, TraeCS4B02G343100 can be considered as a strong candidate for *Snn5*. Although genes with disease resistance domains are attractive candidates, other genes within the interval can not be ignored. Nevertheless, the isolation and cloning of *Snn5* in wheat will add deeper insight to the functioning of compatible host gene-NE interactions resulting in cell death.

Table 4.2. Putative genes or gene fragments identified in the a) Chinese Spring and b) Svevo genomes between markers *fcp759* and *fcp764*. The genes followed by * are the common genes identified in both genomes.

a.

Locus ID in CS	tblastx	e-value
TraeCS4B02G342800	DELLA protein SLR1-like (*Aegilops tauschii*)*	0.0
TraeCS4B02G342900	predicted uncharacterized protein (*Hordeum vulgare*)	9e-115
TraeCS4B02G343000	cation/H(+) antiporter 15 (*Sorghum bicolor*, *Brachypodium distachyon*)*	0.0
TraeCS4B02G343100	serine/threonine-protein kinase PBL28 (*Sorghum bicolor*)	3e-152
TraeCS4B02G343300	gamma-gliadin protein gene (*Triticum aestivum*)	1e-133
TraeCS4B02G343500	predicted transcript variant (*Brachypodium distachyon*)	4e-129
TraeCS4B02G343700	predicted uncharacterized protein (*Aegilops tauschii*, *Setaria italica*, *Sorghum bicolor*)*	0.0
TraeCS4B02G343800	ABC transporter C family member (*Aegilops tauschii*)*	0.0
TraeCS4B02G344000	transcription factor MYB2 (*Brachypodium distachyon*)	2e-84
TraeCS4B02G344100	ubiquitin-protein ligase WAV3 (*Oryza sativa*)*	0.0
TraeCS4B02G344200	predicted uncharacterized protein (*Aegilops tauschii*, *Hordeum vulgare*)	0.0
TraeCS4B02G344300	beta-amylase 1, chloroplastic (*Aegilops tauschii*)*	0.0
TraeCS4B02G344400	60S ribosomal protein L21 (RPL21) gene (*Triticum aestivum*)*	0.0
TraeCS4B02G344500	putative C3H2C3 RING-fimger protein (6G2) gene (*Triticum turgidum*)	8e-21

b.

Predicted genes in Durum Svevo	tblastx	e-value
1	DELLA protein SLR1-like (*Aegilops tauschii*)*	0.0
2	mitochondrial ribosomal protein L11 (*Triticum aestivum*)	5e-99
3	cation/H(+) antiporter 15 (*Sorghum bicolor*, *Brachypodium distachyon*)*	0.0
4	predicted uncharacterized protein (*Setaria italica*)*	0.0
5	ABC transporter C family member (*Triticum polonicum*)	0.0
6	ubiquitin-protein ligase WAV3 (*Oryza sativa*)*	0.0
7	beta-amylase 1, chloroplastic (*Aegilops tauschii*)*	0.0
8	60S ribosomal protein L21 (RPL21) gene (*Triticum aestivum*)*	0.0

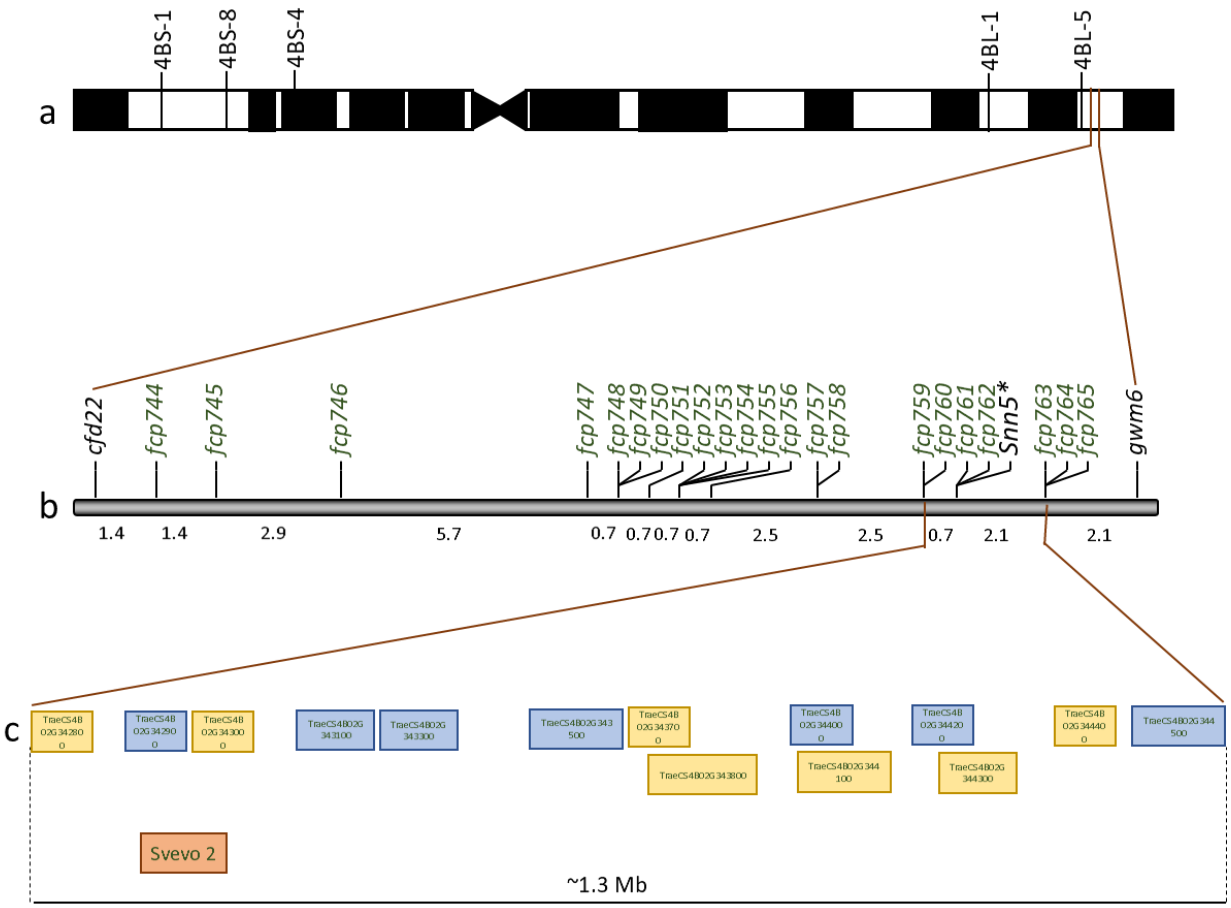

Figure 4.3. Saturated genetic map and predicted genes in the candidate interval for map-based cloning of *Snn5*. a) The physical map of chromosome 4B. The genomic region containing the *Snn5* gene on the long arm of chromosome 4B is shown in brown. b) The genetic linkage map of the *Snn5* region on chromosome 4B. Markers in green are developed in this study. The distance interval between markers are shown below the map in cM units. c) Predicted genes in the candidate interval are shown in blue, and pink for Chinese Spring, and Svevo, respectively. The yellow ones are common in CS and Svevo reference genome.

The co-dominant markers developed in this study should be useful for marker-assisted selection of *Snn5* especially in backcrossing schemes because insensitivity to *Snn5* is recessive and heterozygous genotypes cannot be distinguished from homozygous plants for *Snn5* alleles based on NE infiltration reactions. These user-friendly markers along with data from reaction to SnTox5-containing CFs can be highly useful to eliminate sensitivity alleles from wheat cultivars. A saturated map is the first step towards map-based cloning of gene and next steps include high-resolution (HR) mapping, mutagenesis, and gene complementation. HR mapping was initiated

using a segregating F_2 population developed from a cross between LP29 and PI 94749 to capture more recombination events (ideally one recombination per 100 kb). Markers *fcp756* and *fcp765* were chosen for screening of 2000 F_2 plants (4000 gametes) because they flanked *Snn5*, were codominant, and delineated the gene regin to a 7.9 cM interval. Sn2000K06-1 and Sn99CH1A7a SnTox5 containing CFs were used for subsequent analysis that revealed 121 putative recombinants. Progeny tests are currently being underway using 16 F_3 seeds per F_2 plant. It will validate the genotyping of F_2 plants with critical recombination events flanking the *Snn5* locus either in homozygous or heterozygous state in F_2 plants. These critical recombinants will then be used to obtain more closely linked markers and further narrow down the candidate region. Once the target region is identified, the next step includes identification and validation of candidate genes. The availability of reference genomes has made chromosome walking relatively easy as compared to traditional BAC cloning. The candidate genes in the physical interval can be analyzed using expression data, mutant analysis, or gene transformation. The candidate genes can be sequenced from the mutants and compared with the wild type to determine if it is the target gene or not. Six hundred seeds of LP29 were also treated with 0.25% v/v ethyl methanesulfonate (EMS) in 0.5 M phosphate buffer to generate mutants. M_1 mutants have been harvested and mutant screening are ongoing to identify SnTox5 insensitive mutants.

With the help of critical recombinants and mutants, the most promising candidate gene will be identified, and gene-complementation studies will be performed to validate the gene function. Once the gene is cloned, allelic diversity and expression analysis can be done to further study the gene evolution and function.

4.6. References

Abeysekara NS, Faris JD, Chao S, et al (2012) Whole-genome QTL analysis of *Stagonospora nodorum* blotch resistance and validation of the SnTox4-*Snn4* interaction in hexaploid wheat. Phytopathology 102:94–104. doi: 10.1094/PHYTO-02-11-0040

Abeysekara NS, Friesen TL, Keller B, et al (2009) Identification and characterization of a novel host-toxin interaction in the wheat-*Stagonospora nodorum* pathosystem. Theor Appl Genet 120:117–126. doi: 10.1007/s00122-009-1163-6

Cavanagh CR, Chao S, Wang S, et al (2013) Genome-wide comparative diversity uncovers multiple targets of selection for improvement in hexaploid wheat landraces and cultivars. PNAS 110:8057–8062. doi: 10.1073/pnas.1217133110

Chisholm ST, Coaker G, Day B, et al (2006) Host-microbe interactions: shaping the evolution of the plant immune response. Cell 124:803–814. doi: 10.1016/j.cell.2006.02.008

Chu CG, Chao S, Friesen TL, et al (2010) Identification of novel tan spot resistance QTLs using an SSR-based linkage map of tetraploid wheat. Mol Breeding 25:327–338. doi: 10.1007/s11032-009-9335-2

Faris JD, Fellers JP, Brooks SA, Gill BS (2003) A Bacterial Artificial Chromosome contig spanning the major domestication locus *Q* in wheat and identification of a candidate gene. Genetics 164:311–321

Faris JD and Friesen TL (2009) Reevaluation of a tetraploid wheat population indicates that the *Tsn1*-ToxA interaction is the only factor governing Stagonospora nodorum blotch susceptibility. Phytopathology 99:906–912. doi: 10.1094/PHYTO-99-8-0906

Faris JD, Haen KM, Gill BS (2000) Saturation mapping of a gene-rich recombination hot spot region in wheat. Genetics 154:823–835

Faris JD, Zhang Z, Lu H, et al (2010) A unique wheat disease resistance-like gene governs effector-triggered susceptibility to necrotrophic pathogens. PNAS USA 107:13544–13549. doi: 10.1073/pnas.1004090107

Faris JD, Zhang Z, Rasmussen JB, et al (2011) Variable expression of the *Stagonospora nodorum* effector SnToxA among isolates is correlated with levels of disease in wheat. Mol Plant Microbe Interact 24:1419–1426. doi: 10.1094/MPMI-04-11-0094

Flor HH (1956) The complementary genetics systems in flax and flax rust. Adv. Genet. 8:29-54

Friesen TL, Chu C, Xu SS, et al (2012) SnTox5-*Snn5*: a novel *Stagonospora nodorum* effector-wheat gene interaction and its relationship with the SnToxA-*Tsn1* and SnTox3-*Snn3-B1* interactions. Mol Plant Pathol 13:1101–1109. doi: 10.1111/j.1364-3703.2012.00819.x

Friesen TL, Chu CG, Liu ZH, et al (2009) Host-selective toxins produced by *Stagonospora nodorum* confer disease susceptibility in adult wheat plants under field conditions. Theor Appl Genet 118:1489–1497. doi: 10.1007/s00122-009-0997-2

Friesen TL and Faris JD (2010) Characterization of the wheat-*Stagonospora nodorum* disease system: what is the molecular basis of this quantitative necrotrophic disease interaction?. Can J Plant Pathol 32:20–28. doi: 10.1080/07060661003620896

Friesen TL, Meinhardt SW, Faris JD (2007) The *Stagonospora nodorum*-wheat pathosystem involves multiple proteinaceous host-selective toxins and corresponding host sensitivity genes that interact in an inverse gene-for-gene manner. Plant J 51:681–692. doi: 10.1111/j.1365-313X.2007.03166.x

Friesen TL, Stukenbrock EH, Liu Z, et al (2006) Emergence of a new disease as a result of interspecific virulence gene transfer. Nature Genetics 38:953–956. doi: 10.1038/ng1839

Friesen TL, Zhang Z, Solomon PS, et al (2008) Characterization of the interaction of a novel *Stagonospora nodorum* host-selective toxin with a wheat susceptibility gene. Plant Physiol 146:682–693. doi: 10.1104/pp.107.108761

Gao Y, Faris JD, Liu Z, et al (2015) Identification and characterization of the SnTox6-*Snn6* interaction in the *Parastagonospora nodorum*-wheat pathosystem. Mol Plant Microbe Interact 28:615–625. doi: 10.1094/MPMI-12-14-0396-R

Garcia-Seco D, Chiapello M, Bracale M, et al (2017) Transcriptome and proteome analysis reveal new insight into proximal and distal responses of wheat to foliar infection by *Xanthomonas translucens*. Sci Rep 7:10157. doi: 10.1038/s41598-017-10568-8

Gill KS, Gill BS, Endo TR, et al (1996) Identification and high-density mapping of gene-rich regions in chromosome group 5 of wheat. Genetics 143:1001–1012

Jones JDG, Dangl JL (2006) The plant immune system. Nature 444:323–329. doi: 10.1038/nature05286

Kosambi DD (1943) The estimation of map distances from recombination values. Ann Eugen 12:172–175. doi: 10.1111/j.1469-1809.1943.tb02321.x

Lichten M, Goldman AS (1995) Meiotic recombination hotspots. Annu Rev Genet 29:423–444. doi: 10.1146/annurev.ge.29.120195.002231

Liu Z, Faris JD, Oliver RP, et al (2009) SnTox3 Acts in Effector Triggered Susceptibility to Induce Disease on Wheat Carrying the *Snn3* Gene. PLoS Pathog 5(9):e1000581. doi: 10.1371/journal.ppat.1000581

Liu Z, Friesen TL, Ling H, et al (2006) The *Tsn1*-ToxA interaction in the wheat-*Stagonospora nodorum* pathosystem parallels that of the wheat-tan spot system. Genome 49:1265–1273. doi: 10.1139/g06-088

Liu Z, Zhang Z, Faris JD, et al (2012) The cysteine rich necrotrophic effector SnTox1 produced by *Stagonospora nodorum* triggers susceptibility of wheat lines harboring *Snn1*. PLoS Pathog 8(1):e1002467. doi: 10.1371/journal.ppat.1002467

Liu ZH, Faris JD, Meinhardt SW, et al (2004a) Genetic and physical mapping of a gene conditioning sensitivity in wheat to a partially purified host-selective toxin produced by *Stagonospora nodorum.* Phytopathology 94:1056–1060. doi: 10.1094/PHYTO.2004.94.10.1056

Liu ZH, Friesen TL, Rasmussen JB, et al (2004b) Quantitative Trait Loci analysis and mapping of seedling resistance to *Stagonospora nodorum* leaf blotch in wheat. Phytopathology 94:1061–1067. doi: 10.1094/PHYTO.2004.94.10.1061

Lorieux M (2012) MapDisto: fast and efficient computation of genetic linkage maps. Mol Breeding 30:1231–1235. doi: 10.1007/s11032-012-9706-y

Lu H and Faris JD (2006) Macro- and microcolinearity between the genomic region of wheat chromosome 5B containing the *Tsn1* gene and the rice genome. Funct Integr Genomics 6:90–103. doi: 10.1007/s10142-005-0020-1

Martin GB, Brommonschenkel SH, Chunwongse J, et al (1993) Map-based cloning of a protein kinase gene conferring disease resistance in tomato. Science 262:1432–1436

Oliver RP and Solomon PS (2010) New developments in pathogenicity and virulence of necrotrophs. Curr Opin Plant Biol 13:415–419

Oliver RP, Friesen TL, Faris JD, et al (2012) *Stagonospora nodorum*: from pathology to genomics and host resistance. Annu Rev Phytopathol 50:23–43. doi: 10.1146/annurev-phyto-081211-173019

Phan HTT, Rybak K, Furuki E, et al (2016) Differential effector gene expression underpins epistasis in a plant fungal disease. Plant J 87:343–354. doi: 10.1111/tpj.13203

Röder MS, Korzun V, Wendehake K, et al (1998) A microsatellite map of wheat. Genetics 149:2007–2023

Rozen S and Skaletsky H (2000) Primer3 on the WWW for general users and for biologist programmers. Methods Mol Biol 132:365–386

Schnurbusch T, Paillard S, Fossati D, et al (2003) Detection of QTLs for *Stagonospora* glume blotch resistance in Swiss winter wheat. Theor Appl Genet 107:1226–1234. doi: 10.1007/s00122-003-1372-3

Shi G, Friesen T, Saini J, et al (2015) The Wheat gene *Snn7* confers susceptibility on recognition of the necrotrophic effector SnTox7. Plant Genome 8(2):1-10. doi: 10.3835/plantgenome2015.02.0007

Shi G, Zhang Z, Friesen TL, et al (2016a) Marker development, saturation mapping, and high-resolution mapping of the Septoria nodorum blotch susceptibility gene *Snn3-B1* in wheat. Mol Genet Genomics 291:107–119. doi: 10.1007/s00438-015-1091-x

Shi G, Zhang Z, Friesen TL, et al (2016b) The hijacking of a receptor kinase–driven pathway by a wheat fungal pathogen leads to disease. Science Advances 2(10):e1600822. doi: 10.1126/sciadv.1600822

Shiroishi T, Sagai T, Moriwaki K (1993) Hotspots of meiotic recombination in the mouse major histocompatibility complex. Genetica 88:187–196

Smith GR (1994) Hotspots of homologous recombination. Experientia 50:234–241

Somers DJ, Isaac P, Edwards K (2004) A high-density microsatellite consensus map for bread wheat (*Triticum aestivum* L.). Theor Appl Genet 109:1105–1114. doi: 10.1007/s00122-004-1740-7

Song QJ, Shi JR, Singh S, et al (2005) Development and mapping of microsatellite (SSR) markers in wheat. Theor Appl Genet 110:550–560. doi: 10.1007/s00122-004-1871-x

Sourdille P, Singh S, Cadalen T, et al (2004) Microsatellite-based deletion bin system for the establishment of genetic-physical map relationships in wheat (*Triticum aestivum* L.). Funct Integr Genomics 4:12–25. doi: 10.1007/s10142-004-0106-1

Swiderski MR and Innes RW (2001) The Arabidopsis *PBS1* resistance gene encodes a member of a novel protein kinase subfamily. Plant J 26:101–112

Torada A, Koike M, Mochida K, et al (2006) SSR-based linkage map with new markers using an intraspecific population of common wheat. Theor Appl Genet 112:1042–1051. doi: 10.1007/s00122-006-0206-5

Tsuda K and Katagiri F (2010) Comparing signaling mechanisms engaged in pattern-triggered and effector-triggered immunity. Curr Opin Plant Biol 13:459–465. doi: 10.1016/j.pbi.2010.04.006

Wang S, Wong D, Forrest K, et al (2014) Characterization of polyploid wheat genomic diversity using a high-density 90,000 single nucleotide polymorphism array. Plant Biotechnol J 12:787–796. doi: 10.1111/pbi.12183

Xue S, Zhang Z, Lin F, et al (2008) A high-density intervarietal map of the wheat genome enriched with markers derived from expressed sequence tags. Theor Appl Genet 117:181–189. doi: 10.1007/s00122-008-0764-9

You FM, Wanjugi H, Huo N, et al (2010) RJPrimers: unique transposable element insertion junction discovery and PCR primer design for marker development. Nucleic Acids Res 38:W313–W320. doi: 10.1093/nar/gkq425

Zhang Z, Friesen TL, Simons KJ, et al (2009) Development, identification, and validation of markers for marker-assisted selection against the *Stagonospora nodorum* toxin sensitivity genes *Tsn1* and *Snn2* in wheat. Mol Breeding 23:35–49. doi: 10.1007/s11032-008-9211-5

Zhang Z, Friesen TL, Xu SS, et al (2011) Two putatively homoeologous wheat genes mediate recognition of SnTox3 to confer effector-triggered susceptibility to *Stagonospora nodorum*. Plant J 65:27–38. doi: 10.1111/j.1365-313X.2010.04407.x

Zipfel C (2009) Early molecular events in PAMP-triggered immunity. Curr Opin Plant Biol 12:414–420. doi: 10.1016/j.pbi.2009.06.003

APPENDIX. GENBANK ACCESSION NUMBERS OF *Q* SEQUENCES USED IN PHYLOGENETIC ANALYSIS

Source	GenBank accession number
T. spelta Iranian type PI 572915 (6X) (*Q*)	MK443259
T. spelta Iranian type PI 367199 (6X) (*Q*)	MK443261
T. spelta Iranian type PI 572914 (6X) (*Q*)	MK443258
T. spelta Iranian type P503 (6X) (*Q*)	MK443262
T. aestivum ND495 (6X) (*Q*)	MK493444
T. compactum TA2601 (6X) (*Q*)	MK493446
T. polonicum Cltr 191826 (4X) (*Q*)	AY714339
T. aestivum Renan (6X) (*Q*)	MK493445
T. carthlicum TA2801 (4X) (*Q*)	AY702959
T. durum Langdon (4X) (*Q*)	AY702955
T. aestivum Chinese Spring (6X) (*Q*)	AY702956
T. aestivum Bobwhite (6X) (*Q*)	MK493451
T. dicoccoides 16-1 (4X) (*q*)	MK493450
T. dicoccoides PI 466995 (4X) (*q*)	MK493447
T. dicoccoides TA106 (4X) (*q*)	MK493448
T. dicoccoides PI 355459 (4X) (*q*)	MK493449
T. dicoccoides Cltr 14621 (4X) (*q*)	AY714343
T. macha PI 361862 (6X) (*q*)	AY714342
T. urartu TA704 (2X) (*q*)	AY702958
T. spelta European type PI 266848 (6X) (*q*)	MK450626
T. spelta European type PI 272573 (6X) (*q*)	MK443263
T. spelta European type PI 286060 (6X) (*q*)	MK443524
T. spelta European type PI 585008 (6X) (*q*)	MK443260
T. spelta European type PI 348189 (6X) (*q*)	MK443256
T. spelta European type PI 355651 (6X) (*q*)	MK443257
T. spelta European type PI 378469 (6X) (*q*)	MK450625
T. spelta European type PI 348483 (6X) (*q*)	MK443253
T. spelta European type PI 338367 (6X) (*q*)	MK443255
T. spelta European type (Sears) (6X) (*q*)	AY714341
T. spelta European type TA2603 (6X) (*q*)	AY702960